



國立臺灣大學生命科學院生態學與演化生物學研究所

博士論文

Institute of Ecology and Evolutionary Biology, College of Life Science

National Taiwan University

Doctoral dissertation

現行與未來氣候下的台灣森林植物分布預測研究

PREDICTING THE POTENTIAL DISTRIBUTIONS

OF PLANT SPECIES AND FORESTS IN TAIWAN

UNDER PRESENT AND FUTURE CLIMATES

林奐宇

Huan-Yu Lin

指導教授：胡哲明教授

Advisor: Prof. Jer-Ming Hu

中華民國 109 年 3 月

March, 2020




誌謝

花了七個半年頭，終於寫出一部稍微完整的故事，從科學的角度講述臺灣森林植群與氣候環境的關係。首要歸功於臺灣大學生態學與演化生物學研究所的兩位老師——胡哲明教授與謝長富教授的多年指導、支持與科學訓練，使我的研究腳步能夠踏得紮實穩固，在此致上無限感激。論文初成階段，得蒙王震哲教授、陳子英教授、曾彥學教授及鍾國芳研究員指正，使文字表述臻於精準，更感謝諸位師長審查過程中的觀點交換與討論激盪，讓本研究獲得許多未來的發展與想像。

這是一部由無數前人數據堆砌而成的論文。在展現研究成果之前，我必須慎重地向諸多前輩表達我的敬意與謝意。包含曾經投入國家植群多樣性調查與製圖計畫的師長、野外工作夥伴、調繪製圖與資料庫建置人員；林務局外來入侵植物調查計畫團隊；臺灣四大植物標本館（TAI, TAIF, HAST, TNM）的標本採集與數位典藏工作同仁；以及科技部臺灣氣候變遷推估資訊與調適知識平台（TCCIP）團隊。由於眾多先進的支持，本論文才能站在充足的森林植物分布與氣候資料基礎上，對臺灣森林植群與氣候的關係展開研究探索；也期許這篇論文能延續前輩的分享精神，替臺灣未來的森林生態研究添磚加瓦，略盡一份棉薄之力。

猶記論文研究初期，單憑己力摸索著氣候變遷與物種分布的統計方法，頗有摸石過河的無助與焦慮。感謝陳子英老師帶領我認識兩位貴人——不列顛哥倫比亞大學（UBC）的王同立教授與王光玉教授，經由兩位師長的經驗技術傳授，以及亞太森林復育與永續經營網絡（APFNet）的訓練課程支持，才使論文獲得長足進展。此外，我的研究概念、邏輯思辨及統計方法，亦多得益於臺大森林系李靜峯教授、關秉宗教授與邱祈榮教授。在此一併表達個人的點滴謝意。

這個博士學位，是在職進修獲得的。我的歷任服務單位，包含農林航空測量所、林務局及林業試驗所，都為本研究提供了充足的調查資料、計畫經費與設備資



源。深切感謝臺灣林業部門的支持，也希望我的研究成果能回饋給林業界，對未來的森林保育與經營管理做出貢獻。科學研究是一個快樂而充實的過程，然而，在工作與進修並進下，難免壓縮了與家人共處的假日時光。謝謝我的家人，包括妻子、父母及妹妹幫忙分擔了三個孩子的照顧工作，使我能專心處理研究工作疑難而免於家庭牽掛，謹與我的所有親人，共享走完臺大學業段落的喜悅。

最後，借用指導教授胡哲明老師的一段講評：「這部論文除了整理出臺灣植物分布的趨勢，更重要的，是它挖掘出更多值得探討的研究議題」。學術研究是沒有止盡的，期望我的論文成果能作為後人探討森林生態的另一個起點，也期許來者秉持合作分享的精神，擴大臺灣森林研究的力量。

於林業試驗所

2020年3月

中文摘要




氣候與森林植物的分布緊密關連，而多項研究也證實，臺灣山地的帶狀植群分化、以及部分泛域植群類型的分布，均與氣候條件高度相關，尤其受到溫度與年間降水分配差異的影響。為瞭解臺灣森林植群與氣候的關係，進一步建立森林植群氣候棲位資訊，以及推估氣候變遷的可能影響，本論文整合臺灣既有植群調查及長期氣候資料，建立預測森林植物現生與未來分布的流程方法，並提出森林分布變遷之研究結果。茲就各章節研究成果摘述如下：

一、動態氣候降尺度模型與高解析氣候圖層之產製

氣候資料是生態研究的重要基礎，然而一般泛用氣候圖資之空間解析度以數公里至數十公里不等，難以反映山區起伏地形導致的氣溫與降水的劇烈變化。本章節利用臺灣氣候變遷推估與資訊平台 (TCCIP) 5 公里網格氣候資料，經動態局部迴歸方法獲得區域範圍之海拔遞減率，作為內插校正參數，於 R 軟體設計一套自由尺度化之氣候降尺度模型，命名為 *clim.regression*。經 15 處不同海拔氣象測站實測驗證，*clim.regression* 推估月尺度氣候之平均絕對誤差為 0.56°C (月均溫)、0.79°C (月均低溫)、0.80°C (月均高溫) 及 36.26mm (月累積降水)，改善了 TCCIP 原始資料 54.6–66.7% 的誤差。*Clim.regression* 共可針對歷史年度 (1960–2009) 及三個未來階段產製 73 種氣候因子，其自由尺度化、高準確度的特色，極適合在山地氣候與生態關係研究應用，亦是本論文進行後續章節研究之氣候資料來源。

二、以氣候為基礎的臺灣山地植群分布模擬與預測方法

相較於傳統航遙測影像判釋或現場調查方法，森林植群氣候的棲位模擬預測，是相對簡易而迅速獲得森林植群空間分布資訊的方法。本章節使用林務局國家植群多樣性調查計畫樣區資料，以及李靜峯等人建立之森林分類架構，經由




clim.regression 產生各森林類型之氣候幅度，再利用隨機森林方法，建立 13 種與氣候相關森林類型的棲位模型，並完成 13 種森林類型的現生分布預測。依據 3817 個樣區交叉驗證顯示，隨機森林對於現生植群分布預測之平均錯誤率為 6.59%，森林分布預測結果與地形高度擬合，並反映出不同森林類型交會帶之過渡現象。本章節證實高解析度、高準確度的氣候資料，配合野外調查樣本及充分的機器學習訓練，可提供良好的植群現生分布資訊，作為預測未來變遷的基礎工具。

三、海拔梯度下，氣候變遷對於臺灣山地森林植群的影響程度為何？

目前全球森林與氣候變遷相關研究，主要集中在北半球中緯度，對熱帶森林的研究較少。以山地森林而言，普遍認為暖化可能導致森林植物的向上遷徙，對高海拔或山頂植群造成威脅與衝擊。臺灣山地森林跨越近 4000 公尺的海拔梯度，涵蓋熱帶至亞高山森林類型，利用前一章獲得之山地植群模擬預測方法，於本章節探討不同暖化情境下各森林類型的面積與海拔分布變化。所有暖化情境一致顯示，高海拔森林及中海拔雲霧林可能出現面積縮減，尤其以亞高山刺柏灌叢及臺灣水青岡落葉霧林首當其衝，將喪失大多數棲地（RCP 4.5）或瀕臨滅絕（RCP 8.5）。對於熱帶山地森林的預測結果則較為分歧，雖然熱帶森林的棲地面積在多數暖化情境下呈現逐步擴張的趨勢，然而在極端暖濕、或極端暖乾的狀況下，可能因水分有效性劇烈變化因素，導致熱帶山地霧林完全失去適存環境，熱帶季風林亦將出現顯著的棲地縮減，是不可忽視的氣候變遷威脅。綜上研究結果，本章節可推測出氣候變遷下的易危森林類型，並提出相對應的保育建議，作為後續監測及管理工作的參考。

四、被子植物雌雄異株物種的地理分布與其生態相關因子之研究



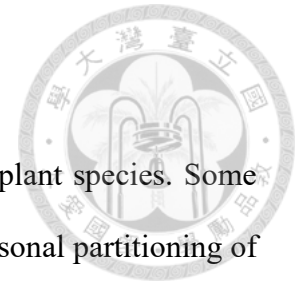
本論文收集大量的植物分布紀錄與氣候資料，不僅限於氣候變遷研究應用，也是生態與生物地理分布研究的珍貴素材。本章節運用上述資料，以植物性別表現的空間分布型式為例進行研究，希能激發其他生態研究者的興趣與更多的參與。

雌雄異株是相對罕見的植物生殖模式，藉由不同雌雄個體異交產生種子延續後代。過去調查統計全球被子植物的雌雄異株種類約佔所有種類的 6%，但許多例子指出不同區域的雌雄異株物種比例會有差異，地形起伏劇烈的海洋島嶼、熱帶森林、木本生活型、蟲媒授粉等現象，通常與較高的雌雄異株比例相關。臺灣的地理環境具有大陸至海洋的過渡特性，本研究發現，臺灣本島被子植物的雌雄異株整體比例約為 8.2%，但從臺灣海峽至太平洋間，臺灣諸島被子植物相的雌雄異株比例呈現逐漸升高的梯度，呼應了 Bawa 氏提出的海洋島嶼較多雌雄異株物種的理論。此外，沿本島海拔梯度則發現，自然植群皆存在雌雄異株比例隨海拔升高而降低的現象，並在海拔 2200 公尺處存在顯著的遞減率轉折點；高海拔的雌雄異株比例劇烈陡降，推測可能與闊葉林與針葉林的交會轉換，以及高海拔授粉昆蟲相趨於單純化所致。但人工植群之雌雄異株比例則與海拔無顯著相關。搭配氣候因子分析，顯示雌雄異株植物常見於溫暖環境，兩性花植物則偏好於低溫的高海拔地區，雜性物種的出現則與氣候條件無顯著關聯。

關鍵字：

氣候、氣候變遷衝擊、生態棲位模型、山地森林植群、隨機森林、臺灣

Abstract

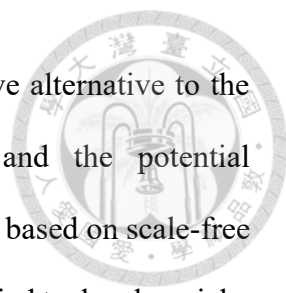


Climate plays a vital role in shaping the distribution of forest and plant species. Some authors had reported that climate, especially the temperature and seasonal partitioning of rainfall, is significantly correlated with the altitudinal zonation of mountain forests and also to some of the distribution of azonal vegetation. This dissertation incorporated vegetation survey and historical climate data to reconstruct climatic niches for mountain forests of Taiwan, and project their distributional changes under future climatic scenarios. The critical outcomes of each chapter summarized as below:

1. A dynamic downscaling approach to generate scale-free regional climate data.

Climate variables, particularly temperature and precipitation, are the most well-known key factors related to vegetation zonation. However, to obtain climate data adequately for the requirement of ecological studies is challenging due to the difficulty of data integration and the complexity of downscaling, especially for mountainous regions. In this section, a synthetic approach combining bilinear interpolation and dynamic local regression was conducted to develop a scale-free climate downscaling model in R environment, namely *clim.regression*. Based on the original 5km x 5km gridded climate surface from TCCIP, *clim.regression* can generate 73 climatic variable estimates specific to the user-defined points of interest for historical (1960–2009) and future periods (2016–2035, 2046–2065 and 2081–2100), which reduced prediction error by 54.6–66.7% relative to the original gridded climate data for temperatures. The result is adapted to the uses of ecological researches and is the source of climate data of this dissertation.

2. Climate-based approach for modeling the distribution of montane forest vegetation.

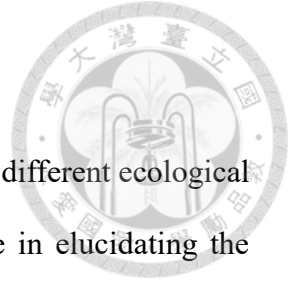


A climate-based ecological niche model may provide an effective alternative to the traditional approach for assessing limitations, thresholds, and the potential distribution of forests. In this section, a machine-learning method based on scale-free climate variable estimates and classified vegetation plots was applied to develop niche models for the 13 climate-related forest types in Taiwan, and to generate a fine-scale predicted vegetation map. The result supported that the machine-learning approach is sufficient to handle a large number of variables and to provide accurate predictions, which has the potentials in projecting the distributional changes of forests under different climate change scenarios.

3. How much does climate change alter the distribution of forests across a great altitudinal gradient?

Taiwan is a high-mountain island with substantial altitudinal variations and diverse forest types driven by climate. In this study, we used the scale-free climate variable estimates and an established machine-learning approach to project the distributional changes of 13 climate-related mountain forest types under selected global warming scenarios. The results demonstrated a consistent trend of the drastic habitat contractions of subalpine *Juniperus* woodland and the deciduous *Fagus* broadleaved forests. It also revealed that tropical montane cloud forest and tropical winter monsoon forest might be highly vulnerable under the extreme warm-humid or warm-dry climatic conditions because of the sever change of water availability. For mitigating the risk of climate change to the vulnerable forest types, adapted conservation strategies were suggested according to the environmental characteristic of each forest type.

4. Geographical distribution of dioecy and its ecological correlates based on fine-



scaled species distribution data.

A great deal of species occurrence and climate data is valuable in different ecological researches. An example is shown here to demonstrate such use in elucidating the complicate distribution patterns of plant sexual systems. In this section, I used species occurrence and historical climate data in exploring the geographical distribution of sexual expression systems of the flowering plants in Taiwan.

It was reported that the incidence of dioecy varied among local floras and suggested inclining to tropical and oceanic environments. We found the average incidence of dioecy in the flora of Taiwan to be 8.2%, but it exhibits geographical variations from islets in the Taiwan Strait to the Pacific Ocean. An apparent two-step decreasing pattern of dioecy percentages with elevation was also found, which shows a distinct transition at the altitude of 2200m. The overall analysis indicated that spatial variations of dioecy were associated with eco-correlates of land cover, elevation, woodiness, species richness, and mean annual temperature. Results of this section partially support Bawa's hypothesis of a higher incidence of dioecy on oceanic islands, and consistent with Baker and Cox's observations of more prosperous dioecious species on high-mountain islands in the tropics and subtropics.

Key words:

Climate, Climate change impacts, Ecological niche modeling, Mountain forest vegetation, Random forest, Taiwan.

Comparison table of abbreviations

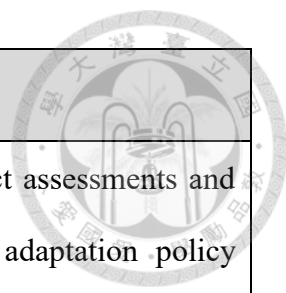


Abbreviation	Definition
AR5	<p>The IPCC Fifth Assessment Report. AR5 is a report announced by IPCC in 2014, it provides an overview of the state of knowledge concerning the science of climate change, emphasizing new results since the publication of the IPCC Fourth Assessment Report (AR4) in 2007.</p> <p>(https://www.ipcc.ch/report/ar5/syr/)</p>
CMIP5	<p>The Coupled Model Intercomparison Project (CMIP) is a standard experimental framework for studying the output of coupled atmosphere-ocean general circulation models. CMIP5 is the most current and extensive of the CMIPs. The objectives of CMIP5 are to:</p> <ol style="list-style-type: none"> 1. evaluate how realistic the models are in simulating the recent past, 2. provide projections of future climate change on two time scales, near term (out to about 2035) and long term (out to 2100 and beyond), and 3. understand some of the factors responsible for differences in model projections, including quantifying some key feedbacks such as those involving clouds and the carbon cycle. <p>(https://climatedataguide.ucar.edu/climate-model-evaluation/cmip-climate-model-intercomparison-project-overview)</p>
CoDeK	<p>Cocktail determination key. CoDeK is a software application, based</p>

Abbreviation	Definition
	<p>on R program (R Development Core Team 2012), which allows automatic classification of vegetation samples into vegetation types defined by Cocktail determination key. The Cocktail Determination Key has been published as supplementary materials in Li et al. (2013), it allows automatic assignment of vegetation plots into predefined vegetation types (supervised classification).</p> <p>(https://www.davidzeleny.net/doku.php/software)</p>
GCM	<p>General circulation model. GCM is a type of climate model. It employs a mathematical model of the general circulation of a planetary atmosphere or ocean based on the basic laws of physics, fluid motion, and chemistry. Scientists divide the planet into a 3-dimensional grid, apply the basic equations, and evaluate the results. The calculations include winds, heat transfer, radiation, relative humidity, and surface hydrology within each grid and evaluate interactions with neighboring points.</p> <p>(https://en.wikipedia.org/wiki/General_circulation_model)</p>
IPCC	<p>Intergovernmental Panel on Climate Change. IPCC is the United Nations body for assessing the science related to climate change. It provides regular assessments of the scientific basis of climate change, its impacts and future risks, and options for adaptation and mitigation.</p> <p>(https://www.ipcc.ch/)</p>
LGM	<p>Last Glacial Maximum. LGM was the most recent time during the</p>

Abbreviation	Definition
	<p>Last Glacial Period that ice sheets were at their greatest extent. The growth of ice sheets commenced 33,000 years ago and maximum coverage was between 26,500 years and 19–20,000 years ago.</p> <p>(https://en.wikipedia.org/wiki/Last_Glacial_Maximum)</p>
LOESS	<p>Local polynomial regression. LOESS is a nonparametric technique for smoothing scatter plots and modeling functions. For each point, x_0, a low-order polynomial regression is fit using only points in some “neighborhood” of x_0. The result is a smooth function over the support of the data.</p> <p>Avery, M. (2010). Literature Review for Local Polynomial Regression.</p>
MAP	<p>Mean annual precipitation. It refers to the sum of precipitation of 12 months a year.</p>
MAT	<p>Mean annual temperature. It refers to the average of mean temperatures of 12 months a year.</p>
OOB error	<p>Out-of-bag error. OOB error is a method of measuring the prediction error of random forests, boosted decision trees, and other machine learning models utilizing bootstrap aggregating (bagging) to sub-sample data samples used for training. Subsampling allows one to define an out-of-bag estimate of the prediction performance improvement by evaluating predictions on those observations which were not used in the building of the next base learner.</p>

Abbreviation	Definition
	<p>(https://en.wikipedia.org/wiki/Out-of-bag_error)</p>
RCP	<p>Representative Concentration Pathways. RCPs usually refer to the portion of the concentration pathway extending up to 2100, corresponding emission scenarios. Four RCPs, RCP 2.6, RCP 4.5, RCP 6.0, and RCP 8.5, produced from Integrated Assessment Models were selected from the published literature and are used in the Fifth IPCC Assessment as a basis for the climate predictions and projections.</p> <p>(https://www.ipcc-data.org/guidelines/pages/glossary/glossary_r.html)</p>
RF	<p>Random forests. RF is an ensemble learning method for classification, regression and other tasks that operate by constructing a multitude of decision trees at training time and outputting the class that is the mode of the classes (classification) or mean prediction (regression) of the individual trees. This method has been recommended for modeling the ecological niche of organisms and predicting their potential distribution.</p> <p>(https://en.wikipedia.org/wiki/Random_forest)</p>
TCCIP	<p>Taiwan Climate Change Information and Projection. The TCCIP coordinated by National Science and Technology Center for Disaster Reduction (NCDR) is one of the major climate change projects funded by Ministry of Science and Technology. The TCCIP project</p>



Abbreviation	Definition
	not only produces climate change data for impact assessments and adaptations but also aims to support national adaptation policy framework. (https://tccip.ncdr.nat.gov.tw/au_eng.aspx)



Contents



口試委員會審定書	i
誌謝	iii
中文摘要	v
Abstract	viii
Comparison table of abbreviations	xi
Chapter 1. General introduction	1-1
Chapter 2. A dynamic downscaling approach to generate scale-free regional climate data in Taiwan	
2.1 Introduction	2-2
2.2 Materials and methods	2-4
2.3 Results	2-11
2.4 Discussion	2-25
2.5 Author contributions	2-30
2.6 Literature cited	2-30
Chapter 3. Climate-based approach for modeling the distribution of montane forest vegetation in Taiwan	
3.1 Introduction	3-2
3.2 Materials and methods	3-6
3.3 Results	3-13
3.4 Discussion	3-24
3.5 Author contributions	3-31
3.6 Literature cited	3-32

**Chapter 4. How much does climate change alter the distribution of
forests across a great altitudinal gradient on a subtropical
island?**



4.1	Introduction	4-2
4.2	Materials and methods	4-6
4.3	Results	4-11
4.4	Discussion	4-24
4.5	Author contributions	4-29
4.6	Literature cited	4-29

**Chapter 5. Geographical distribution of dioecy and its ecological
correlates based on fine-scaled species distribution data
from a subtropical island**

5.1	Introduction	5-2
5.2	Materials and methods	5-5
5.3	Results	5-10
5.4	Discussion	5-20
5.5	Author contributions	5-25
5.6	Literature cited	5-25

Supplementary: Committee's comments and the responses	S-1
--	------------

Chapter 1

General introduction



Climate is one of the most important factors shaping the distribution of species, communities, ecosystems, and biomes (Whittaker, 1975; Woodward and Williams, 1987; Davis and Shaw, 2001). To understand the vegetation-climate relationship is not only the kernel that most ecologists interested in but also being a piece of equipment for exploring the possible changes of organisms in a changing environment. Anthropogenic climate change in recent decades has emerged as a major driver affected the characteristics of vegetation worldwide, such as the directional range shift of plants and animals (IPCC, 2014), the disrupted interspecies phenological synchrony (Ovaskainen et al., 2013), and local extinction events in particular localities (Pauli et al., 2012), which may cause severe impacts to the management of natural resources, biological conservation, and ecosystem functions and services.

The directional range shift, including the poleward and upward migration of species under global warming, is an issue of growing concern for many ecologists. A first-order approximation regarding the response of organisms to a warming climate is that species will migrate upward or poleward to find a suitable climate to survive (Beniston, 2003). Mountain environment is a region with dramatic climatic gradient in a very short distance that species could find and access a cooler habitat easily. However, the accompanied competition, substitution, and progressively replacement of mountain forest communities may also occur.

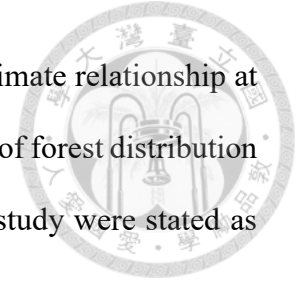
Taiwan is a mountainous island with territories over 70% occupied by hills and mountains, and a total of 58% of this island is covered by forests. It's already known that regional climate, especially the altitudinal temperature gradient and seasonal precipitation

differences, shapes the diverse mountain forests of Taiwan (Su, 1984). Since mountain forest vegetation plays important role in harboring the plentiful biodiversity of our home island, it is needed to study the relationship of forest vegetation with the concurrent climatic environment, and to map the possible influence of climate change on forest ecosystems. The results, e.g. the estimated range shift of a specific or a rare forest type in the coming decades, can be applied in the use of protected area evaluation or threatened species conservation.

Studies of niche modeling for plant species/communities were launched around 20 years in Taiwan (Lee et al., 2006), and the climatic characteristics of a few species (Yen et al., 2008; Nakao, et al., 2014; Lin and Chiu, 2019) or forest types (Chiu et al., 2013; Lin et al., 2014) have been reported accordingly. However, intact modeling for the distribution of forests at the whole-island scale and the assessment for their future change have still received little research attention. Furthermore, most climatic niche modeling studies used the worldwide and online accessible climate database such as WorldClim (Hijmans, et al., 2005), rather than using the fine-scale interpolated climatic surface from historical observations of local meteorological stations. Weng and Yang (2012) compared the prediction accuracy between East-Asia regional climate model and Taiwan's local observations, and they utilized historical data from thousands of local meteorological stations to establish a gridded climate surface improving the performance of regional climate model. From 2012 on, a gridded climate surface covers the historical period of 1960–2012 and the future stages of 2016–2035, 2046–2065, and 2081–2100 was released by Taiwan Climate Change Projection and Information Platform (TCCIP), which has become the ideal and fundamental materials for conducting climate-relevant researches.

In this dissertation, my research goal is to incorporate the plant distribution data and the

latest released climate surface to model the concurrent vegetation-climate relationship at the whole-island scale, which can be applied in projecting the change of forest distribution under different climate change scenarios. The main layouts of this study were stated as follows:




- (1) Accurate and fine-resolution climate data is essential for modeling forest distribution corresponding to the diverse topography in the mountains. We developed a statistical approach to downscale the 5 km x 5 km climate data provided by TCCIP to a scale-free format being environmental factor estimates for the climate niche models. (Chapter 2)
- (2) Establishment of a climate-based approach for modeling the vegetation-climate relationship based on field sampling data and its corresponding climatic parameters. This model framework can be used to generate a predicted vegetation map under the selected climatic scenario. (Chapter 3)
- (3) An extended application of the vegetation-climate model. Based on climate data of different general circulation models (GCMs) and emission scenarios provided by TCCIP, we explored the possible change of forest distribution, including the area change and altitudinal range shift, and to evaluate the impact of climate change on each forest type. (Chapter 4)
- (4) A further example of using the developed data from above. I used the geographical distribution of plant sexual expression system in Taiwan as an example to illustrate the extended application of our data. It would be an ideal demonstration for more ecological studies to be involved in. (Chapter 5)



LITERATURE CITED

- Beniston, M.** 2003. Climatic change in mountain regions: A review of possible impacts. *Climatic Change* **59**: 5–31.
- Chiu, C.-A., T.-Y. Chen, C.-C. Wang, C.-R. Chiou, Y.-J. Lai and C.-Y. Tsai.** 2013. Using BIOMOD2 to model the species distribution of *Fagus hayatae*. *Quarterly Journal of Forest Research* **35**: 253–272. [In Chinese with English summary.]
- Davis, M. B. and R. G. Shaw.** 2001. Range shifts and adaptive responses to quaternary climate change. *Science* **292**: 673–679.
- Hijmans, R. J., S. E. Cameron, J. L. Parra, P. G. Jones and A. Jarvis.** 2005. Very high resolution interpolated climate surface for global land areas. *International Journal of Climatology* **25(15)**: 1965–1978. <http://doi.org/10.1002/joc.1276>
- IPCC.** 2014. Summary for policymakers. In: *Climate Change 2014: Impacts, adaptation, and vulnerability. Part A: Global and sectoral aspects. Contribution of Working Group II to the Fifth Assessment Report of the Intergovernmental Panel on Climate Change.* Cambridge University Press, Cambridge, United Kingdom and New York, NY, USA, pp. 1–32.
- Lee, P.-F., K.-Y. Lue and S.-H. Wu.** 2006. Predictive distribution of Hynobiid salamanders in Taiwan. *Zoological Studies* **45**: 244–254.
- Lin, C.-T. and C.-A. Chiu.** 2019. The relic *Trochodendron aralioides* Siebold & Zucc. (Trochodendraceae) in Taiwan: Ensemble distribution modeling and climate change impacts. *Forests* **10(1)**: 7. <http://doi.org/10.3390/f10010007>
- Lin, W.-C., Y.-P. Lin, W.-Y. Lien, Y.-C. Wang, C.-T. Lin, C.-R. Chiou, J. Anthony and N. D. Crossman.** 2014. Expansion of protected areas under climate change: An example of mountainous tree species in Taiwan. *Forests* **2014(5)**: 2882–2904.
- Nakao, K., M. Higa, I. Tsuyama, C.-T. Lin, S.-T. Sun, J.-R. Lin, C.-R. Chiou, T.-Y. Chen, T. Matsui and N. Tanaka.** 2014. Changes in the potential habitats of 10 dominant evergreen broad-leaved tree species in the Taiwan-Japan archipelago. *Plant Ecology* **215**: 639–650.

- 
- Ovaskainen, O., S. Skorokhodova, M. Yakovleva, A. Sukhov, A. Kutenkov, N. Kutenkova, A. Shcherbakov, E. Meyke and M. M. Delgado.** 2013. Community-level phenological response to climate change. *PNAS* **110(33)**: 13434–13439.
- Su, H.-J.** 1984. Studies on the climate and vegetation types of the natural forests in Taiwan (II). Altitudinal vegetation zones in relation to temperature gradient. *Quarterly Journal of Chinese Forestry* **17(4)**: 57–73.
- Whittaker, R. H.** 1975. *Communities and ecosystems*. 2nd Revised Edition, MacMillan Publishing Co., New York.
- Weng, S.-P. and C.-T. Yang.** 2012. The construction of monthly rainfall and temperature dataset with 1km gridded resolution over Taiwan area (1960–2009) and its application to climate projection in the near future (2015–2039). *Atmospheric Sciences* **40(4)**: 349–369. [in Chinese with English summary]
- Woodward, F. I. and B. G. Williams.** 1987. Climate and plant-distribution at global and local scales. *Vegetatio* **69**: 189–197.
- Yen, S.-M., C.-R. Chiou and K.-T. Chang.** 2008. Modeling the species distribution of three dominant coniferous species in Taiwan. *Taiwan Journal of Forest Science* **23(2)**: 165–181.



Chapter 2

A dynamic downscaling approach to generate scale-free regional climate data in Taiwan



This chapter is a published paper in Taiwania 63(3): 251–266, 2018, co-authored by Huan-Yu Lin, Jer-Ming Hu, Tze-Ying Chen, Chang-Fu Hsieh, Guangyu Wang, and Tongli Wang.

Abstract

Plenty of climate data from various sources have become available in recent years. However, to obtain climate data adequately meeting the requirement of ecological studies remains a challenge in some cases due to the difficulty of data integration and the complexity of downscaling, especially for mountainous regions. Lapse rate is one of the most important factors that influence the change of climatic variables in the mountains, and it should be incorporated into climatic models. In this study, we applied a synthetic approach combining bilinear interpolation (to produce seamless surfaces) and dynamic local regression (to obtain local lapse rates) to develop a scale-free and topography-correspondent downscaling model in R environment for Taiwan, called *clim.regression*. This model can generate 73 climatic variable estimates specific to the user-defined points of interest, including primary climatic variables and additional biologically relevant derivatives for historical (1960–2009) and future periods (2016–2035, 2046–2065 and 2081–2100). Results of our evaluation indicated that *clim.regression* reduced prediction error by 54.6%–66.7% relative to the original gridded climate data for temperatures. In addition, we demonstrated the spatiotemporal patterns of lapse rate for different climate variables.

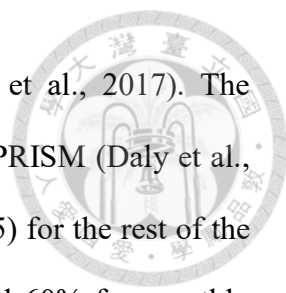
KEY WORDS: Climate change, Downscaling model, Dynamic local regression, Historical and future climate scenarios, TCCIP.



INTRODUCTION

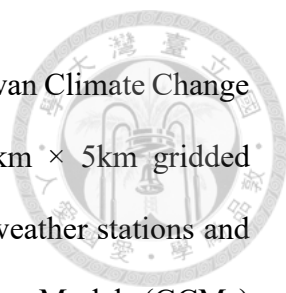
Climate variables, particularly temperature and precipitation, are the most well-known key factors related to vegetation zonation. A high-quality and accessible climate dataset is essential for ecological studies and applications, especially in regions with diverse topography and high climatic heterogeneity. However, to obtain and to process substantial climate data were difficult for ecologists in the past, and scientists often use statistically interpolated climate data from a few existing stations as substitutes for the continuous climate surface (Su, 1984a; Tang and Ohsawa, 1997).

Over the last decade, a large volume of climate data has become available through various sources; most of them were represented in grid format with the finest resolution of arc-seconds or kilometers in global or regional scale (Hannaway et al., 2005; Hijmans et al., 2005; Harris et al., 2014). Although such gridded data are suitable for modeling general patterns and trends at global and regional scales, they are still too coarse to provide detailed climatic information in mountainous and topographically diverse areas to facilitate local ecological studies and resources management. To overcome this limitation, several downscaling methods have been developed to generate high-resolution spatial climate data, such as Ordinary Kriging (Chiu and Lin, 2004), a combination of Kriging and polynomial linear regression (Chiou et al., 2004), a combination of bilinear interpolation and partial derivative functions for elevational adjustment (Wang et al., 2006; 2012), and an approach of dynamic local regression (Wang et al., 2016; 2017). ClimateAP, a scale-free climate downscaling model based on dynamic local regression approach, was



recently developed and covered Asia-Pacific (AP) region (Wang et al., 2017). The baseline data of this model used a 4-km gridded climate data from PRISM (Daly et al., 2002) for China and Mongolia, and WorldClim (Hijmans et al., 2005) for the rest of the Asia-Pacific. The model reduces prediction error by up to 27% and 60% for monthly temperature and precipitation, respectively, relative to the original baseline data. However, the prediction accuracy for a specific region varies depending on the quality of the baseline data, which is affected by the density of weather stations used for developing the baseline data for the region. Unfortunately, historical climate data from weather stations in Taiwan were not included in the climate mapping project of PRISM (Hannaway et al., 2005). Thus, it could adversely impact the prediction accuracy of ClimateAP in Taiwan.

Taiwan is a subtropical island on the west edge of the Pacific Ocean with diverse and complicated topography. The climate of Taiwan is mainly affected by the northeast monsoon during winter and by the southwest monsoon and typhoons in the summer. The Central Range occupying more than 70% of the area of Taiwan, runs through the whole island from northeast to southwest with the highest peak of 3,952 meters asl, and creates an obvious altitudinal temperature zonation (Su, 1984a), as well as the seasonal allocation of precipitation (Su, 1985). Many studies have revealed a strong relationship between the natural vegetation and the large-scale altitudinal climate zonation (Su, 1984b; Chiu, 2004; Chiou et al., 2010; Lin et al., 2012; Li et al., 2013). Furthermore, the local climate is induced by the co-effects of monsoon and topography (Sun, 1993; Sun et al., 1998; Chao et al., 2007; Chao et al., 2010; Li et al., 2013). Ecologists have a strong demand on fine-scale climate data to depict the ecological and environmental correlations in detail. However, most studies can only utilize indirect variables such as elevation and topography as substitutes to climatic variables due to the lack of a high-quality and high-resolution spatial climate dataset for the island.



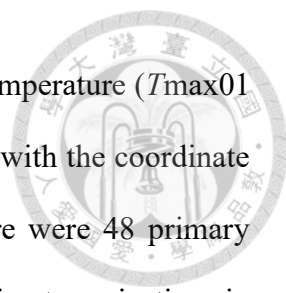
Meteorologists in Taiwan have accomplished a framework called Taiwan Climate Change Projection and Information Platform (TCCIP) and generated a $5\text{km} \times 5\text{km}$ gridded climate surface based on historical observations from thousands of weather stations and provided future projections based on different AR5 General Circulation Models (GCMs) and scenarios (Hsu et al., 2011; Weng and Yang, 2012). TCCIP's datasets are powerful supplements to the remote and observation-sparse mountains, but its resolution is not fine enough to represent the diverse climate situation due to the steep topography within a $5\text{km} \times 5\text{km}$ grid.

In this study, our main objectives were to: (1) establish a statistical downscaling model named as *clim.regression* in R environment to downscale the $5\text{km} \times 5\text{km}$ gridded climate data of TCCIP to a scale-free format based on the algorithm of bilinear interpolation and dynamic local regression from ClimateNA (Wang et al., 2016) and ClimateAP (Wang et al., 2017); (2) generate additional biologically relevant derivatives for ecological studies; (3) analyze the spatiotemporal patterns of variation in lapse rate; and (4) evaluate the prediction accuracy of *clim.regression* in comparison to the original TCCIP data.

MATERIALS AND METHODS

Source of historical and future climate data

The $5\text{km} \times 5\text{km}$ gridded surfaces of historical meteorological data used in this study were developed by TCCIP (Weng and Yang, 2012). The dataset covers the main island of Taiwan and spans the period from 1960 to 2009. TCCIP incorporated historical records of air temperature from 1,152 weather stations and precipitation from 1,497 rainfall stations to construct the gridded dataset through a conventional spatial interpolation process. There are four sets of primary climate variables including monthly precipitation (precip01 to precip12), monthly minimum temperature (*T*_{min01} to *T*_{min12}), monthly



mean temperature (T_{mean01} to T_{mean12}) and monthly maximum temperature (T_{max01} to T_{max12}). The values of these variables were obtained and united with the coordinate (latitude, longitude and elevation) of the center of each grid. There were 48 primary monthly climate variables in total. TCCIP has also provided future climate projections in the same resolution of $5\text{km} \times 5\text{km}$, which were downscaled from GCMs of CMIP5 and rectified by observations of Aphrodite (Asia Precipitation Highly-Resolved Observational Data Integration Towards Evaluation of the Water Resources) and historical climate data of Taiwan (Lin et al., 2016). Projections of 49 GCMs (Table 2.1) covering different RCPs (RCP 2.5, RCP 4.6, RCP 6.0 and RCP 8.5) and periods (2016–2035, 2046–2065, 2081–2100).

The downscaling process of historical and future climate data

To obtain smooth and continuous climate surface estimates, *clim.regression* utilized the combination of bilinear interpolation and dynamic local regression approach to downscale the original $5\text{km} \times 5\text{km}$ gridded climate dataset to scale-free point estimates, which is the same as in ClimateNA (Wang et al., 2016) and ClimateAP (Wang et al., 2017). The downscaling process included four steps for each of the 48 primary monthly climate variables as illustrated in Fig. 2.1:

- (1). Extraction of a primary climate variable and elevation from the grid covering the point of interest and eight neighboring grids (Fig. 2.1A);
- (2). Calculation of the bilinear interpolated estimate of the primary monthly climate variable (t'_p) and elevation (Z'_p) of the location of interest from the nearest four grids (Fig. 2.1B, Formula 1 & 2);
- (3). Calculation of the differences in the primary monthly climate variable (Δt) and in



elevation (Δz) between each of the 36 unique pairs among the nine neighbor grids (Fig. 2.1C, Formula 3);

- (4). Construction of a simple linear regression based on the 36 pairs to represent the local relationship between Δt and Δz with the slope of the regression line, m , representing the local lapse rate of the cell where the interest point is located. Elevation adjustment was based on the lapse rate (m) and the difference between actual elevation (Z_p) and the bilinear interpolate (Z'_p) of the interest point (Fig. 2.1D, Formula 4).

Table 2.1. All the 49 GCMs and emission scenarios provided by TCCIP available for *clim.regression*.

GCM	RCP 2.6	RCP 4.5	RCP 6.0	RCP 8.5	GCM	RCP 2.6	RCP 4.5	RCP 6.0	RCP 8.5
10th-percentile	V	V	V	V	GFDL-ESM2M		V	V	V
25th-percentile	V	V	V	V	GISS-E2-H	V	V	V	V
75th-percentile	V	V	V	V	GISS-E2-H-CC		V		V
90th-percentile	V	V	V	V	GISS-E2-R	V	V	V	V
ACCESS1-0		V		V	GISS-E2-R-CC		V		V
ACCESS1-3		V		V	HadGEM2-AO	V	V	V	V
bcc-csm1-1	V	V	V	V	HadGEM2-CC		V		V
bcc-csm1-1-m	V	V	V	V	HadGEM2-ES	V	V	V	V
BNU-ESM	V	V		V	inmcm4		V		V
CanESM2	V	V		V	IPSL-CM5A-LR	V	V	V	V
CCSM4	V	V	V	V	IPSL-CM5A-MR	V	V	V	V
CESM1-BGC		V		V	IPSL-CM5B-LR		V		V
CESM1-CAM5	V	V	V	V	maximum	V	V	V	V
CESM1-CAM5-1-FV2		V		V	media	V	V	V	V
CMCC-CESM				V	minimum	V	V	V	V
CMCC-CM		V		V	MIROC5	V	V	V	V
CMCC-CMS		V		V	MIROC-ESM	V	V	V	V
CNRM-CM5	V	V		V	MIROC-ESM-CHEM	V	V	V	V
CSIRO-Mk3-6-0	V	V	V	V	MPI-ESM-LR	V	V		V
EC-EARTH				V	MPI-ESM-MR	V	V		V
ensemble	V	V	V	V	MRI-CGCM3	V	V	V	V
FGOALS-g2	V	V		V	MRI-ESM1				V
FIO-ESM	V	V	V	V	NorESM1-M	V	V	V	V
GFDL-CM3	V	V	V	V	NorESM1-ME	V	V	V	V
GFDL-ESM2G	V	V	V	V					

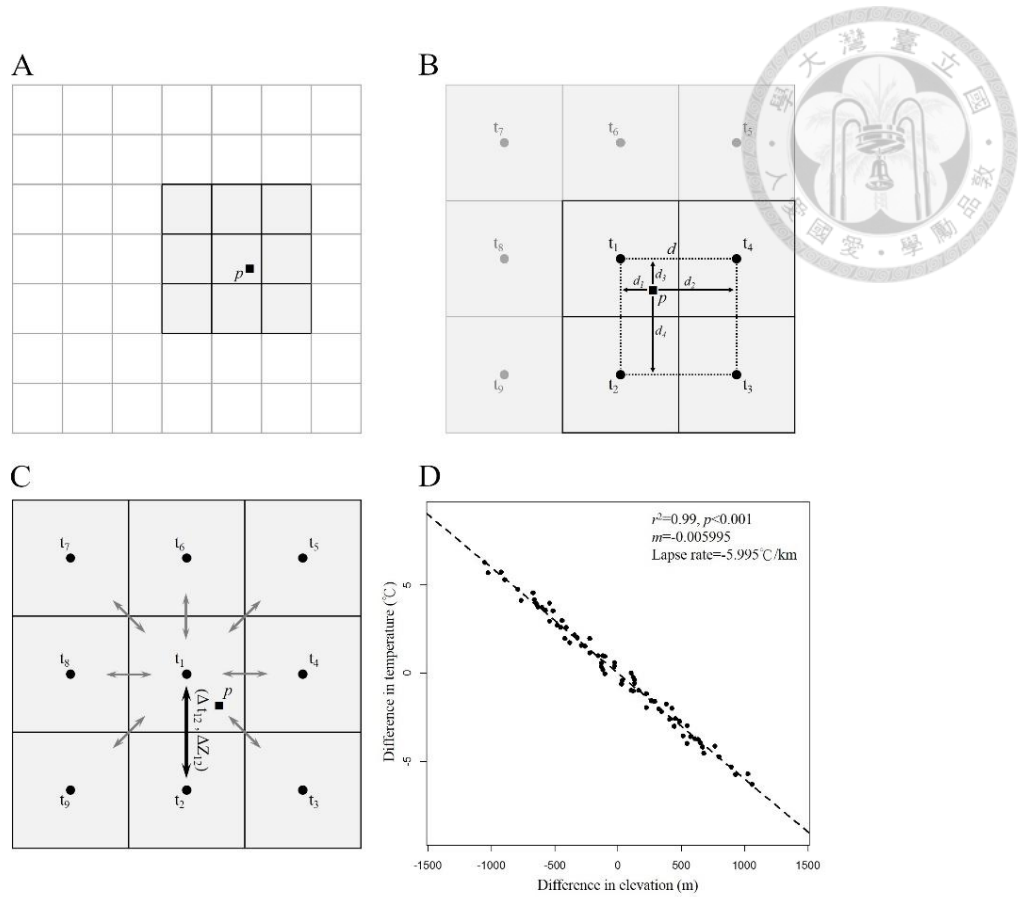
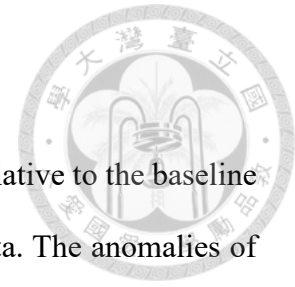


Fig. 2.1. Four steps of the downscaling process. (A) The grid tiles covering the point of interest p and its eight neighbors were extracted from the original climate dataset. (B) Bilinear interpolated estimates of temperature, precipitation and elevation of the point p were calculated by the weighting of distance to the center of the four nearest grid tiles. (C) A total of 36 unique pairs were subset to calculate the paired differences for temperature, precipitation (Δt) and elevation (Δz), respectively. (D) A simple linear regression of $\Delta t_{mn} \sim \Delta Z_{mn}$ was conducted to obtain the slope m , representing the local lapse rate of the nine grids surround point of interest for each of the climate variables.

Clim.regression generated 73 climate variable estimates (Table 2.2) for either a single point location or a continuous surface. These climate variables were either directly calculated from the four primary climate variables or derived as indicated in Table 2.2.

The formula for the downscaling process included:

- (1)
$$t'_p = \frac{t_1 d_2 d_4 + t_2 d_2 d_3 + t_3 d_1 d_3 + t_4 d_1 d_4}{d^2}$$
- (2)
$$Z'_p = \frac{Z_1 d_2 d_4 + Z_2 d_2 d_3 + Z_3 d_1 d_3 + Z_4 d_1 d_4}{d^2}$$
- (3) $\Delta t_{mn} \sim \Delta Z_{mn}, m = \{1, 2, 3, \dots, 9\}, n = \{1, 2, 3, \dots, 9\}, m \neq n$
- (4) $t_p = t'_p + m |Z_p - Z'_p|$



Future climate projections of TCCIP were presented as anomalies relative to the baseline of 1986–2005 at the same spatial resolution of historical climate data. The anomalies of 5km × 5km gridded future climate projections were added to the baseline portion (1986–2005) to create a ‘gridded future climate data’ prior to the downscaling procedure.

Table 2.2. Primary climate variables and the biologically relevant derivatives generated by *clin_regression*

(1) Primary climate variable estimates.

Category	Climate variables	
Precipitation		Monthly precipitation (precip01 to precip12)
		Seasonal precipitation (PPT_DJF, PPT_MAM, PPT_JJA, PPT_SON)
		Mean annual precipitation (MAP)
		Mean annual summer precipitation (MSP)
Temperature	Minimum	Mean monthly minimum temperature (T_{min01} to T_{min12})
		Mean seasonal minimum temperature (T_{min_DJF} , T_{min_MAM} , T_{min_JJA} , T_{min_SON})
	Average	Mean monthly temperature (T_{mean01} to T_{mean12})
		Mean seasonal temperature (T_{ave_DJF} , T_{ave_MAM} , T_{ave_JJA} , T_{ave_SON})
		Mean annual temperature (MAT)
	Maximum	Mean monthly maximum temperature (T_{max01} to T_{max12})
Mean seasonal maximum temperature (T_{max_DJF} , T_{max_MAM} , T_{max_JJA} , T_{max_SON})		

(2) Derivative estimates.

Derivative variable	Definition
Temperature difference (TD)	T_{mean07} minus T_{mean01}
Summer heat:moisture index (SHM)	$(T_{mean07})/(MSP/1000)$
Annual heat:moisture index (AHM)	$(MAT+10)/(MAP/1000)$
Ratio of winter precipitation (WPR)	PPT_DJF/MAP (Li et al., 2013)
Warmth index (WI)	Annual summation of mean monthly temperature higher than 5°C. (Su, 1984b)
Precipitation deficiency (PD)	Difference between annual potential evapotranspiration and MAP. (Su, 1985)
Dry month (DM)	The month with rainfall less than 2X mean monthly temperature. DM is a factor variable in 0/1. (Su, 1985)



Evaluations of climate variable estimates

We collected historical records covering the period of 1961 to 2009 from 15 weather stations to evaluate the accuracies of *clim.regression* model. Ten of the 15 stations are subordinate to the Central Weather Bureau (CWB), which is the main corporation agency of TCCIP. The remaining five stations belong to the Taiwan Forestry Research Institute (TFRI), which is independent of the samples of TCCIP network. The observations from the 15 weather stations were also used to evaluate the magnitude of improvement over the original TCCIP gridded surfaces. Four sets of climate variable estimates generated by *clim.regression*, including monthly precipitation, monthly minimum temperature, monthly mean temperature and monthly maximum temperature, were evaluated against observations from the 15 weather stations (Table 2.3, Fig. 2.2). Prediction errors of *clim.regression* were assessed and compared using the following three statistical measures:

$$\text{Mean error (ME): } \frac{1}{n} \sum (y_i - f_i)$$

where n is the number of samples, f_i is the predicted value of the i -th sample and y_i its real value.

$$\text{Mean absolute error (MAE): } \frac{1}{n} \sum |y_i - f_i|$$

$$\text{Root mean squared error (RMSE): } \sqrt{\frac{1}{n} \sum (y_i - f_i)^2}$$

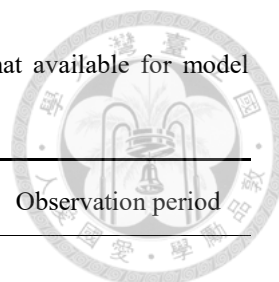


Table 2.3. Localities of 15 weather stations and the period of observed data that available for model evaluation.

Subordination/ Station	Longitude	Latitude	Altitude (m)	Observation period
Central Weather Bureau (CWB) Incorporated by TCCIP				
Kaohsiung	120.32	22.57	2	1961–2009
Taitung	121.15	22.75	9	
Hualien	121.61	23.98	16	
Hengchun	120.75	22.00	22	
Keelung	121.74	25.13	27	
Taichung	120.68	24.15	84	
Anbu	121.53	25.18	826	
Sunmoon Lake	120.91	23.88	1,018	
Alishan	120.81	23.51	2,413	
Yushan	120.96	23.49	3,845	
Taiwan Forestry Research Institute (TFRI) independent from TCCIP				
Taimali	120.98	22.60	120	1980–2009
Liukuei	120.63	23.00	230	1999–2009
Fushan	121.60	24.76	634	1992–2003
Lienhuachih	120.90	23.93	666	1999–2009
Piluhsi	121.31	24.23	2,150	1991–2009

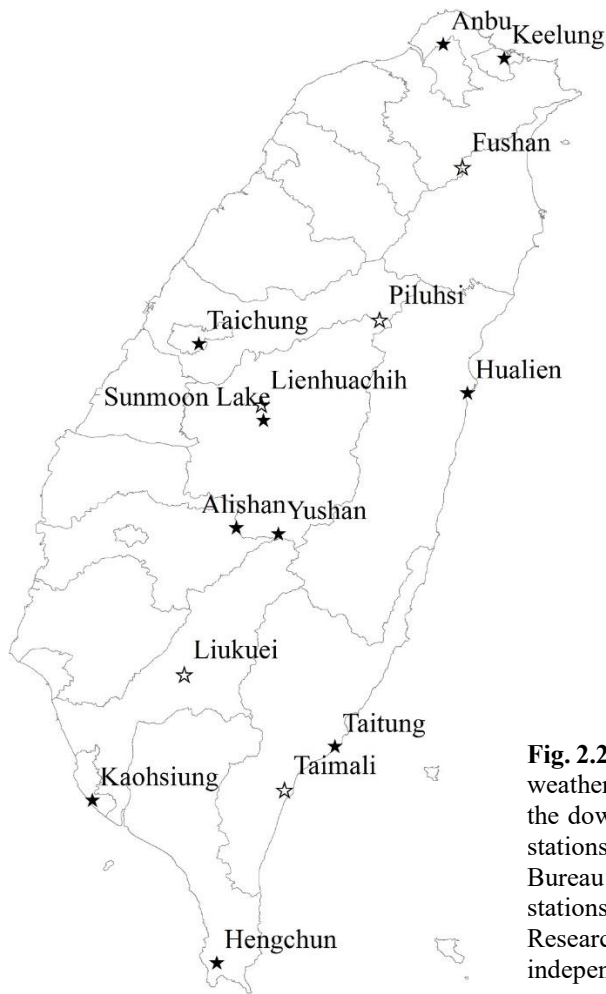


Fig. 2.2. Long-term observation data from fifteen weather stations were incorporated to evaluate the downscaling model. Solid stars demonstrate stations subordinate to the Central Weather Bureau of Taiwan (CWB). Open stars represent stations belonging to the Taiwan Forestry Research Institute (TFRI), which were independent from TCCIP system.

RESULTS

Scale-free climate surfaces from the downscaling model

Clim.regression is a scale-free and topography-correspondent downscaling model, which attributes to the continuous and smooth characteristics of bilinear interpolation and the elevational adjustment by lapse rate from a dynamic local regression. Regular grids for MAT (mean annual temperature) and MAP (mean annual precipitation) surfaces were generated by the model at the spatial resolution of the original baseline data ($5\text{km} \times 5\text{km}$) and a downscaled spatial resolution ($250\text{m} \times 250\text{m}$) (Fig. 2.3). The results showed that MAT in Taiwan ranges from 1°C to 28°C and exhibits a trend of decline from lowland to

alpine and from south to north. A more detailed spatial distribution of temperature due to geographical effect, such as warm basin of Puli and cool tablelands of Linkou and Pagua, could also be revealed by the downscaled surface (Fig. 2.3A–B). The spatial distribution of MAP demonstrated a different pattern from that of MAT; it exhibited two-ended humid regions in the northeast and the southwest of Taiwan. The northeastern mountains in Taipei and Ilan and the southwestern edge of the Central Mountain Range in Kaohsiung and Pingtung are the moistest regions of Taiwan, and the downscaled surface more clearly revealed some precipitation hotspots with annual rainfall up to 6,000mm (Fig. 2.3C–D).

In comparison with the original climate dataset at the resolution of 5km × 5km, the downscaled one offers a detail depiction on the climatic alternation with topographies as the examples showed in Fig. 2.3. The scale-free modeling approach not only has the advantage in providing continuous and seamless climatic surface for large-scale studies (e.g., the classification of ecological-climatic regions, climatic niche modeling, and projections, etc.), but also generates accurate and point-specific climatic estimates as environmental correlates for plot-based researches (e.g., vegetation survey and plotting, etc.).

Table 2.4. The r-squared values of the local linear regressions for different monthly climate variables.

Monthly variable	r ² value / Month												
	1	2	3	4	5	6	7	8	9	10	11	12	Average
<i>T</i> mean	0.82	0.82	0.81	0.84	0.86	0.87	0.88	0.88	0.88	0.87	0.86	0.84	0.85
<i>T</i> min	0.79	0.80	0.81	0.83	0.85	0.85	0.85	0.85	0.86	0.84	0.83	0.80	0.83
<i>T</i> max	0.79	0.79	0.78	0.81	0.84	0.85	0.85	0.86	0.85	0.82	0.81	0.79	0.82
Precipitation	0.20	0.21	0.24	0.23	0.25	0.26	0.23	0.25	0.22	0.21	0.22	0.22	0.23

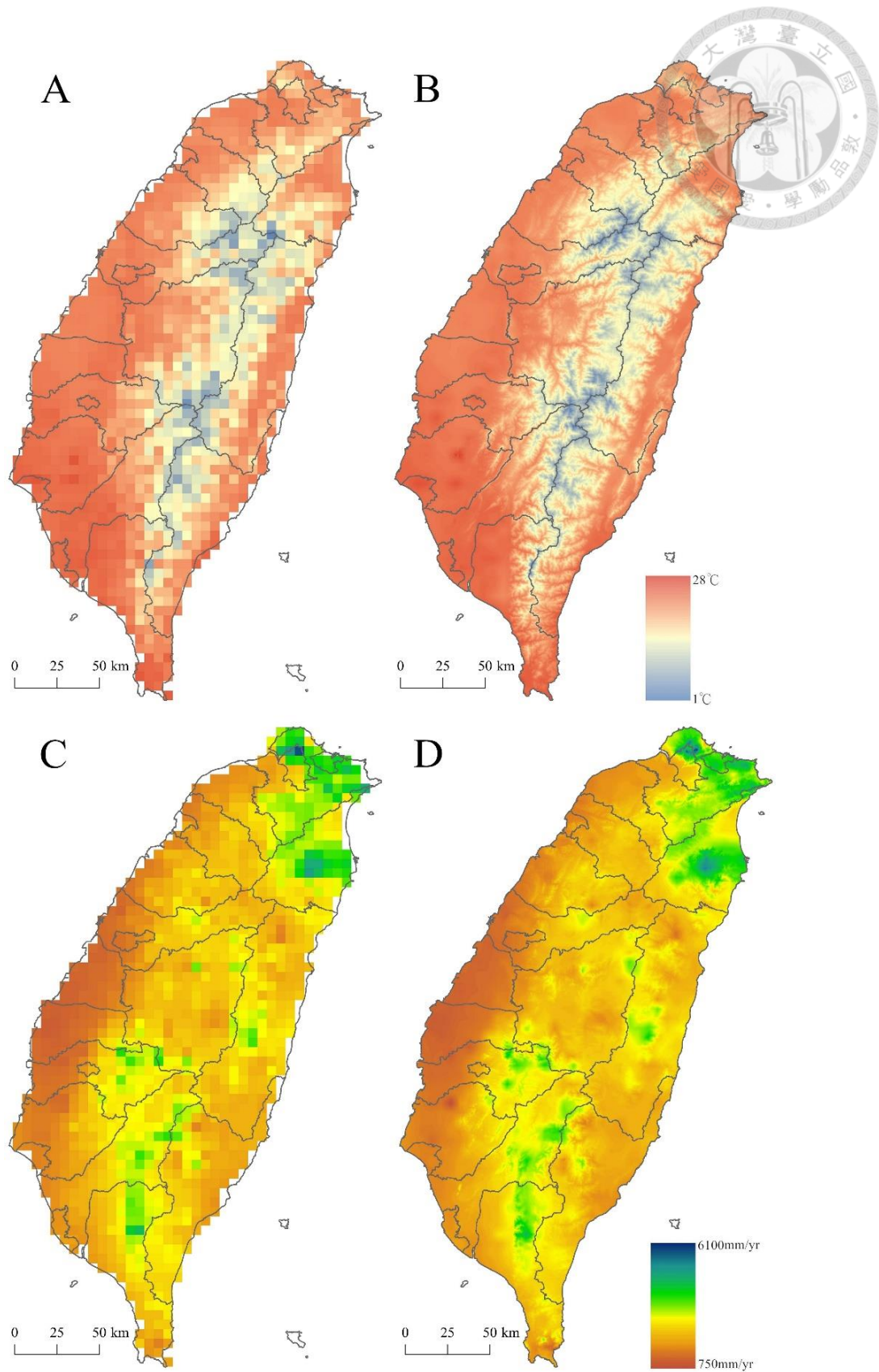
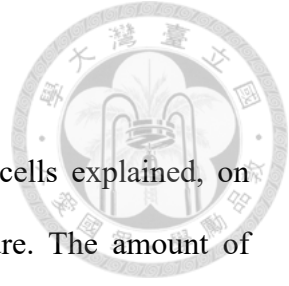


Fig. 2.3. Spatial distributions of mean annual temperature (MAT) and mean annual precipitation (MAP) for original climate data at the resolution of 5km and downscaled to the resolution of 250m. (A) Original and (B) downscaled MAT; (C) Original and (D) downscaled MAP. Data period: 1986–2005.



Lapse rate and effectiveness of the elevational adjustment

The dynamic local linear regression among the nine neighboring cells explained, on average, 85.3% of the total variation in monthly mean temperature. The amount of variance explained for monthly minimum temperature (83.1%) and monthly maximum temperature (81.9%) were slightly lower (Table 2.4). The average temperature lapse rate in the mountain areas was $-5.65^{\circ}\text{C}/\text{km}$ but displayed an obvious seasonal variation. Fig. 2.4A–C illustrate the same pattern in three primary temperature variables with a higher variation of lapse rate in winter (from Nov. to Apr.) than in summer (from May to Sep.). The relationships revealed in the local regressions were weaker for precipitation than for temperatures. Only 20.3–25.7% of precipitation’s variation can be explained by the local regressions (Fig. 2.4D, Table 2.4).

We compared the relationships between the changes in temperature and the elevation between two mountains, Alishan and Taipingshan. Such a relationship was stronger for Alishan with a steady lapse rate from -6.00 to $-6.44^{\circ}\text{C}/\text{km}$ from winter to summer. In contrast, a higher seasonal variation and a weaker relationship between temperature and elevation were observed in Taipingshan (Fig. 2.5).

The spatial distributions of the estimated lapse rates varied among seasons and regions. In winter, lower lapse rates for monthly average temperature (from -2 to $-5^{\circ}\text{C}/\text{km}$) were exhibited in the central and western parts of the Central Mountain Range, especially in the hills from Hsinchu, Miaoli, Nantou, Chiayi to Kaohsiung. In contrast, very steep lapse rates (from -6 to $-9^{\circ}\text{C}/\text{km}$) were demonstrated in the northeastern mountains and Hengchun peninsula (Fig. 2.6A). The spatial differentiation in lapse rate in most areas mitigated in summer, and demonstrated a mild geographical divergence with a range from -4 to $-7^{\circ}\text{C}/\text{km}$ (Fig. 2.6C). In some regions, such as the northeastern mountains in Taipei

and Ilan, Hengchun peninsula, Tawu Mountain and the Costal Mountain Range, the steep lapse rates ($< -6^{\circ}\text{C}/\text{km}$) could be found across all seasons of the year. Our dynamic local regression approach revealed the variation in the lapse rate both spatially and temporally over the island, and thus produced accurate adjustment for elevation.



Table 2.5. Summaries of statistical evaluations of *clim.regression* against historical observed data from Central Weather Bureau (CWB) and Taiwan Forestry Research Institute (TFRI).

Subordination	Climate variable	<i>Clim.regression</i>			TCCIP		
		MAE	RMSE	Variance explained (%)	MAE	RMSE	Variance explained (%)
CWB (10 stations)	T_{mean} ($^{\circ}\text{C}$)	0.56	0.73	99.10	1.73	3.40	87.83
	T_{min} ($^{\circ}\text{C}$)	0.79	0.98	98.72	1.92	3.51	87.04
	T_{max} ($^{\circ}\text{C}$)	0.71	1.00	98.22	1.67	3.25	88.29
	Precipitation (mm)	34.65	64.63	94.39	31.10	67.08	93.75
TFRI (5 stations)	T_{mean} ($^{\circ}\text{C}$)	0.58	0.74	98.56	1.34	1.56	96.75
	T_{min} ($^{\circ}\text{C}$)	0.82	1.17	97.27	1.24	1.49	96.51
	T_{max} ($^{\circ}\text{C}$)	1.52	1.85	95.61	2.53	2.78	92.27
	Precipitation (mm)	49.56	105.39	79.77	46.39	106.14	79.62
Average (15 stations)	T_{mean} ($^{\circ}\text{C}$)	0.56	0.73	99.06	1.68	3.25	86.71
	T_{min} ($^{\circ}\text{C}$)	0.79	1.00	98.52	1.85	3.35	86.61
	T_{max} ($^{\circ}\text{C}$)	0.80	1.13	97.61	1.76	3.21	84.76
	Precipitation (mm)	36.26	70.16	93.00	32.74	72.30	92.43

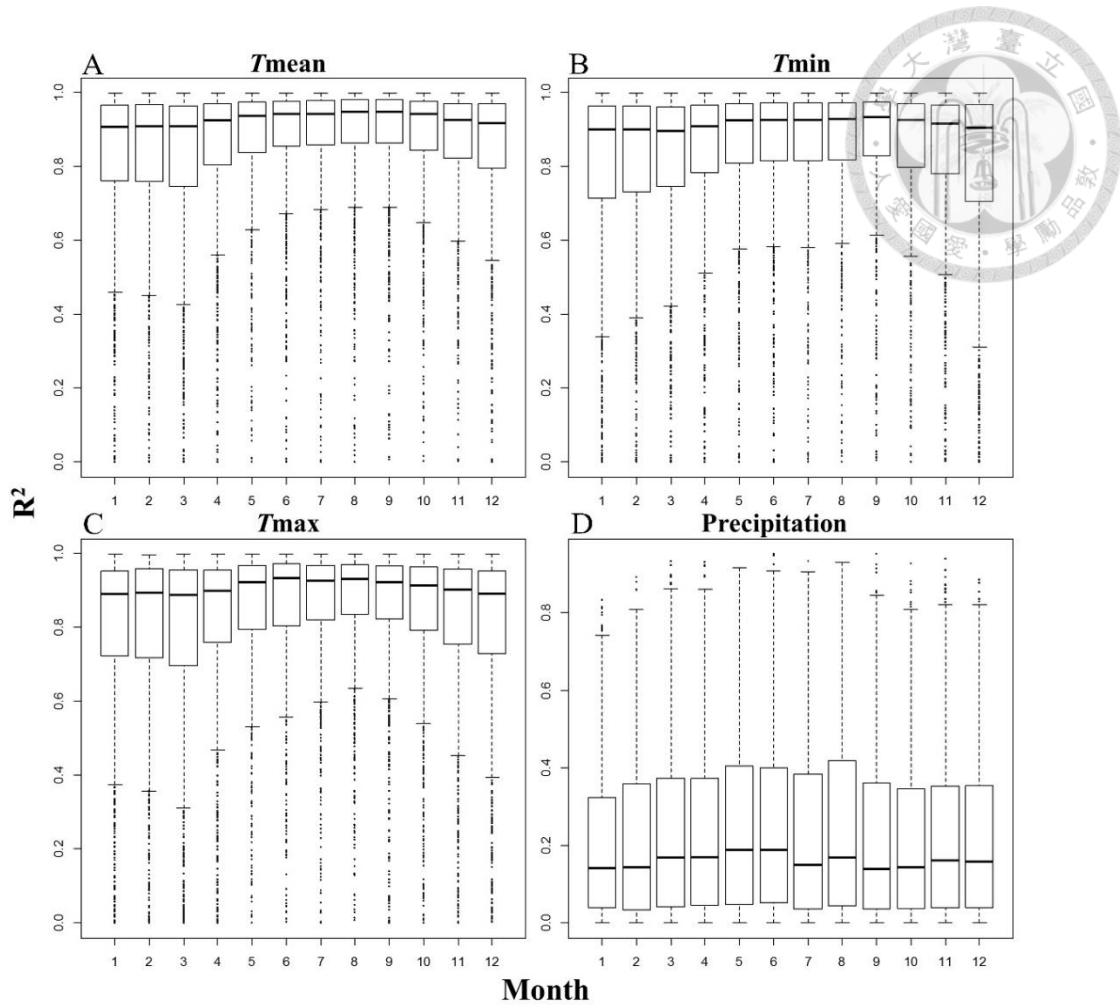


Fig. 2.4. Proportions of variance explained by local linear regressions in total variation among the nine neighboring cells for the four primary climate variables: (A) monthly mean temperature (T_{mean}), (B) monthly minimum temperature (T_{min}), (C) monthly maximum temperature (T_{max}) and (D) monthly precipitation, by month. The black horizontal solid lines inside the boxes indicate the median. For temperature variables, a similar trend of higher variation in winter and lower variation in summer can be observed. Data period: 1961–2009.

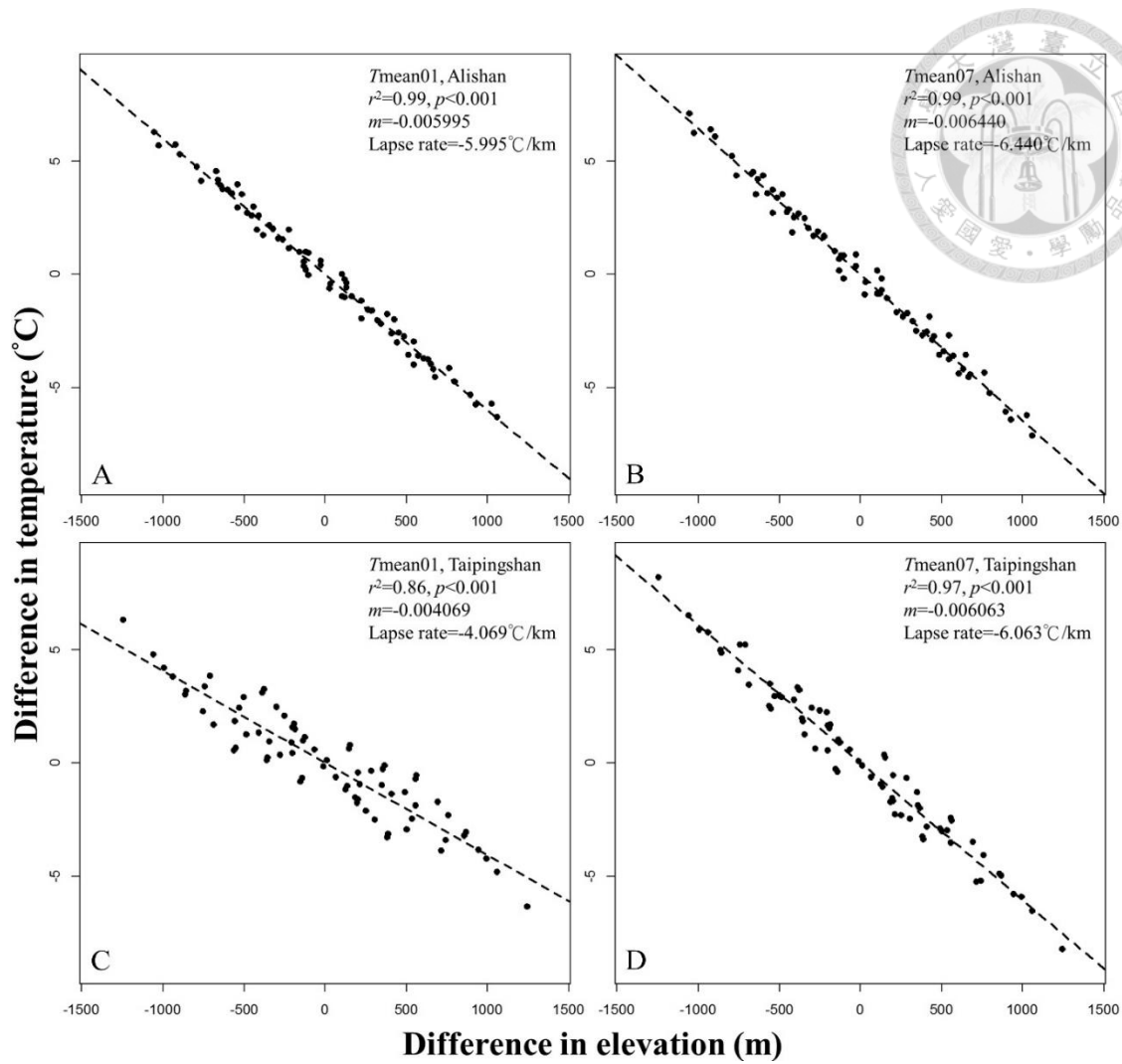


Fig. 2.5. Comparisons in lapse rates for winter and summer between two mountains, Alishan (A, B) and Taipingshan (C, D). Alishan (120.81E, 23.51N) is a mountain located in the south-west Taiwan, while Taipingshan (121.53E, 24.49N) is located in the north-east part. The two mountains have a similar elevation around 2,000m. Data period: 1961–2009.

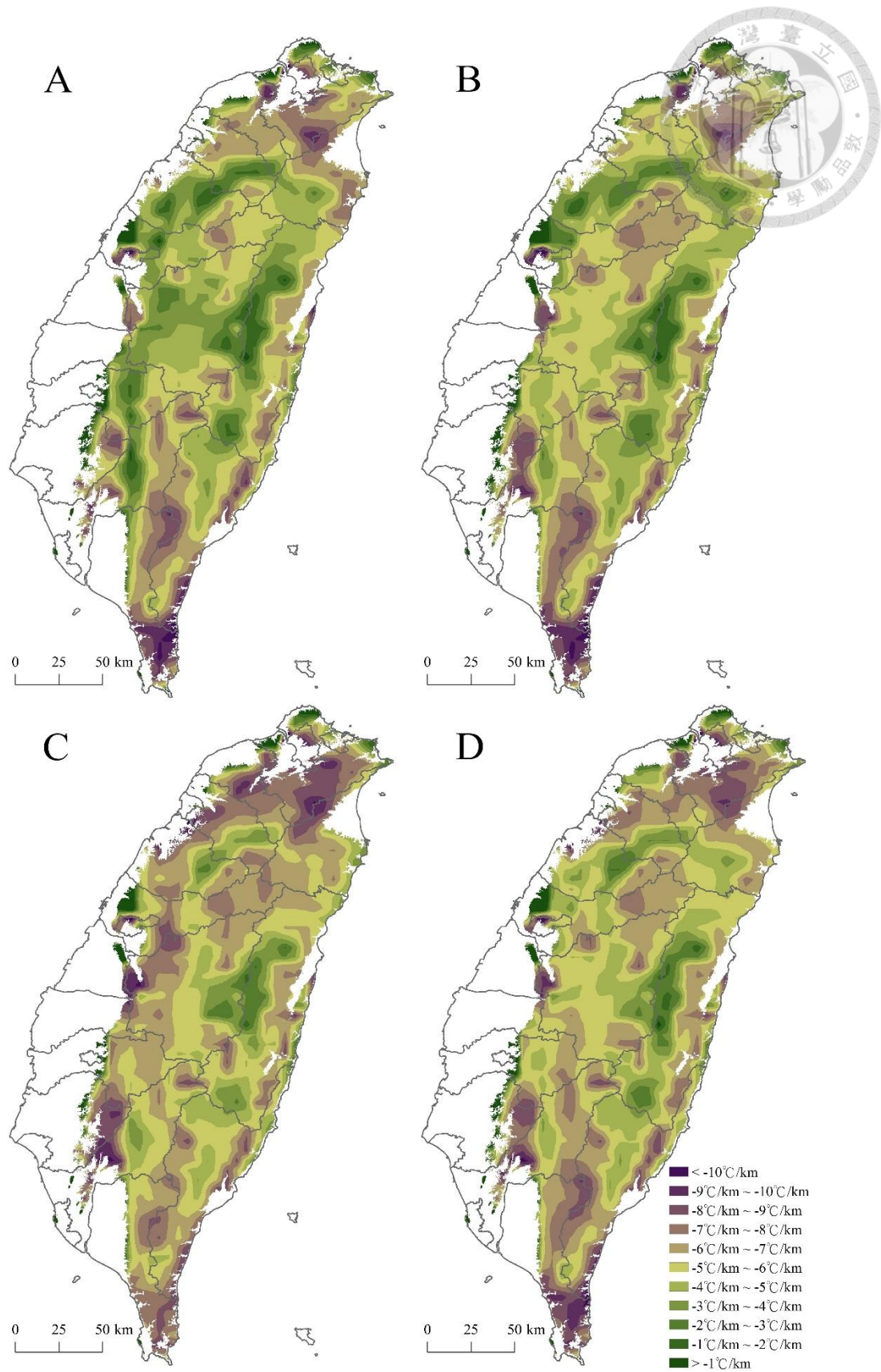


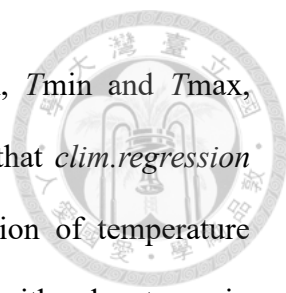
Fig. 2.6. Spatial distributions of estimated lapse rate for monthly mean temperature in the mountain areas (regions higher than 100m asl) in Taiwan: (A) January, (B) April, (C) July and (D) October. Data period: 1961–2009; resolution: 250m.

Statistical evaluations of the downscaling model and its improvement over TCCIP dataset

The prediction accuracy of *clim.regression* was evaluated by comparing to historical observations from the 15 weather stations (Table 2.5). *Clim.regression* demonstrated a high prediction accuracy for monthly mean temperature with a low prediction error (0.56°C in MAE) and a high percent of variance explained (99.1%). The prediction accuracy and variance explanation were slightly lower for monthly minimum temperature and monthly maximum temperature in terms of the prediction error (0.79°C and 0.80°C) and the percent of variance explained (98.5% and 97.6%, respectively). However, the prediction accuracy was considerably lower for precipitation. The precipitation estimates explained 93.0% of the total variance of observations with a prediction error of 36.26mm in MAE.

Monthly mean temperature was the most predictable climate variable. The prediction accuracy of monthly mean temperature in regions lower than 2,500m asl could reach the level of 0.3–0.6°C in MAE. However, we found that the prediction error increased with elevation ($r^2=0.55$, $p=0.0015$). For example, in the subalpine area of Taiwan, *clim.regression* had a comparatively weak predict ability with the MAE of 1.02°C. Interestingly, such a relationship was not observed for monthly minimum temperature and monthly maximum temperature ($r^2=0.07$ and 0.35 , $p=0.3252$ and 0.0209). The prediction accuracy for precipitation was lower and accompanied with a higher variation and a less amount of variance explained (92.1%). In addition, there was no obvious trend found between prediction error in precipitation and altitude ($r^2=0.01$, $p=0.7612$). It suggests that the pattern of precipitation could be dominantly influenced by regional terrains rather than a local elevational gradient within the 5km × 5km grids.

In comparisons to TCCIP original dataset, *clim.regression* reduced prediction errors by



1.12°C (66.7%), 1.06°C (52.3%) and 0.96°C (54.6%) for T_{mean} , T_{min} and T_{max} , respectively (Fig. 2.7A–C, Table 2.5). These results demonstrated that *clim.regression* effectively improved the accuracy and refined the spatial resolution of temperature estimates relative to the original dataset from TCCIP, especially with advantages in temperature projection for mountains with diverse topography. However, the improvement in precipitation is limited (Fig. 2.7D). Both TCCIP baseline and *clim.regression* had a higher prediction error for precipitation during summer months (May to Oct.). As illustrated in Fig. 2.8, the magnitude of the improvement was more substantial at higher elevations (the lower end of the temperatures), especially in the alpine area of Yushan (3,952 m) and Alishan (2,413 m). The downscaled temperatures followed a 1:1 relationship with observations much closer than the TCCIP predictions.

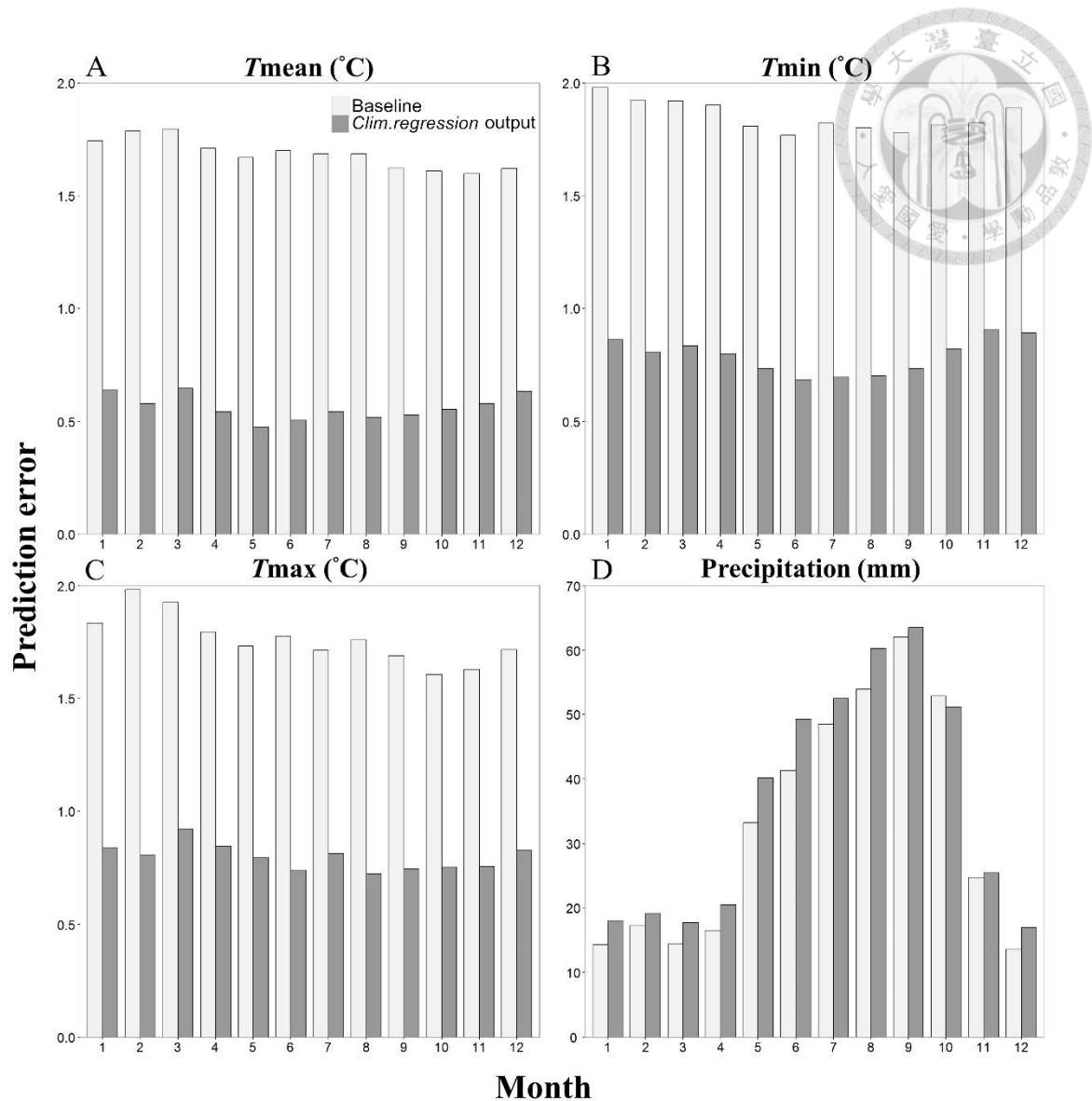


Fig. 2.7. Comparison in prediction error between baseline data (directly from TCCIP) and *Clim. regression* output of 15 weather stations for: (A) monthly mean temperature (T_{mean}), (B) monthly minimum temperature (T_{min}), (C) monthly maximum temperature (T_{max}) and (D) monthly precipitation.

Downscaling for future climate projections

Based on the estimated lapse rate of future scenarios, *clim. regression* was also effective to downscale the ‘gridded future climate data’ to a scale-free and continuous surface with the same 73 climate variables as for the historical period. Downscaled MAT by *clim. regression* for the reference period and future scenario in the mountainous area of Taiwan were illustrated in Fig. 2.9. The benefit of the downscaled MAT is clearly shown

in this example in term of fine spatial resolution and high topographical correspondence. Based on the comparison among current and future climate under the RCP 4.5 scenario, not only an evident warming can be found in the valleys and plains but also demonstrate an obvious retreat of isothermals to the subalpine area (Fig. 2.9). *Clim.regression* has a solid advantage in generating current and future climate data with the same and desirable spatial resolution, which is a convenient for modeling biological response to climate change and for advanced comparative studies.

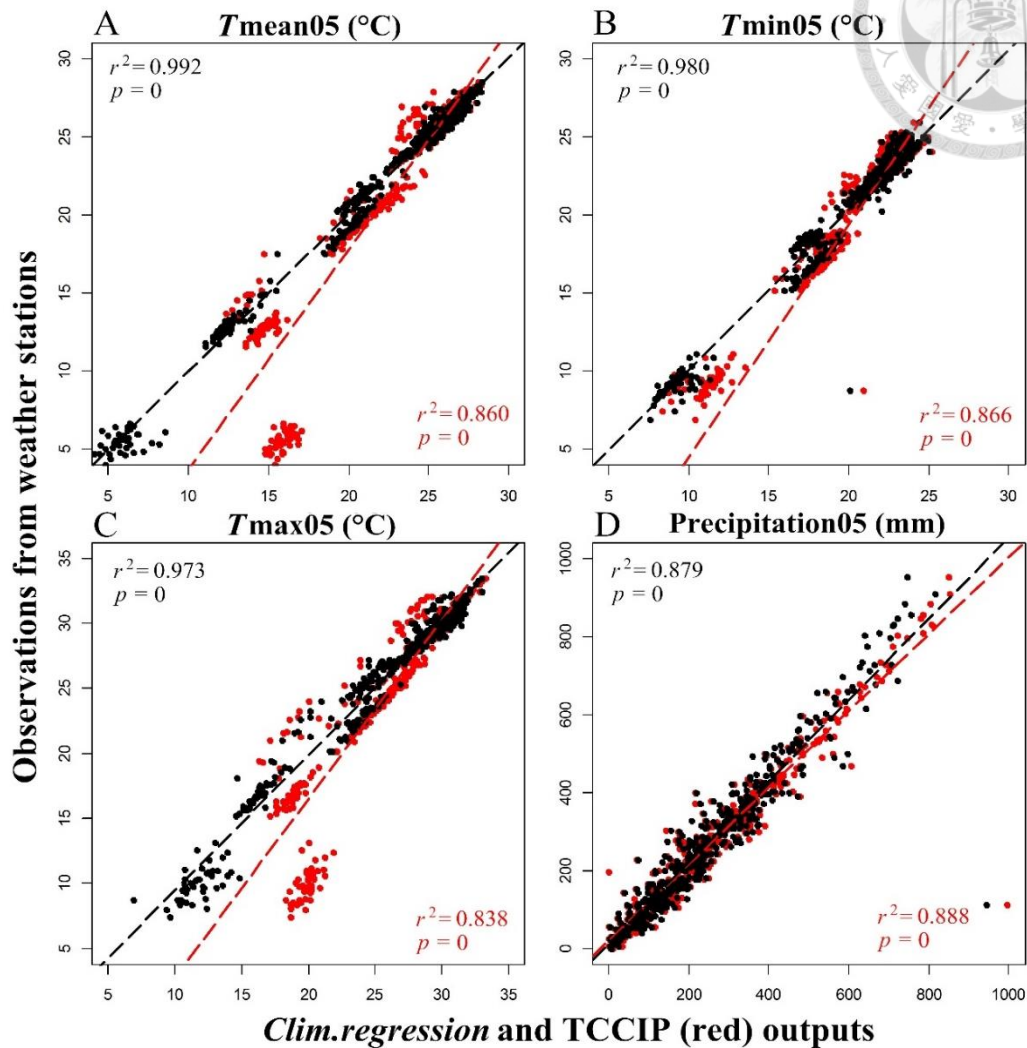


Fig. 2.8. An illustration to demonstrate the difference between observations from 15 weather stations and its corresponding climatic estimates from TCCIP outputs (red) and *clim.resgression* in May for (A) monthly mean temperature (*Tmean05*), (B) monthly minimum temperature (*Tmin05*), (C) monthly maximum temperature (*Tmax05*) and (D) monthly precipitation (*Precipitation05*). It was clearly revealed that TCCIP outputs are biased as the decreasing of observed temperature, which is highly correspond to the raise of altitude.

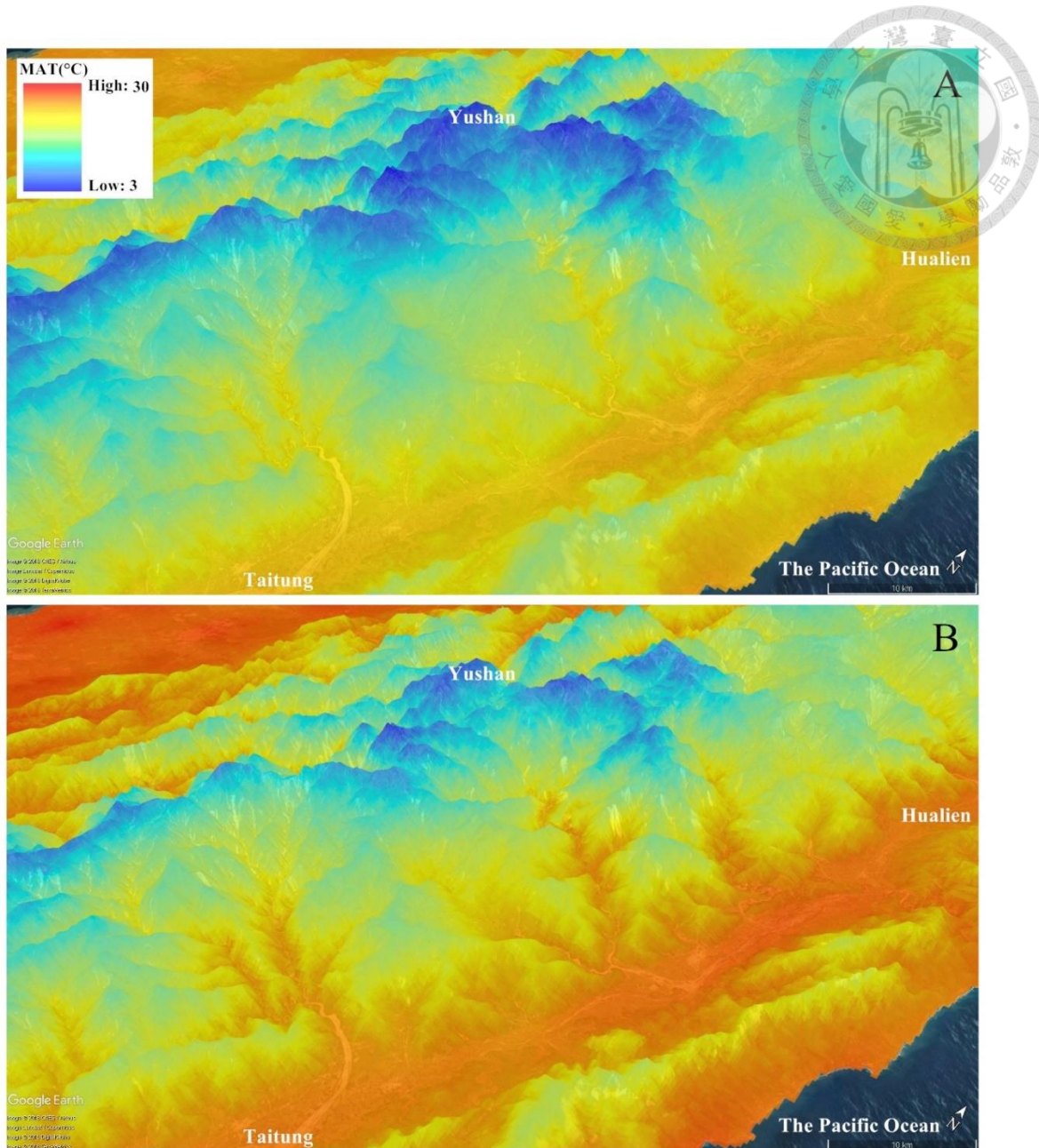


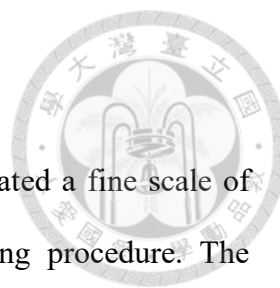
Fig. 2.9. Illustration of the effectiveness of downscaled climatic surface in the mountainous area of Taiwan, stretching from the coast of the Pacific Ocean up to the highest peak, Yushan, at 3,952m asl. (A) Downscaled mean annual temperature (MAT) by *clim.regression* in the resolution of 250m for the reference period of 1986–2005; (B) downscaled future MAT for the period of 2090–2100 based on the GCM of CSIRO-Mk3-6-0 in RCP 4.5 scenario.

DISCUSSION

Spatio-temporal heterogeneity of temperature lapse rate in Taiwan



Temperature lapse rate, the rate of change in temperature with elevation in the troposphere, is widely used as the most important predictor in mountain climate (Su, 1984a; Tang, 2006; Chiu et al., 2014). Many authors have revealed the spatio-temporal variation of lapse rate caused by atmospheric processes, interaction of prevailing monsoon, geographical and topographical positions, etc. (Su, 1984a; Tang and Ohsawa, 1997; Pepin, 2001; Chiu et al., 2014), thus suggested using regional observed data to derive the lapse rate as a local climate predictor rather than the commonly used global constant ($-6.5^{\circ}\text{C}/\text{km}$ in Barry and Chorley, 2009; or $-6.0^{\circ}\text{C}/\text{km}$ in Willmott and Matsuura, 2009). In Taiwan, a high spatio-temporal variation of lapse rate has been reported. Su (1984a) mentioned that temperature in the mountain area is highly correlated to elevations, and represented a lapse rate ranges from -3.08 to $-6.98^{\circ}\text{C}/\text{km}$ but varies among regions and seasons. Guan et al. (2009) has modeled a steeper temperature lapse rate from April to December with a range between -4.93 and $-5.62^{\circ}\text{C}/\text{km}$, and a shallower rate from -3.22 to $-3.61^{\circ}\text{C}/\text{km}$ during January to March according to historical observation data from 43 meteorological stations, mostly located in the west of the Central Mountain Range and Snow Mountain. A full exploration of the spatio-temporal variation of lapse rate was accomplished by Chiu et al. (2014). Based on historical records from 219 weather stations, Chiu et al. (2014) depicted that the average temperature lapse rate for all of Taiwan is $-5.17^{\circ}\text{C}/\text{km}$ with a general tendency to be steeper in summer and shallower in winter. They also found that the lapse rate exhibits a pronounced contrast between the windward side (steeper, $-5.97^{\circ}\text{C}/\text{km}$) and the leeward side of the Central Mountain Range (shallower, $-4.51^{\circ}\text{C}/\text{km}$) due to the atmospheric effect of prevailing winter monsoon. However, to



obtain a lapse rate for specific locations remained a challenge.

Through the approach of dynamic local regression, we have delineated a fine scale of lapse rate and used it as the key adjustment for the downscaling procedure. The distribution maps of lapse rate for the monthly temperature (Fig. 2.6) have shown a similar spatio-temporal pattern to that of Chiu et al. (2014), which exhibited a steeper lapse rate in regions exposed to the northeast monsoon (e.g., The northeast mountains, the Coastal Mountain Range from Hualien to Taitung, and Hengchun peninsula) and shallower in the leeward side (e.g., The west of the Central Mountain Range) during winter, and became obscure in summer. In the context of high spatio-temporal variation of lapse rate in Taiwan, *clim.regression* shows an excellent performance by using the local lapse rate to facilitate a high-resolution downscaling. Our evaluations have proved that this model considerably improves prediction accuracy relative to the original TCCIP climate data and it is suitable for the steep and mountainous areas and provides accurate and topography-corresponded climate variable estimates.

In addition, Lenoir et al. (2008) have pointed out that temperature lapse rate is the most important predictor of temperature variability in mountains, and can be one of the key contributions to predict the response of plants to climate change. In this study, steep lapse rates ($<-6^{\circ}\text{C}/\text{km}$) are found all year round in several areas, such as the northeast mountains, Hengchun peninsula, Tawu Mountain and Coastal Mountain Range. Some studies have reported the compression of vegetation zones in these areas due to a dramatic change in temperature along the altitudinal gradient (Su, 1984a; Su, 1984b; Chiou et al., 2010). In consequence of the feature of local regression, *clim.regression* can provide a deep insight into the entire spatial and temporal distribution of lapse rate in Taiwan, and our results show a great promise for providing high quality scale-free climate variables

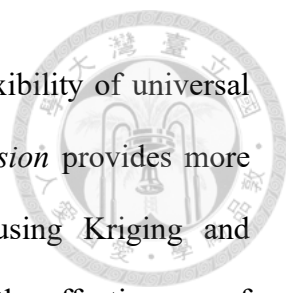
for a wide spectrum of research and application activities in biology, ecology, and adaptation to climate change.



Benefits of the dynamic local downscaling model

Dynamic local regression is a simple but effective method to achieve a scale-free downscaling. This method has been utilized to develop ClimateNA for North America (Wang et al., 2016) and ClimateAP for Asia-Pacific region (Wang et al., 2017) to downscale WorldClim and PRISM gridded datasets to scale-free climate estimates. The model evaluation demonstrated that the prediction error of ClimateNA and ClimateAP are 0.77°C and 1°C (in MAE). *Clim.regression* is a R script based on the same algorithm of ClimateNA and ClimateAP but use TCCIP 5km × 5km gridded climate surface, an interpolation based on historical data from thousands of weather stations of Taiwan, as the data source. Our statistical evaluations revealed that the prediction error of *clim.regression* is 0.56°C in monthly mean temperature and 36.26mm in monthly precipitation, which are substantially smaller than that for the original TCCIP data (in MAE, Table 2.5). These results suggest that the dynamic local regression approach is effective in downscaling climate variables to meet the requirement for ecological studies in mountain areas in Taiwan.

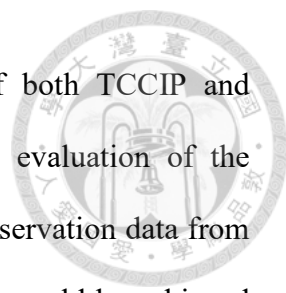
Chiu and Lin (2004) utilized regression and Ordinary Kriging to develop a scale-free model based on 219 meteorological stations and 877 rainfall stations to interpolate the distribution of monthly temperature and monthly precipitation. A cross validation revealed that the prediction errors of monthly temperature ranged from 1.57–1.74°C and monthly precipitation ranged from 17.51–53.07mm (in RMSE). In addition, some authors applied polynomial regression to model the distribution of monthly temperature based on historical observations from 156 weather stations, but exhibited a lower prediction



accuracy ranging from -5.15°C to 4.68°C (in ME) due to the inflexibility of universal regression coefficient (Chiou et al., 2004). In contrast, *clim.regression* provides more accurate temperature estimates ($0.73\text{--}1.13^{\circ}\text{C}$ in RMSE) than using Kriging and polynomial regression, due to its flexibility of local lapse rate and the effectiveness of elevational adjustment. However the rainfall prediction error of our model is 70.16mm in RMSE, it does not meet the level shown in Chiu and Lin (2004).

We found that *clim.regression* is not effective in downscaling precipitation (Fig. 2.7D). In Taiwan, the co-effect of humid monsoons and strong typhoons with diverse topography creates dramatic changes of precipitation in the mountains. For a windward slope at the middle elevation, the monthly precipitation during wet seasons can reach $2,000\text{mm}/\text{month}$ but decrease to less than $800\text{mm}/\text{month}$ as the change of aspect in a short distance of kilometers at the same elevation. Bilinear interpolation with a sampling window of 2 by 2 cells ($10\text{km} \times 10\text{km}$) and the dynamic local regression within a sampling unit of 3 by 3 cells ($15\text{km} \times 15\text{km}$) are the kernel of *clim.regression* to produce climatic estimates for the point of interest, however, the severe change of precipitation in mountains may neither linearly correlate with the change of elevation nor correspondently fit with the coverage of sampling windows to lead to a poor performance in precipitation prediction than temperature. It is worthy of advanced researches to explore the spatial pattern and its statistical correlates of precipitation to achieve an accurate predict model in the future.

The results of validation by weather stations of CWB and TFRI demonstrated that the estimates of *clim.regression* were more approximate to observations from CWB rather than TFRI. It could be partly attributed to the reason that most historical observation data of CWB stations were the main component of TCCIP system, so that it might not be an

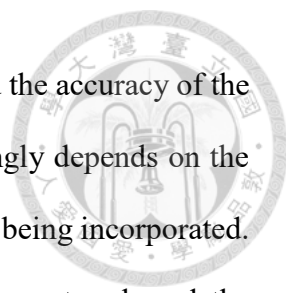


independent validation and could lead to an over estimation of both TCCIP and *clim.regression* model performances, but it would not affect the evaluation of the improvement in prediction accuracy relative to TCCIP. Historical observation data from TFRI was not included by TCCIP, so that an independent validation could be achieved theoretically. However, due to the lack of sustainable maintenance and long-term financial support, data quality of these independent weather stations could be harsher than CWB. It could be another effect leading to an under estimation of the downscaling model.

Applications and future works for *clim.regression* model

Ecologists have accumulated a large amount of field investigation data in Taiwan. Many studies exploring vegetation-climate relationship have also been published. However, due to the difficulty in accessing climate data in the past, researchers usually used geographical variables, such as elevation, longitude, latitude, aspect, the distance to seashore and exposure to prevailing monsoon as substitutions for climate variables in data analysis. Results of these studies based on indirect variables could lead to a biased result of ecological-climate relationships. The scale-free climate variables generated by *clim.regression* offer a solution to this problem. Users not only can generate a continuous and seamless surface for climate niche modeling but also possible to estimate historical and future climate condition for specific locations such as numerous vegetation survey plots. It provides a large number of climate variables for scientists to explore, delineate and quantify the relationships between climate and vegetation.

However, some limitations still exist in our downscaling approach. *Clim.regression* downscales gridded source climate variables through a combination of bilinear interpolation and concise elevational adjustment. Therefore, the performance of *clim.regression* is mostly determined by two factors in addition to the effectiveness of the



downscaling algorithm: the quality of the original climate dataset and the accuracy of the imported digital elevation surface. The quality of baseline data strongly depends on the number of historical observations and the number of weather stations being incorporated. Therefore, we regard both of the robust meteorological observation network and the effective interpolation approaches are the critical issues to provide a high-quality gridded dataset for downscaling. TCCIP has an ongoing project to improve the accuracy and the coverage of periods for gridded climate data of Taiwan, which serves as an ideal baseline data to be used in *clim.regression* to generate high-resolution and high-quality climate data for ecological studies.

AUTHOR CONTRIBUTIONS

HYL and TW conceived the research; HYL, TW, and JMH led the writing; TYC, and CFH contributed the data and background information; HYL performed the statistical analyses with contributions from GW and TW; all authors discussed the results and commented on the manuscript.

LITERATURE CITED

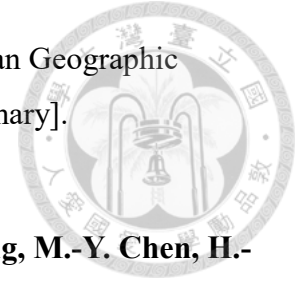
Barry, R. G. and R. J. Chorley. 2009. *Atmosphere, Weather and Climate*, 9th edition, Routledge, London, 536 pp.

Chao, W.-C., G.-Z. M. Song, K.-J. Chao, C.-C. Liao, S.-W. Fan, S.-H. Wu, T.-H. Hsieh, I.-F. Sun, Y.-L. Kuo and C.-F. Hsieh. 2010. Lowland rainforests in southern Taiwan and Lanyu, at the northern border of Paleotropics and under the influence of monsoon wind. *Plant Ecology* **210(1)**: 1–17. <http://doi.org/10.1007/s11258-009-9694-0>

Chiou, C.-R., Y.-C. Liang, Y.-J. Lai and M.-Y. Huang. 2004. A study of delineation

and application of the climatic zones in Taiwan. *Journal of Taiwan Geographic Information Science* **1(1)**: 41–62. [in Chinese with English summary].

<http://doi.org/10.29790/JTGIS.200410.0004>



Chiou, C.-R., G.-Z. M. Song, J.-H. Chien, C.-F. Hsieh, J.-C. Wang, M.-Y. Chen, H.-Y. Liu, C.-L. Yeh, Y.-J. Hsia and T.-Y. Chen. 2010. Altitudinal distribution patterns of plant species in Taiwan are mainly determined by the northeast monsoon rather than the heat retention mechanism of Massenerhebung. *Botanical Studies* **51**: 89–97.

Chiu, C.-A. 2004. Regionalized mountain vegetation and predicted potential vegetation—The application of climate-vegetation classification scheme. Shei-Pa National Park Headquarters, Miaoli, Taiwan, ROC, 42pp. [in Chinese]

Chiu, C.-A. and P.-H. Lin. 2004. Spatial Interpolation of air temperature and precipitation from meteorological stations at Taiwan. *Atmospheric Sciences* **32(4)**: 329–350. [in Chinese with English summary]

Chiu, C.-A., P.-H. Lin and C.-Y. Tsai. 2014. Spatio-temporal variation and monsoon effect on the temperature lapse rate of a subtropical island. *Terrestrial Atmospheric and Oceanic Sciences* **25(2)**: 203–217.

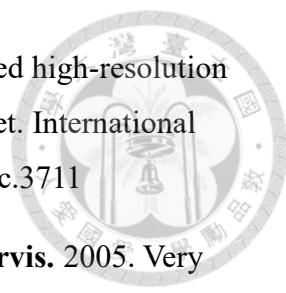
[http://doi.org/10.3319/TAO.2013.11.08.01\(A\)](http://doi.org/10.3319/TAO.2013.11.08.01(A))

Daly, C., W. P. Gibson, G. H. Taylor, G. L. Johnson and P. Pasteris. 2002. A knowledge-based approach to the statistical mapping of climate. *Climate Research* **22**: 99–113. <http://doi.org/10.3354/cr022099>

Guan, B.-T., H.-W. Hsu, T.-H. Wey and L.-S. Tsao. 2009. Modeling monthly mean temperatures for the mountain regions of Taiwan by generalized additive models. *Agricultural and Forest Meteorology* **149(2)**: 281–290.

<http://doi.org/10.1016/j.agrformet.2008.08.010>

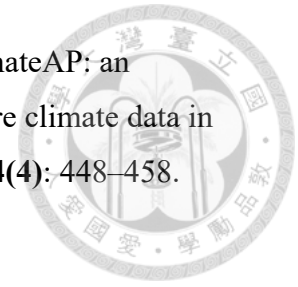
Hannaway, D. B., C. Daly, W.-X. Cao, W.-H. Luo, Y.-R. Wei, W.-L. Zhang, A.-G. Xu, C.-A. Lu, X.-Z. Shi and L.-X. Li. 2005. Forage species suitability mapping for China using topographic, climatic and soils spatial data and quantitative plant tolerances. *Agricultural Science in China* **4(9)**: 660–667.

- 
- Harris, I., P. D. Jones, T. J. Osborn and D. H. Lister.** 2014. Updated high-resolution grids of monthly climatic observations—the CRU TS 3.10 Dataset. *International Journal of Climatology* **34(3)**: 623–642. <http://doi.org/10.1002/joc.3711>
- Hijmans, R. J., S. E. Cameron, J. L. Parra, P. G. Jones and A. Jarvis.** 2005. Very high resolution interpolated climate surface for global land areas. *International Journal of Climatology* **25(15)**: 1965–1978. <http://doi.org/10.1002/joc.1276>
- Hsu, H.-H., C. Chou, Y.-C. Wu, M.-M. Lu, C.-T. Chen and Y.-M. Chen.** 2011. Climate Change in Taiwan: Scientific Report 2011 (Summary). National Science Council, Taipei, Taiwan, ROC, 67pp.
- Lenoir, J., J. C. Gegout, P. A. Marquet, P. de Ruffary and H. Brisse.** 2008. A significant upward shift in plant species optimum elevation during the 20th century. *Science* **320(5884)**: 1768–1771. <http://doi.org/10.1126/science.1156831>
- Li, C.-F., M. Chytrý, D. Zelený, M.-Y. Chen, T.-Y. Chen, C.-R. Chiou, Y.-J. Hsia, H.-Y. Liu, S.-Z. Yang, C.-L. Yeh, J.-C. Wang, C.-F. Yu, Y.-J. Lai, W.-C. Chao and C.-F. Hsieh.** 2013. Classification of Taiwan forest vegetation. *Applied Vegetation Science* **16**: 698–719.
- Lin, C.-T., C.-F. Li, D. Zelený, M. Chytrý, Y. Nakamura, M.-Y. Chen, T.-Y. Chen, Y.-J. Hsia, C.-F. Hsieh, H.-Y. Liu, J.-C. Wang, S.-Z. Yang, C.-L. Yeh and C.-R. Chiou.** 2012. Classification of the high-mountain coniferous forests in Taiwan. *Foilia Geobot* **47**: 373–401.
- Lin, L.-Y.** 2011. Annual report on Taiwan Climate Change Projection and Information Platform (TCCIP) project. NSC98-2625-M-492-011. National Science Council, Taipei, Taiwan, ROC, 166 pp. [in Chinese with English summary]
- Pepin, N.** 2001. Lapse rate changes in northern England. *Theoretical and Applied Climatology* **68(1-2)**: 1–16. <http://doi.org/10.1007/s007040170049>
- Su, H.-J.** 1984a. Studies on the climate and vegetation types of the natural forests in Taiwan (I). Analysis of the variations in climatic factors. *Quarterly Journal of Chinese Forestry* **17(3)**: 1–14.
- Su, H.-J.** 1984b. Studies on the climate and vegetation types of the natural forests in

Taiwan (II). Altitudinal vegetation zones in relation to temperature gradient. *Quarterly Journal of Chinese Forestry* **17(4)**: 57–73.

- Su, H.-J.** 1985. Studies on the climate and vegetation types of the natural forests in Taiwan (III). A scheme of geographical climatic regions. *Quarterly Journal of Chinese Forestry* **18(3)**: 33–44.
- Sun, I.-F.** 1993. The species composition and forest structure of a subtropical rain forest at southern Taiwan. PhD Thesis, University of California, Berkeley, USA.
- Sun, I.-F., C.-F. Hsieh and S.-P. Hubbell.** 1998. The structure and species composition of a subtropical monsoon forest in southern Taiwan on a steep wind-stress gradient. In: Dallmeier F., J. A. Comiskey (eds) *Forest Biodiversity Research, monitoring and modeling: conceptual background and old world case studies*. Parthenon Publishing Co., Paris, France, pp 565–635.
- Tang, C. Q.** 2006. Forest vegetation as related to climate and soil conditions at varying altitudes on a humid subtropical mountain, Mount Emei, Sichuan, China. *Ecological Research* **21(2)**: 174–180. <http://doi.org/10.1007/s11284-005-0106-1>
- Tang, C. Q. and M. Ohsawa.** 1997. Zonal transition of evergreen, deciduous, and coniferous forests along the altitudinal gradient on a humid subtropical mountain, Mt. Emei, Sichuan, China. *Plant Ecology* **133**: 63–78.
- Wang, T., A. Hamann, D. Spittlehouse and S. N. Aitken.** 2006. Development of scale-free climate data for western Canada for use in resource management. *International Journal of Climatology* **26(3)**: 283–397. <http://doi.org/10.1002/joc.1247>
- Wang, T., A. Hamann, D. Spittlehouse and C. Carroll.** 2016. Locally downscaled and spatially customizable climate data for historical and future periods for North America. *PLoS One* **11(6)**: e0156720. <http://doi.org/10.1371/journal.pone.0156720>
- Wang, T., A. Hamann, D. Spittlehouse and T. Q. Murdock.** 2012. ClimateWNA-high-resolution spatial climate data for Western North America. *Journal of Applied Meteorology and Climatology* **51(1)**: 16–29. <http://doi.org/10.1175/JAMC-D-11-043.1>

Wang, T., G. Wang, J. L. Innes, B. Seely and B. Chen. 2017. ClimateAP: an application for dynamic local downscaling of historical and future climate data in Asia Pacific. *Frontiers of Agricultural Science and Engineering* **4(4)**: 448–458. <https://doi.org/10.15302/J-FASE-2017172>



Weng, S.-P. and C.-T. Yang. 2012. The construction of monthly rainfall and temperature dataset with 1km gridded resolution over Taiwan area (1960–2009) and its application to climate projection in the near future (2015–2039). *Atmospheric Sciences* **40(4)**: 349–369. [in Chinese with English summary]

Willmott, C. J. and K. Matsuura. 2009. Terrestrial Air Temperature and Precipitation: Monthly Climatologies (version 4.01). Global Air Temperature and Precipitation Archive.

Chapter 3

Climate-based approach for modeling the distribution of montane forest vegetation in Taiwan



This chapter is a published paper in in Applied Vegetation Science (DOI: 10.1111/AVSC.12485) co-authored by Huan-Yu Lin, Ching-Feng Li, Tze-Ying Chen, Chang-Fu Hsieh, Guangyu Wang, Tongli Wang, and Jer-Ming Hu.

Abstract

Climate shapes forest types on our planet and also drives the differentiation of zonal vegetation at regional scale. A climate-based ecological model may provide an effective alternative to traditional approach for assessing limitations, thresholds, and the potential distribution of forests. The main objective of this study is to develop such a model, with a machine-learning approach based on scale-free climate variable estimates and classified vegetation plots, to generate a fine-scale predicted vegetation map of Taiwan, a subtropical mountainous island. In this paper, a total of 3,824 plots from 13 climate-related forest types and 57 climatic variable estimates for each plot were used to build an individual ecological niche model for each forest type with Random Forest (RF). A predicted vegetation map was developed through the assemblage of RF predictions for each forest type at the spatial resolution of 100m. It displays a distinct altitudinal zonation from subalpine to montane cloud forests, followed by the latitudinal differentiation of subtropical mountain forests in the north and tropical montane forests in the south, with an average mismatch rate of 6.59%. An elevational profile and 3-D visualization demonstrate the excellence of the model in estimating a fine, precise, and topographically-corresponded potential distribution

of forests. This study supports that machine-learning approach is effective to handle a large number of variables and to provide accurate predictions.

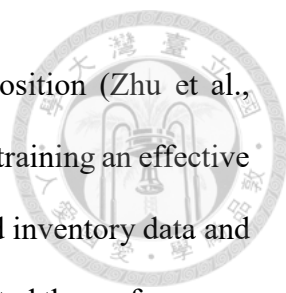


KEY WORDS: Climate, Eastern Asia, Ecological niche modeling, Montane forest, Subtropical forest, Random Forest, Vegetation mapping, Taiwan.

INTRODUCTION

Climate is the primary element that governs the distribution of plant species, and most species are adapted to a specific range of climatic conditions, which is referred to as their climatic niche (Pearson and Dawson, 2003; Wang et al., 2016a). The vegetation-climate relationship has long been recognized by ecologists, and the concept has been applied to depict the regionalization of ecoregions or vegetation types for decades (Holdridge, 1947; Bailey, 1983; Su, 1984b; Fang et al., 2002). Recent progress in ecological niche modeling and the accessibility of accurate and fine-scale climate data have enabled vegetation-climate relationships to be used in numerous studies for a variety of purposes, including projection of the historical and current distribution of biomes and forests for management purposes (Rehfeldt et al., 2006), prediction of changes in species (Matsui et al., 2018) or ecosystems (Brinkmann et al., 2011; Rehfeldt et al., 2012; Wang et al., 2012) under various global warming scenarios, and provision of strategic tools for conservation and adaptation to the impact of climate change (Hansen and Phillips, 2015; Klassen and Burton, 2015; Wang et al., 2016a).

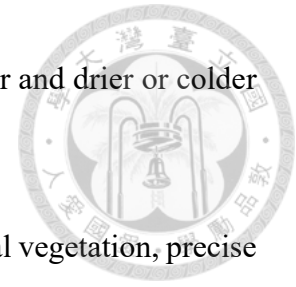
Most predictive ecological niche modeling studies focused on large landscapes and dominant forests in temperate zones, but these studies seldom explored the complex, highly mixed, and species-diverse forests in tropical and subtropical regions. Distinguishing the boundaries of tropical and subtropical forest communities is difficult



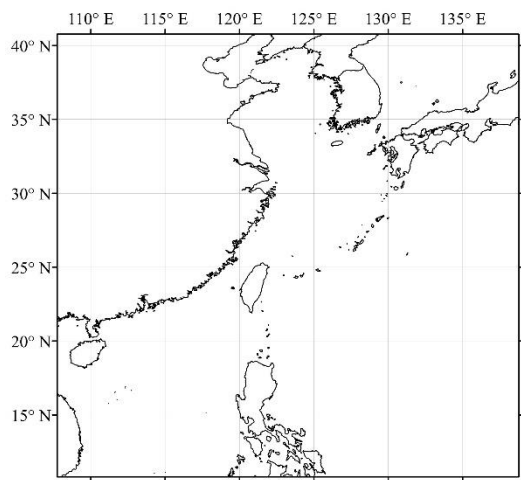
due to their similar broad-leaved physiognomy and variable composition (Zhu et al., 2015). Comprehensively and clearly-tagged samples are requisite for training an effective and robust statistical classifier, however, the lack of high-quality field inventory data and the variable species composition in tropics and subtropics greatly limited the performance of statistical models in these extensive territories (Martin et al., 2007).

Taiwan is an island located in middle of the monsoon region of Asia with more than 200 peaks over 3,000m asl. The diverse climatic conditions along the altitudinal gradient create a distinct altitudinal zonation of forests within the island, from tropical lowland rainforest (Chao et al., 2010) to subalpine coniferous forest (Lin et al., 2012). The overall vegetation patterns on the island have been studied over the past few decades, recognizing and characterizing six distinct altitudinal vegetation zones within mesic to humid habitats (Su, 1984b). A national vegetation inventory was completed by the Taiwan Forestry Bureau in 2008. This inventory revealed that 58% of Taiwan's territory was covered by forests, 53% of which are broad-leaved forests, with the remainder approximately 47% of the forested lands comprised of coniferous or mixed forests. Li et al. (2013) established a vegetation classification scheme based on the floristic data of 8804 plots from the National Vegetation Database of Taiwan, which included 922 tree and shrub species in the analysis. They used the Cocktail determination key (CoDeK), a software application to formalize classification definitions, and developed automatic assignments of new plots to the defined vegetation classification scheme. Based on the formalized approach, a total of 6574 plots were successfully classified into 21 forest types in which 12 types were zonal while 9 types were azonal. Li et al. (2013) suggested that the main factors responsible for the differentiation of zonal forests are temperature and moisture, which vary according to the latitudinal distribution and altitudinal stratification in mesic to humid habitats. In contrast, most azonal forests are affected by specific soil properties or

disturbance rather than climate, and their habitats are usually warmer and drier or colder and wetter than those of zonal forests.



Since climate is the main factor controlling the differentiation of zonal vegetation, precise and fine-scaled climate data are considered to be a reasonable alternative for assessing limitations, thresholds, and the potential distribution of forests across a large landscape, if an effective statistical classifier exists. Machine learning is a new, high-performance approach applied in ecological niche modeling, which works outstandingly when a continuous supply of information for improving its performance is available. In Taiwan, intensive sampling plots tagged by the classification scheme and its corresponding climate variable estimates would be ideal sources to train a machine-learning model for exploring the vegetation-climate relationship. The main objectives of this study were to: (1) reveal the climatic factors responsible for the current distribution of dominant forest types in Taiwan; (2) develop an effective and reproducible statistical model for predicting the potential distribution of climate-related forests; and (3) use Taiwan's zonal vegetation as an example to evaluate the performance of the model.



Elevation (m)

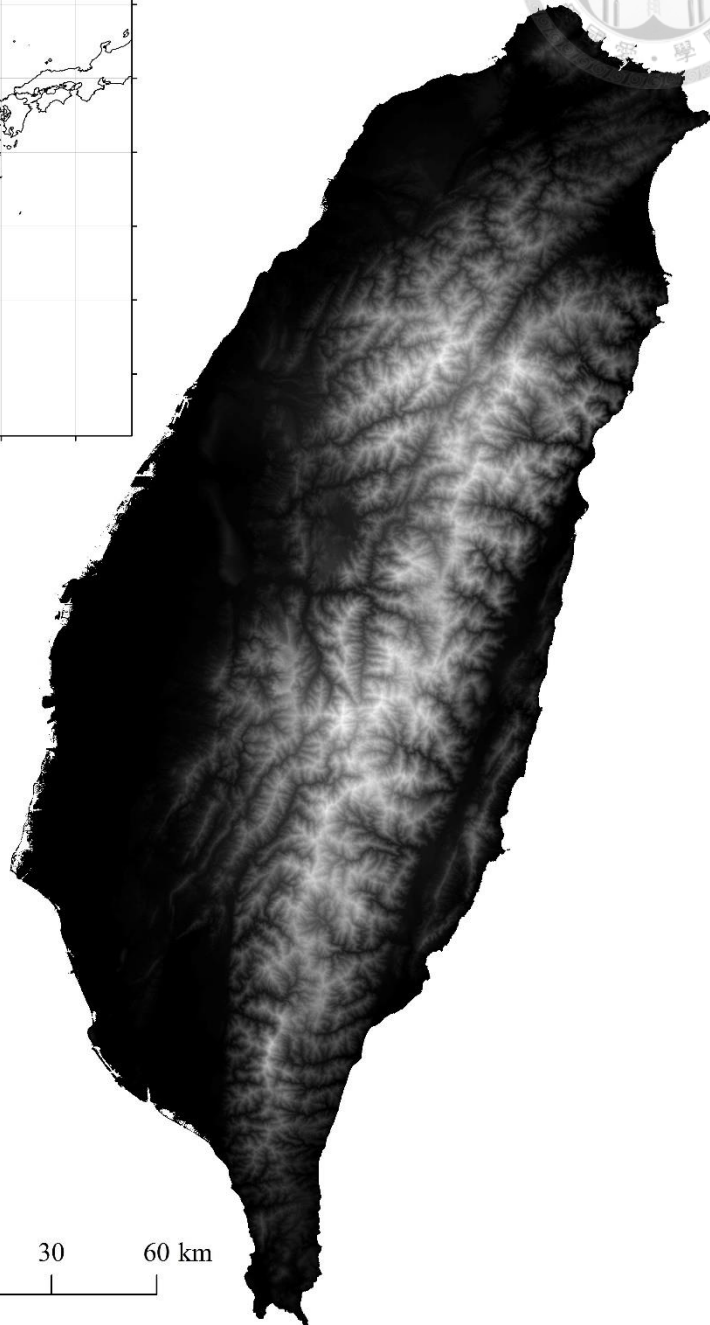
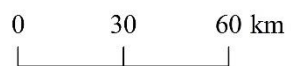
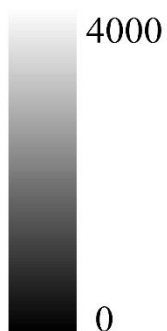


Fig. 3.1. Location and digital elevation surface of Taiwan island.

MATERIALS AND METHODS

Study area

Taiwan (21.83°–25.33° N, 120.00°–122.00° E) is a subtropical island on the western edge of the Pacific Ocean. Hills and mountains occupy more than 70% of the island's 36,000km². A principle mountain range, the Central Mountain Range, runs through the whole island in a NNE–SSW trend, and the highest peak is 3,952m asl (Fig. 3.1). The climate in Taiwan is mainly affected by prevailing monsoons and typhoons. In winter, the northeast monsoon from Siberia passes through Japan and the East China Sea, bringing plentiful precipitation and cold temperature to the windward slopes of northeast Taiwan. By contrast, the southwest monsoon from Indochina and the South China Sea brings heavy rains and a humid climate in the summer, inducing the rainy season in south Taiwan (Su, 1984a; Lin et al., 2009). Typhoons occur only occasionally but they represent severe climatic events in Taiwan. They contribute a sizable portion of the annual rainfall and are the primary trigger of landslides and disturbances in mountain areas.

Topographical variations in the form of lofty mountains and steep gorges result in a wide temperature range that forms distinct stratification of climatic zones in mountain areas and creates diverse microhabitats harboring many vascular plant species (~4,200 species). The zonation of forest types along the altitudinal gradient of Taiwan was first reported by Sasaki (1924), which was followed by a series of studies depicting the physiognomy and species composition of native flora (Suzuki, 1938; Liu and Su, 1972; Chang, 1974). Su (1984a, 1984b, 1985) evaluated overall vegetation patterns in Taiwan and concluded that distribution of natural vegetation is governed by the alternating winter and summer monsoons, coupled with the steep topography. He also proposed a widely accepted scheme for classifying six altitudinal vegetation zones in mesic to humid habitats and for

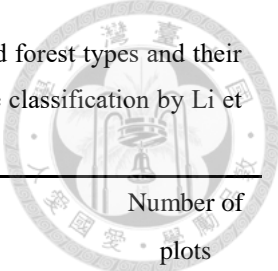


some parts of the azonal vegetation in the drier successional regions of Taiwan.

Vegetation data

The geographic coordinates of 6,574 plots and its corresponding 21 vegetation classification types were received from Li et al. (2013); then, a preliminary inspection was conducted to eliminate coordinate-duplicate plots. Eight forest types, which were climate-unrelated or geographically isolated, were removed from the original dataset: two types were seashore woodlands and mangroves; three types were successional woodland related to historical landslides and disturbances; two types were rock-outcrop forests associated with uplifted coral reef tableland, limestone, and scree slopes; and the last type was tropical forest on Green Island and Orchid Island isolated from the Taiwan main island. Finally, a total of 3,824 plots belonging to 13 climate-related forest types (Table 3.1) were retained to explore the relationship between climate and vegetation.

Table 3.1. The training data incorporated in this study, including 13 climate-related forest types and their corresponding 3,824 field plots. The abbreviations of each forest type followed the classification by Li et al. (2013).



Forest type	Number of plots
High-mountain coniferous woodlands and forests (C1)	
<i>Juniperus</i> subalpine coniferous woodland and scrub (C1A01)	102
<i>Abies-Tsuga</i> upper-montane coniferous forest (C1A02)	89
Subtropical mountain zonal forests (C2)	
<i>Chamaecyparis</i> montane mixed cloud forest (C2A03)	543
<i>Fagus</i> montane deciduous broad-leaved cloud forest (C2A04)	55
<i>Quercus</i> montane evergreen broad-leaved cloud forest (C2A05)	1,058
<i>Machilus-Castanopsis</i> sub-montane evergreen broad-leaved forest (C2A06)	359
<i>Phoebe-Machilus</i> sub-montane evergreen broad-leaved forest (C2A07)	410
<i>Ficus-Machilus</i> foothill evergreen broad-leaved forest (C2A08)	145
Tropical mountain zonal forests (C3)	
<i>Pasania-Elaeocarpus</i> montane evergreen broad-leaved cloud forest (C3A09)	57
<i>Drypetes-Helicia</i> sub-montane evergreen broad-leaved forest (C3A10)	425
<i>Dysoxylum-Machilus</i> foothill evergreen broad-leaved forest (C3A11)	27
Tropical mountain azonal forests (C5)	
<i>Illicium-Cyclobalanopsis</i> tropical winter monsoon forest (C5A13)	40
Subtropical mountain azonal woodlands and forests (C6)	
<i>Pyrenaria-Machilus</i> subtropical winter monsoon forest (C6A15)	514
Total	3,824



Climate data

Grid-based climate data were easily accessible and suitable for modeling general patterns at global and regional scales (Hannaway et al., 2005; Hijmans et al., 2005; Harris et al., 2014). However, for detailed ecological research, such climate data were usually too coarse to provide exact climate estimates for each plot in mountainous and topographically diverse areas. In Taiwan, a meteorological framework named Taiwan Climate Change Projection and Information Platform (TCCIP) has integrated historical observations from thousands of weather stations to develop a $5 \times 5\text{km}^2$ gridded climate surface covering the period of 1960–2012 (Hsu et al., 2011; Weng and Yang, 2012). A climate data downscaling process named *clim.regression* (Lin et al., 2018), which is based on a synthetic approach of bilinear interpolation and dynamic local regression (Wang et al., 2016a; Wang et al., 2017), was used to downscale the TCCIP $5 \times 5\text{km}^2$ dataset to a scale-free and seamless surface by conducting reasonable elevational adjustments using local lapse rate estimates. The accuracy of the climate downscaling model has been evaluated by comparing to historical observations from the 15 weather stations over different altitudinal zones. It demonstrated prediction errors of 0.56°C , 0.79°C , 0.80°C , and 36.26mm in T_{ave} , T_{min} , T_{max} , and PPT (measured by the mean absolute error between monthly estimation and observation), respectively, and these were considerably improved over the TCCIP data (Lin et al., 2018). A total of 73 climate variable estimates were obtained through the downscaling process, including annual, seasonal, and monthly variables, alongside biologically relevant derivatives.

For exploring the relationship between vegetation and climate, 57 of the 73 climate variable estimates (Table 3.2), specific to the location of vegetation survey plots from Li et al. (2013) for the reference period of 1986–2005, were selected and were used as

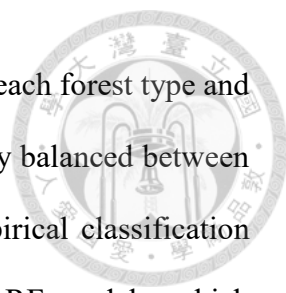
parameters to construct raw climate niche models for each forest type. Seasonal climate variables were not considered because of the large number of monthly variables. A gridded climate surface at a resolution of $100 \times 100\text{m}^2$, which covers regions higher than 100m asl in Taiwan (2.7 million hectares in total), was generated from the same set of 57 climate variable estimates by *clim.regression* for predicting the climatic suitability of forests over the study area.

Table 3.2. The 57 climate variables, which were generated by the climate downscaling process of *clim.regression*, were incorporated in the random forest models.

Climate variables	Definition
Monthly precipitation (PPT1 to PPT12)	
Mean annual precipitation (MAP)	
Mean summer precipitation (MSP)	Summation of precipitation from May to September
Ratio of winter precipitation (WPR)	$(\text{PPT12} + \text{PPT1} + \text{PPT2}) / \text{MAP}$ (Li et al., 2013)
Mean monthly minimum temperature (T_{min1} to T_{min12})	
Mean monthly temperature (T_{ave1} to T_{ave12})	
Mean annual temperature (MAT)	
Mean monthly maximum temperature (T_{max1} to T_{max12})	
Temperature difference (TD)	T_{ave7} minus T_{ave1}
Annual heat:moisture index (AHM)	$(\text{MAT} + 10) / (\text{MAP} / 1000)$
Summer heat:moisture index (SHM)	$(T_{\text{ave7}}) / (\text{MSP} / 1000)$
Warmth index (WI)	Annual summation of mean monthly temperature higher than 5°C (Su, 1984b)
Precipitation deficiency (PD)	Difference between annual potential evapotranspiration and MAP (Su, 1985)

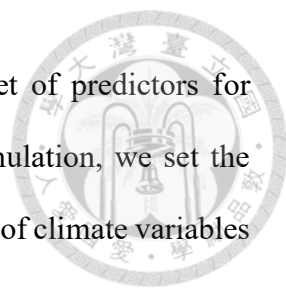
Construction of the ecological niche model and vegetation prediction

The R version (Liaw and Wiener, 2002) of the random forest (RF) algorithm (Breiman,



2001) was used to model the relationship between the occurrence of each forest type and the climatic variables. RF works best when the samples are relatively balanced between classes (Breiman, 2001; Rehfeldt et al., 2006); however, most empirical classification problems and ecological samplings are imbalanced. A total of 13 RF models, which represented the climatic niche of each forest type, were constructed in this study. For each RF model, plots belonging to the target forest type were treated as “presence”, and the remnants were regarded as “absence”. In most cases, occurrences of absence were much more common than those of presence for each forest type, leading to imbalanced samples, which can result in poor predictive performance for the minority (presence) class. Therefore, balanced random forest (Chen et al., 2004) and multiple forest approaches (Wang et al., 2016b) were applied to build an ensemble of RF models to reduce the effect of imbalanced samples. Presence points (in minority) were combined with the same number of randomly selected points of absence (in majority), to establish the training dataset of each RF model. The identical sample size of absence and presence can ensure balanced sampling between classes. The above-mentioned model-building process was repeated 100 times to achieve “multiple forests”—the ensemble predictions from multiple forests were used to represent the climatic suitability of each forest type.

Although RF can handle confounding variables, a final model with the parsimonious set of variables that optimized variance is necessary to reduce the risk of over-fit and speed up the prediction. The R package VSURF was implemented to select a minimum set of predictors (Genuer et al., 2015) from the 57 climate variable estimates provided by *clim.regression* for each forest type. VSURF first calculates the importance scores of all variables and eliminates variables of small importance, based on a descending importance rank. The variables that result in the lowest model out-of-bag (OOB) error are selected as explanatory variables. This set of explanatory variables is further truncated to eliminate



all but one of any correlated variables, resulting in a minimum set of predictors for constructing the most parsimonious prediction model. For each simulation, we set the number of trees as 500 and used the default square root of the number of climate variables at each node (Liaw and Wiener, 2002).

Each geographical cell of the $100 \times 100\text{m}^2$ projecting surface received climatic suitability for the 13 forest types based on predictions from multiple forests. Fig. 3.2 presents a flow diagram evaluating the most suitable forest type for each cell according to the following criteria: (1) cells with climatic suitability lower than 0.3 for all forest types were classified as “uncertain”; (2) cells that shared the same suitability for two (or more) forest types (e.g., forest type *i* and *j*) and had suitability higher than 0.3 (included) were assigned as “mixed stands” between forest type *i* and *j*; and (3) the remnant cells, namely those with high suitability for a single forest type, were defined as “pure stands” of the predicted forest type. The cut-off threshold of 0.3 in the first step affects the proportion of the study areas being identified as an “uncertain” entity. We tested values between 0 and 0.5 for being the threshold and found a slight difference in resulting areas as uncertain type, ranging from 0 to 1418 ha (accounting for 0–0.05% of the total study area). Thus, we arbitrarily chose the midpoint value 0.3 as the threshold, which demonstrates a performance similar to our field experience. The ensemble of climatic suitable forest types and their suitability were composed as a raster layer to produce the predicted vegetation map using ESRI ArcGIS Pro 2.4.

Geographic cell	Climatic suitability of forest type				
	Type 1	Type 2	Type 3	...	Type n
Cell 1	P_{11}	P_{12}	P_{13}	...	P_{1n}
Cell 2	P_{21}	P_{22}	P_{23}	...	P_{2n}
⋮	⋮	⋮	⋮	⋮	⋮
Cell m	P_{m1}	P_{m2}	P_{m3}	...	P_{mn}

The projected forest type of cell k ($k=\{1,2,3,\dots,m\}$) was evaluated by the following workflow.

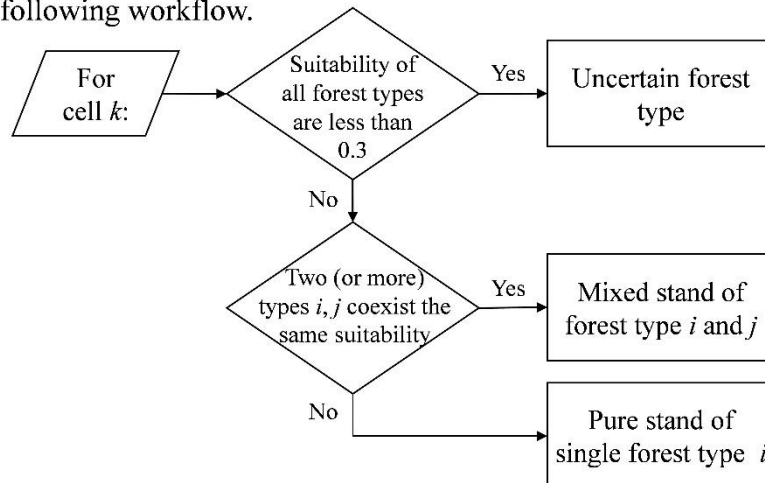
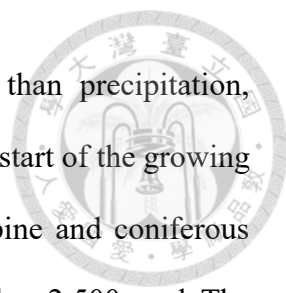


Fig. 3.2. The workflow diagram for the ensemble of RF predictions of each forest type to evaluate the most suitable forest type(s) of each geographic cell.

RESULTS

Climatic niche and important variables of forest types

The result of VSURF variable truncation revealed that the importance and number of selected climate variables varied among forest types. The OOB error arising from the model-building process of 500 trees is 7.9% on average, ranging from 1.2% to 18.2% depending on forest type (Table 3.3). The vegetation-climate relationships of high-mountain, and subtropical mountain zonal forests (from *Juniperus* woodland and scrub to *Ficus–Machilus* forest in Table 3.3) are strongly driven by temperature factors (T_{max} , T_{ave} , and T_{min}); that is, the primary predictors of high-mountain, temperate, and



subtropical forests are usually dominated by temperature rather than precipitation, respectively. Furthermore, the maximum monthly temperature at the start of the growing season (March to June) closely relates to the occurrence of subalpine and coniferous forests (*Juniperus*, and *Abies-Tsuga*) distributed at elevations higher than 2,500m asl. The critical effect shifts to winter temperature (December to February) for cloud forests at elevations of 1,500–2,500m asl, which are dominated by *Chamaecyparis* or *Fagus*. By contrast, precipitation-related factors, especially the relative dryness in spring (March to May), display a more evident correlation with the climatic suitability of tropical mountain zonal forests in south Taiwan (*Pasania-Elaeocarpus* cloud forest, *Drypetes-Helicia* forest, and *Dysoxylum-Machilus* forest). Due to the co-effect of topographical exposure and windward chilling of northeast monsoon during winter, two azonal forest types, the tropical *Illicium-Cyclobalanopsis* monsoon forest and the subtropical *Pyrenaria-Machilus* monsoon forest, exhibit climatic features of higher precipitation and lower temperature than its nearby habitats in winter (Fig. 3.3).

Table 3.3. The most parsimonious RF model for each forest type through the variable selection process of VSURF package. Predictor variables were sorted by its importance (Gini values) in descending order.

Forest type	Predictor variable / proportion of variable importance	OOB error rate
<i>Juniperus</i> woodland and scrub	<i>Tmax6</i> (37.6%), <i>Tmax5</i> (34.2%), <i>Tmax3</i> (15.3%), <i>Tmax4</i> (12.9%)	1.2%
<i>Abies-Tsuga</i> forest	<i>Tmax5</i> (23.6%), <i>Tmax6</i> (22.9%), <i>Tmax3</i> (20.1%), <i>Tave6</i> (12.0%), <i>Tmax4</i> (10.1%), <i>Tmax2</i> (7.3%), <i>Tave5</i> (3.9%)	6.0%
<i>Chamaecyparis</i> cloud forest	<i>Tave12</i> (19.9%), <i>Tmax2</i> (13.1%), <i>Tave1</i> (8.2%), <i>Tmax9</i> (8.1%), <i>Tave6</i> (5.5%), <i>PPT12</i> (5.4%), <i>Tmax11</i> (5.2%), <i>PPT1</i> (5.0%), <i>TD</i> (4.7%), <i>Tave2</i> (3.8%), <i>PPT11</i> (3.7%), <i>WPR</i> (3.5%), <i>PPT6</i> (3.0%), <i>WI</i> (2.6%), <i>Tave3</i> (2.5%), <i>Tmax12</i> (2.3%), <i>PPT10</i> (1.8%), <i>PPT3</i> (1.7%)	8.7%
<i>Fagus</i> cloud forest	<i>Tmax12</i> (21.6%), <i>Tmax2</i> (19.8%), <i>Tmax1</i> (18.6%), <i>TD</i> (11.9%), <i>PPT1</i> (8.1%), <i>Tmax11</i> (8.1%), <i>PPT9</i> (7.6%), <i>WPR</i> (4.3%)	3.4%
<i>Quercus</i> cloud forest	<i>Tave6</i> (14.1%), <i>Tmin12</i> (13.4%), <i>Tmax6</i> (10.2%), <i>Tmin10</i> (9.6%), <i>Tmax7</i> (8.2%), <i>Tmax2</i> (6.7%), <i>PPT1</i> (5.6%), <i>PPT12</i> (5.2%), <i>PPT3</i> (5.0%), <i>PPT9</i> (4.6%), <i>PPT10</i> (4.6%), <i>Tave5</i> (3.3%), <i>Tmin6</i> (2.8%), <i>Tmax8</i> (2.7%), <i>PPT11</i> (2.4%), <i>PPT6</i> (1.8%)	11.0%
<i>Machilus-Castanopsis</i> forest	<i>Tmax4</i> (15.9%), <i>Tmax10</i> (13.6%), <i>Tmax11</i> (10.8%), <i>Tmin6</i> (9.9%), <i>Tmax6</i> (7.9%), <i>Tmax5</i> (7.2%), <i>Tmax3</i> (7.1%), <i>PPT10</i> (6.6%), <i>Tmax12</i> (6.4%), <i>Tmax1</i> (4.9%), <i>Tmax9</i> (4.1%), <i>Tmax7</i> (2.8%), <i>PPT8</i> (2.7%)	16.7%
<i>Phoebe-Machilus</i> forest	<i>Tmax9</i> (18.7%), <i>Tave2</i> (15.1%), <i>Tmax7</i> (12.4%), <i>PPT3</i> (10.8%), <i>PPT7</i> (8.6%), <i>PPT4</i> (8.3%), <i>Tmax11</i> (8.0%), <i>Tave9</i> (7.3%), <i>TD</i> (2.9%), <i>PPT9</i> (2.8%), <i>PPT8</i> (2.6%), <i>PPT10</i> (2.5%)	18.2%
<i>Ficus-Machilus</i> forest	<i>Tmax11</i> (26.1%), <i>Tmax10</i> (25.9%), <i>Tmax9</i> (13.9%), <i>SHM</i> (12.1%), <i>Tmax8</i> (11.6%), <i>AHM</i> (1.3%), <i>MSP</i> (3.1%), <i>PPT5</i> (3.0%)	5.2%
<i>Pasania-Elaeocarpus</i> cloud forest	<i>PPT4</i> (34.4%), <i>PPT2</i> (26.4%), <i>PPT3</i> (20.5%), <i>WPR</i> (9.1%), <i>Tmax9</i> (5.0%), <i>PPT7</i> (4.5%)	6.8%
<i>Drypetes-Helicia</i> forest	<i>PPT3</i> (42.7%), <i>PPT2</i> (16.0%), <i>TD</i> (13.6%), <i>Tmax1</i> (10.8%), <i>PPT1</i> (6.6%), <i>Tmax8</i> (6.5%), <i>PPT8</i> (3.9%)	5.7%
<i>Dysoxylum-Machilus</i> forest	<i>Tave2</i> (45.7%), <i>Tmax1</i> (40.4%), <i>PPT5</i> (13.8%)	7.0%
<i>Illicium-Cyclobalanopsis</i> winter monsoon forest	<i>PPT4</i> (43.2%), <i>Tmin1</i> (31.6%), <i>TD</i> (25.1%)	5.6%
<i>Pyrenaria-Machilus</i> winter monsoon forest	<i>TD</i> (48.1%), <i>PPT11</i> (28.1%), <i>PPT1</i> (15.1%), <i>PPT12</i> (8.6%)	6.8%

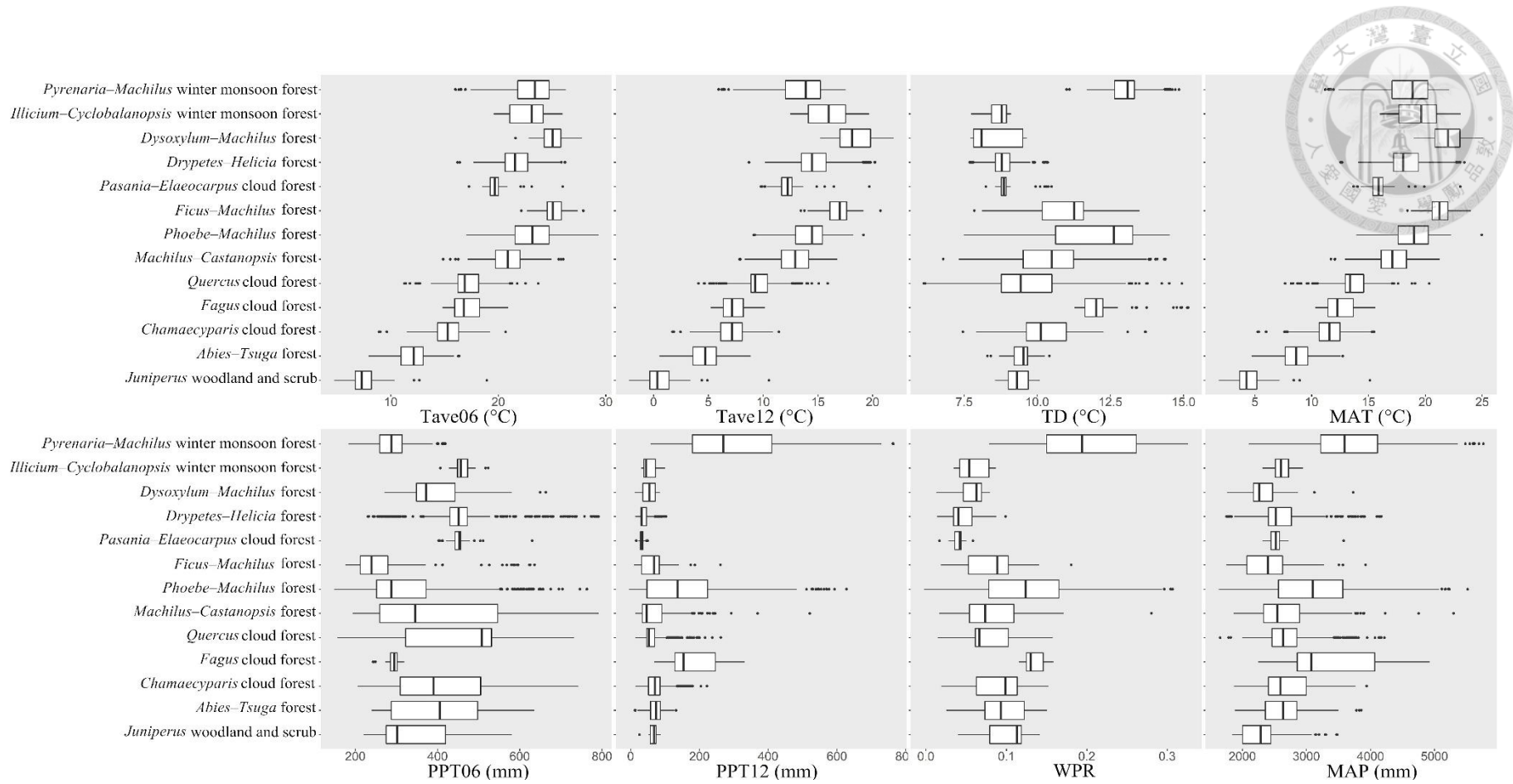
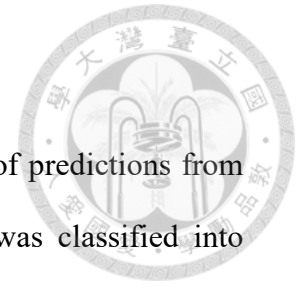


Fig. 3.3. Range of climatic variable estimates on the location of sampling plots of each forest type.

Predicted vegetation map



A predicted vegetation map was obtained based on the ensemble of predictions from multiple forests. Climate environment of the entire study area was classified into potential habitats of 13 forest types (Fig. 3.4). The predicted map displays an obvious altitudinal zonation from high-mountain woodland to montane cloud forests, followed by the latitudinal differentiation of sub-montane and foothill forests in the subtropical and tropical parts of Taiwan. Two azonal forests, the tropical *Illicium–Cyclobalanopsis* forest and the subtropical *Pyrenaria–Machilus* forest, are mapped in the southern peninsula and the northeast corner. *Ficus–Machilus* forest is the most widespread vegetation, occupying 25.64% of Taiwan’s slope land. The rank of occupying area is followed by *Quercus* cloud forest (13.22%), *Machilus–Castanopsis* (12.05%), and *Phoebe–Machilus* forest (11.74%). High-mountain habitats with a total area of 390,000 ha, which are suitable for coniferous woodland and forests such as *Juniperus*, *Abies*, *Tsuga*, and *Chamaecyparis*, account for 14.52% of the study area. The area of habitats suitable for tropical mountain zonal forests is close to high-mountain vegetation (390,000 ha, accounts for 14.49%) but distribution is relatively sparse among the predicted regions (Table 3.4).

The altitudinal distribution of forests showed that most forest types dominate in a distinct altitudinal range (Fig. 3.5); for example, *Juniperus* woodland and scrub occupied a mean elevation of 3,078m asl, *Abies–Tsuga* forest at 2,743m asl, *Chamaecyparis* cloud forest at 2,274m asl, and *Pasania–Elaeocarpus* cloud forest at 1657m asl in southern Taiwan. However, the altitudinal ranges of some forest types are overlapped and mixed; for example, *Fagus* cloud forest co-occurs with *Quercus* cloud forest at an elevation of 1,700m asl, *Machilus–Castanopsis* and *Phoebe–Machilus* forests are generally co-dominant at elevations of 800–1,000m asl, and two foothill

forest types, *Ficus–Machilus* and *Dysoxylum–Machilus* forests, are mixed at elevations of 200–300m asl in southern Taiwan (Fig. 3.5).



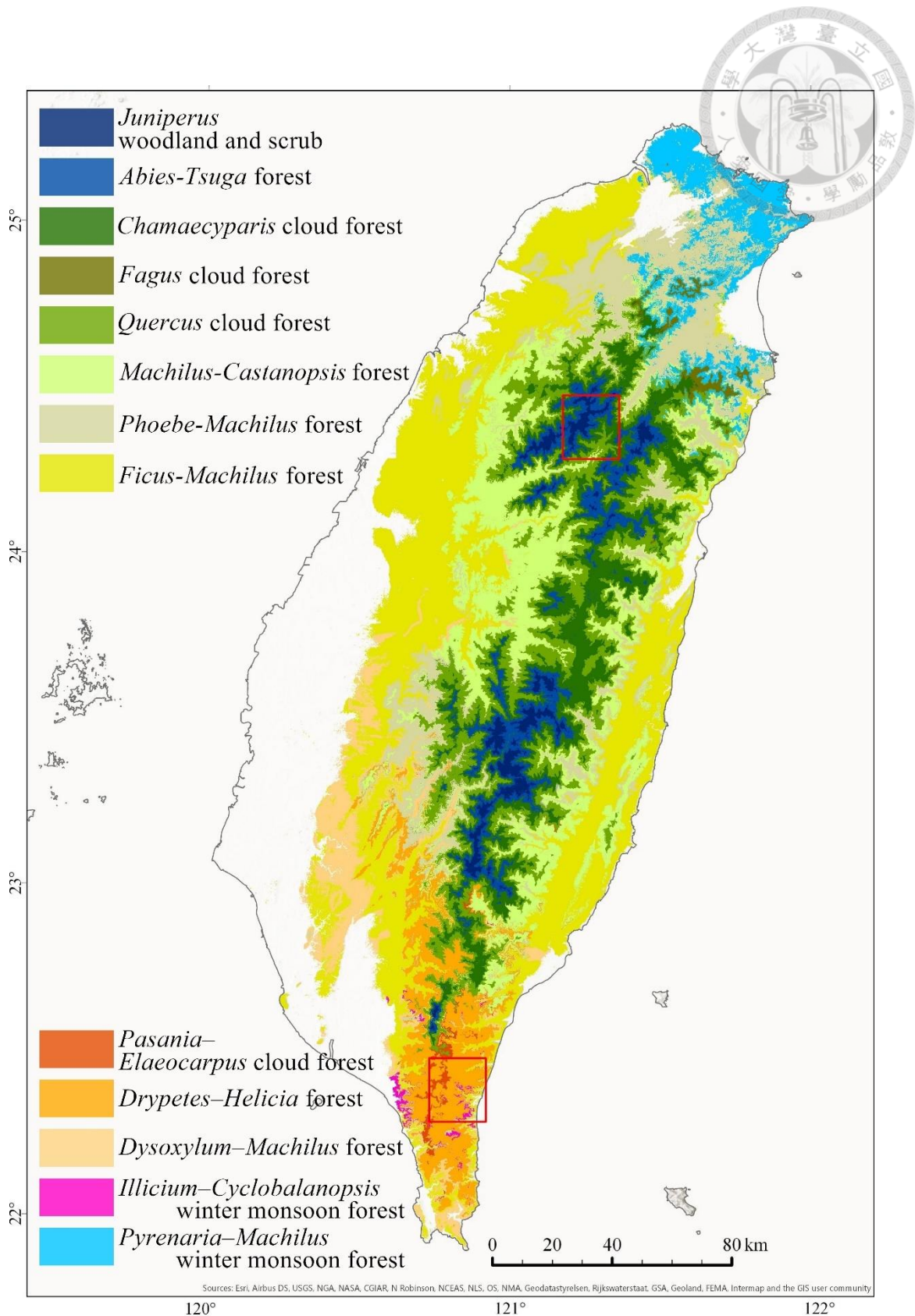


Fig. 3.4. Predicted vegetation map of study area based on the ensemble of suitability of each forest type. The red rectangles are sample areas for illustrating the map in detail (see Fig. 3.6).

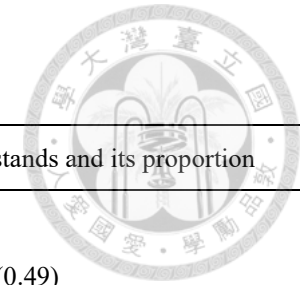


Table 3.4. The area statistics of predicted forest types, pure stand and mixed stand are included (Unit: ha).

Predicted forest type	Total area	%	Pure stand		Mixed stand		Coexisted forest type(s) within mixed stands and its proportion
			Area	%	Area	%	
<i>Juniperus</i>	29,134	1.08%	13,590	46.65%	15,544	53.35%	<i>Abies-Tsuga</i> (1.00)
<i>Abies-Tsuga</i>	114,151	4.21%	76,930	67.39%	37,221	32.61%	<i>Juniperus</i> (0.42), <i>Chamaecyparis</i> (0.58)
<i>Chamaecyparis</i>	250,006	9.23%	204,420	81.77%	45,586	18.23%	<i>Abies-Tsuga</i> (0.47), <i>Fagus</i> (0.04), <i>Quercus</i> (0.49)
<i>Fagus</i>	15,433	0.57%	9,993	64.75%	5,440	35.25%	<i>Chamaecyparis</i> (0.30), <i>Quercus</i> (0.06), <i>Pyrenaria-Machilus</i> (0.64)
<i>Quercus</i>	358,009	13.22%	322,318	90.03%	35,691	9.97%	<i>Chamaecyparis</i> (0.62), <i>Fagus</i> (0.01), <i>Machilus-Castanopsis</i> (0.24), <i>Phoebe-Machilus</i> (0.04), <i>Pasania-Elaeocarpus</i> (0.02), <i>Pyrenaria-Machilus</i> (0.07)
<i>Machilus-Castanopsis</i>	326,277	12.05%	233,338	71.52%	92,939	28.48%	<i>Quercus</i> (0.09), <i>Phoebe-Machilus</i> (0.65), <i>Ficus-Machilus</i> (0.14), <i>Pasania-Elaeocarpus</i> (0.01), <i>Drypetes-Helicia</i> (0.07), <i>Pyrenaria-Machilus</i> (0.04)
<i>Phoebe-Machilus</i>	318,017	11.74%	185,980	58.48%	132,037	41.52%	<i>Quercus</i> (0.02), <i>Machilus-Castanopsis</i> (0.46), <i>Ficus-Machilus</i> (0.28), <i>Drypetes-Helicia</i> (0.02), <i>Pyrenaria-Machilus</i> (0.22)
<i>Ficus-Machilus</i>	694,606	25.64%	531,653	76.54%	162,953	23.46%	<i>Machilus-Castanopsis</i> (0.08), <i>Phoebe-Machilus</i> (0.23), <i>Drypetes-Helicia</i> (0.01), <i>Dysoxylum-Machilus</i> (0.66), <i>Illicium-Cyclobalanopsis</i> (0.02)
<i>Pasania-Elaeocarpus</i>	8,750	0.32%	5,474	62.57%	3,276	37.43%	<i>Quercus</i> (0.19), <i>Machilus-Castanopsis</i> (0.01), <i>Ficus-Machilus</i> (0.02), <i>Drypetes-Helicia</i> (0.62), <i>Dysoxylum-Machilus</i> (0.11), <i>Illicium-Cyclobalanopsis</i> (0.05)
<i>Drypetes-Helicia</i>	143,575	5.30%	111,772	77.85%	31,803	22.15%	<i>Machilus-Castanopsis</i> (0.20), <i>Phoebe-Machilus</i> (0.08), <i>Ficus-Machilus</i> (0.04), <i>Pasania-Elaeocarpus</i> (0.06), <i>Dysoxylum-Machilus</i> (0.20), <i>Illicium-Cyclobalanopsis</i> (0.42)
<i>Dysoxylum-Machilus</i>	240,205	8.87%	122,659	51.06%	117,546	48.94%	<i>Ficus-Machilus</i> (0.91), <i>Drypetes-Helicia</i> (0.06), <i>Illicium-Cyclobalanopsis</i> (0.03)
<i>Illicium-Cyclobalanopsis</i>	27,314	1.01%	8,096	29.64%	19,218	70.36%	<i>Ficus-Machilus</i> (0.17), <i>Pasania-Elaeocarpus</i> (0.01), <i>Drypetes-Helicia</i> (0.68), <i>Dysoxylum-Machilus</i> (0.14)
<i>Pyrenaria-Machilus</i>	182,806	6.75%	142,180	77.78%	40,626	22.22%	<i>Fagus</i> (0.09), <i>Quercus</i> (0.06), <i>Machilus-Castanopsis</i> (0.12), <i>Phoebe-Machilus</i> (0.72), <i>Ficus-Machilus</i> (0.01)
Uncertain	506	0.02%	-	-	-	-	
Total	2,708,789	100.00%	1,968,403	72.67%	739,880	27.33%	

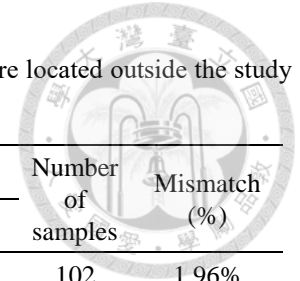
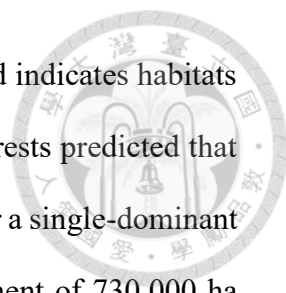


Table 3.5. A confusion matrix of actual forest type versus predicted forest type for evaluating the accuracy of ensemble predictions. Seven plots are located outside the study area and eliminated from this evaluation.

	Predicted forest types													Number of samples	Mismatch (%)	
	<i>J.</i>	<i>A.-T.</i>	<i>C.</i>	<i>F.</i>	<i>Q.</i>	<i>M.-C.</i>	<i>P.-M.</i>	<i>F.-M.</i>	<i>P.-E.</i>	<i>D.-H.</i>	<i>D.-M.</i>	<i>I.-C.</i>	<i>P.-M.</i>			
<i>Juniperus</i>	100	1			1									102	1.96%	
<i>Abies-Tsuga</i>		82	7											89	7.87%	
<i>Chamaecyparis</i>		4	511	3	22	1							2	543	5.89%	
<i>Fagus</i>			1	53										1	55	3.64%
<i>Quercus</i>		3	32	3	992	14	3		10					1	1058	6.24%
<i>Machilus-Castanopsis</i>			1	1	9	308	11	1		17	1	1	9	359	14.21%	
<i>Phoebe-Machilus</i>					3	14	365	8		2		1	17	410	10.98%	
<i>Ficus-Machilus</i>							1	141		1	1			144	2.08%	
<i>Pasania-Elaeocarpus</i>									55	1		1		57	3.51%	
<i>Drypetes-Helicia</i>					1	5		2	3	410	1	3		425	3.53%	
<i>Dysoxylum-Machilus</i>										2	24			26	7.69%	
<i>Illicium-Cyclobalanopsis</i>									4	3		33		40	17.50%	
<i>Pyrenaria-Machilus</i>			1	1	1	1	14						491	509	3.54%	
Outside														7	-	
Number of predictions	100	90	553	61	1029	343	394	152	62	446	27	39	521	3824	6.59%	



The workflow of Fig. 3.2 depicts core region of each forest type and indicates habitats where adjacent forest types coexisted. The ensemble of multiple forests predicted that 72.67% of the study area (1,970,000 ha) was climatically suitable for a single-dominant forest type, classified as a pure stand. However, climatic environment of 730,000 ha (~27.33% of the study area) was predicted to be suitable for two or more coexisting forest types, classified as a mixed stand. The remaining areas, 506 ha (0.02%), could not be identified by the RF models and are classified as uncertain (Table 3.4). Fig. 3.6 shows examples illustrating the predicted pure stands and mixed stands in the high-mountain areas of north Taiwan (Fig. 3.6a) and in the tropical low hills of south Taiwan (Fig. 3.6b). Because of topographical influences on mesoclimate in the mountains, including lapse rate, orographic precipitation, and windward effects, the occurrence of mixed stands usually follow the iso-altitudinal belts on slopes. However, the spatial extent of the predicted mixed stands stretches from hundreds to thousands of meters in width, depending on mountain steepness, aspect, and climate variation. The *Ficus–Machilus* forest is the most widespread forest type but it also shares a broader area of mixed stands of 160,000 ha with other forests, 66% of which (~110,000 ha) are habitats mixed with *Dysoxylum–Machilus* forest, mainly distributed in the tropical lowland of Taiwan. The *Phoebe–Machilus* forest (130,000 ha in total), primarily occurring at a middle elevation of 800m asl, is another forest type which has 46% (~60,000 ha) of mixed stands with its upper neighboring *Machilus–Castanopsis* forest at the ranges of 850–1,000m asl.

Statistical evaluation of the ensemble model

In addition to the OOB error assessed during the model-building process of each forest type, the overall accuracy of the ensemble RF models was evaluated by comparing the prediction at locations of the 3817 forest-type-classified plots (Table 3.5). Model errors

of fit (mismatch rate) were low for most forest types, ranging from 1.96% to 17.50% with an average of 6.59%. The findings revealed that the performance of the RF model was lower for distinguishing three vegetation types, namely *Illicium–Cyclobalanopsis* winter monsoon forest (error = 17.50%), *Machilus–Castanopsis* forest (error = 14.21%), and *Phoebe–Machilus* forest (error = 10.98%). These three forest types mainly occur at elevations from 479 to 1,030m asl, the altitudinal range where several vegetation types tend to coexist and form mixed stands in Taiwan (Fig. 3.5).

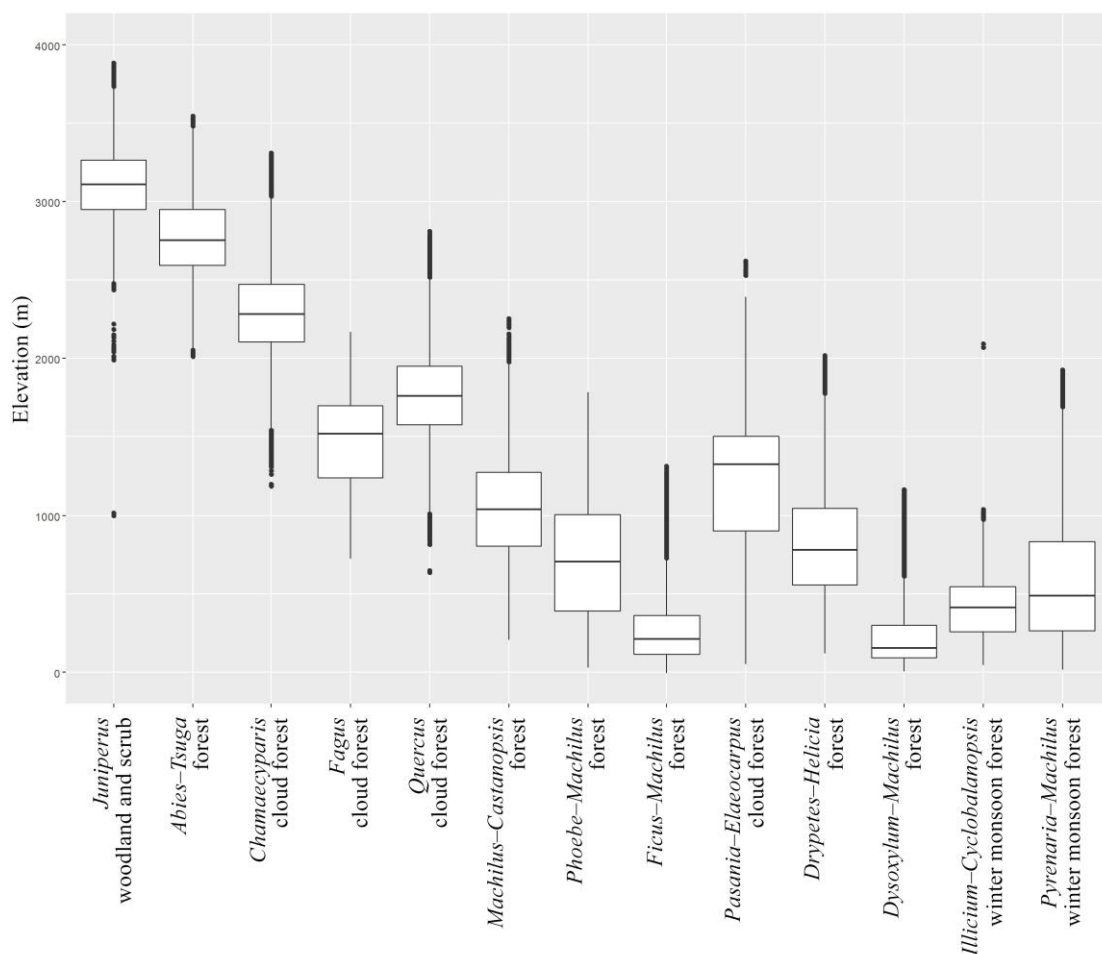
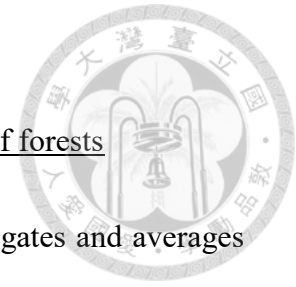


Fig. 3.5. The altitudinal ranges of forests based on the predicted vegetation map. Core habitats of most forest types occupied distinct altitudinal regions, however, habitats of some forests (eg. *Fagus* & *Quercus*, *Machilus–Castanopsis* & *Phoebe–Machilus*, *Pasania–Elaeocarpus* & *Drypetes–Helicia*, *Ficus–Machilus* & *Dysoxylum–Machilus*) were partially overlapped in elevation.

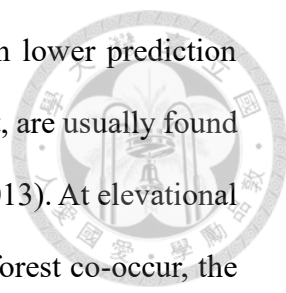
DISCUSSION

Model accuracy and its ability to predict the potential distribution of forests



The Random Forests approach is an ensemble classifier that aggregates and averages predictions across multiple trees to generate robust outcomes. This method has been recommended for modeling the ecological niche of organisms and predicting their potential distribution (Wang et al., 2012; Chiu et al., 2013; Zhang et al., 2015), and it has been widely applied on both regional and global scales for the use of conservation and adaptation to environmental change (Rehfeldt et al., 2006; Attorre et al., 2011; Rehfeldt et al., 2012; Wang et al., 2016b). In this study, RF models performed with a high degree of accuracy in predicting the potential distribution of forest vegetation in Taiwan, with a mismatch rate of 6.59% on average.

However, the prediction accuracy of several forest types is comparatively lower, such as *Illicium–Cyclobalanopsis* winter monsoon forest (with a mismatch rate of 17.50%), *Machilus–Castanopsis* forest (14.21%), and *Phoebe–Machilus* forest (10.98%). Several possible reasons for this result are as follows: (1) *Illicium–Cyclobalanopsis* forest is tropical vegetation exposed to winter monsoon directly, which is characterized by its cold-humid climate during winter, the high stem density, and richness in sclerophyllous species. This forest type is narrowly restricted to windward hill ridges, but converts to high canopy leeward or to valley forests dramatically as the topography changes (Chao et al., 2010; Li et al., 2013). In southern Taiwan, the habitats of *Illicium–Cyclobalanopsis* forest are usually fragmented and form a mosaic with sub-montane and foothill forests such as *Drypetes–Helicia* forest, *Ficus–Machilus* forest, and *Dysoxylum–Machilus* forest. The transition of vegetation can occur in a very short distance, even less than 50m (Chao et al., 2007), which is too localized for the climate downscaling model to detect, resulting in a high percentage of mixed stand and low



accuracy in the RF predictions; (2) the other two forest types with lower prediction accuracy, *Machilus–Castanopsis* forest and *Phoebe–Machilus* forest, are usually found at similar altitudinal ranges of 400–1,800 and 0–1,400m (Li et al., 2013). At elevational ranges where *Machilus–Castanopsis* forest and *Phoebe–Machilus* forest co-occur, the former usually dominates on ridges with drier and well-developed soil, whereas the latter has a low abundance and frequency of Fagaceae and tends to occur in relatively narrow, shaded valleys, and humid habitats. The similarity in altitudinal ranges in combination with differentiation among micro habitats for *Machilus–Castanopsis* forest and *Phoebe–Machilus* forest may explain the lower prediction accuracy.

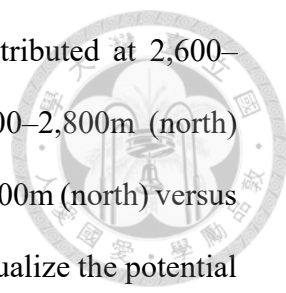
Although a machine-learning model is difficult to interpret due to its complex variables, it can provide a starting point for identifying key predictor variables and testing theory in an experimental framework. For example, our results show that temperature variables contribute to distinctly separate potential habitats of *Juniperus* woodland, *Abies–Tsuga*, *Chamaecyparis*, and *Fagus* forests (Table 3.3). Maximum monthly temperature of growing season, especially at the thresholds of 15°C (May) and 16.5°C (June), closely correspond with the boundaries of *Juniperus* woodland and *Abies–Tsuga* forest. For *Chamaecyparis* and *Fagus* forests, the important variables contribute to the RF model shift to winter temperature; for example the thresholds of 7.2°C (*Tave* of Dec.), 11.9°C (*Tmax* of Feb.), 5.9°C (*Tave* of Jan.) for *Chamaecyparis* forest; and monthly maximum temperatures of 12.4°C (Dec.), 11.6°C (Feb.), 10.7°C (Jan.) for *Fagus* forest. The results also indicate that annual temperature difference (TD) and winter precipitation play important roles in identifying the potential habitat of *Fagus* from other forest types. The range and threshold of predictors from a machine-learning model can provide insight into ways of broader exploration in ecosystems and can lead to a better understanding of forest habitat differentiation.

Detailed inspections of the RF model predictions

Gradients of the physical environment may result in the presence of varying organisms and communities, which can lead to directional changes in the composition, physiognomy, and biological interactions of forests (Whittaker, 1975). A prominent niche model should elucidate factors that critically relate to biological phenomena, and precisely project these factors to their spatial extent.

In Taiwan, it has been reported that the mountain temperatures for a given elevation are higher at the central part of the mountain range, and lower at both the north and the south end (Su, 1984a). This phenomenon may be attributed to the heat retention mechanism of Massenerhebung (Su, 1984a) or the cooling effect induced by northeast monsoon (Chiou et al., 2010), and it is responsible for the altitudinal compression of vegetation zones at the northern and southern tips of Taiwan, while a most extensive and distinguishable zonation in the middle part can be found. This pattern can be well-simulated by our approach. Fig. 3.7 illustrates the north-south profiles on model predictions of seven selected forest types, which are widespread throughout Taiwan, and demonstrates evident downward compression of vegetation zones in the north and south ends while a more extensive altitudinal distribution was modeled in central Taiwan.

Except for the large-scale climate patterns, topo-climatic variations such as rain shadow, radiative difference, and windward cooling, also influence the local distribution of forests. Snow Mountain is a mountain mass located in the middle of the northwest and central west climate region of Taiwan with the highest peak at an elevation of 3886m, where its northeast-facing slope is cool and humid due to the lack of sunlight and moist air brought by the winter monsoon, yet a relatively warm and dry environment is formed on its south slope (Su, 1985). Su (1984b) reported that similar vegetation types occurred



at lower elevations on the north-facing slope, eg. *Abies* zone distributed at 2,600–3,100m (north) versus 2,900–3,400m (south); *Tsuga* zone at 2,200–2,800m (north) versus 2,200–2,900m (south); and *Chamaecyparis* zone at 1,600–2,300m (north) versus 1,700–2,400m (south). We applied the RF models to predict and visualize the potential distributions of forests on Snow Mountain (Fig. 3.6a and Appendix S1, or by the link of <https://youtu.be/NaR76WVDp30>) and verified it with observations by Su in 1984. The predicted forest distributions are in very close agreement with Su’s observation. Based on the work diagram of Fig. 3.2, the RF models also indicate the locations of mixed stand, which is analog to the characteristic of an ecotone—a community comprising part of the ecological features of its neighbors but having a specific site characteristic of its own (Holland and Risser, 1991; Barnes et al., 1997). On Snow Mountain for example, the models identified mixed stands, 400-m in width, between *Juniperus* woodland and *Abies–Tsuga* forest, and also mapped the transition between *Chamaecyparis* forest and *Quercus* forest.

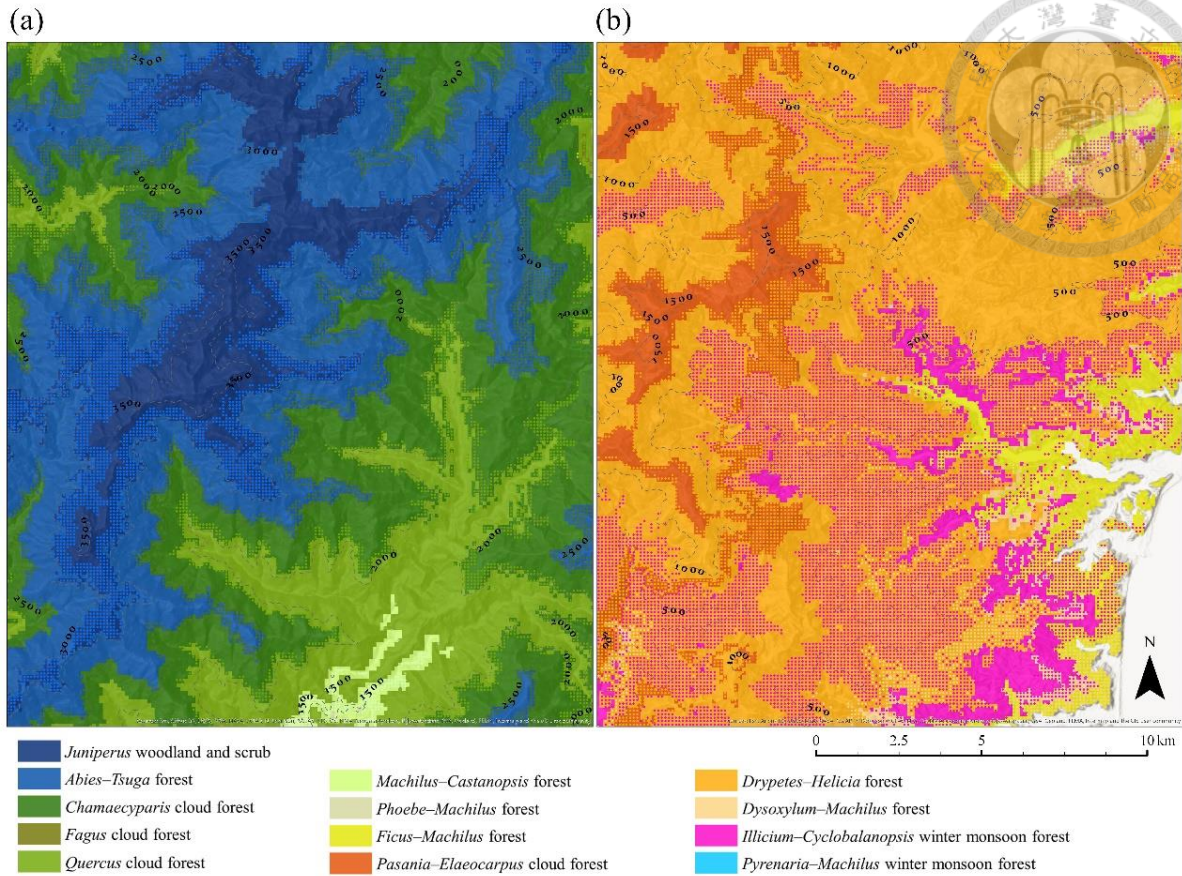


Fig. 3.6. The detailed mapping of predicted forest types. A pure stand is represented by a single color, whereas a mixed stand is indicated by the coexistence of a dot. (a) The prediction of high-mountain and subtropical montane forests with types of *Juniperus*, *Abies–Tsuga*, *Chamaecyparis*, *Quercus*, and *Machilus–Castanopsis*. The belt-like mixed stands usually occur along an iso-elevation hillside. (b) The predicted mapping of tropical forests in southeast Taiwan where tropical montane forests (*Pasania–Elaeocarpus* and *Drypetes–Helicia*) mixed with subtropical foothill forest (*Ficus–Machilus*) and tropical winter monsoon forest (*Illicium–Cyclobalanopsis*). Broadly mixed stands of *Drypetes–Helicia* forest and *Illicium–Cyclobalanopsis* forest occurred at the north slope in a valley, where a cooler habitat exposed to the northeast monsoon during winter is predicted.

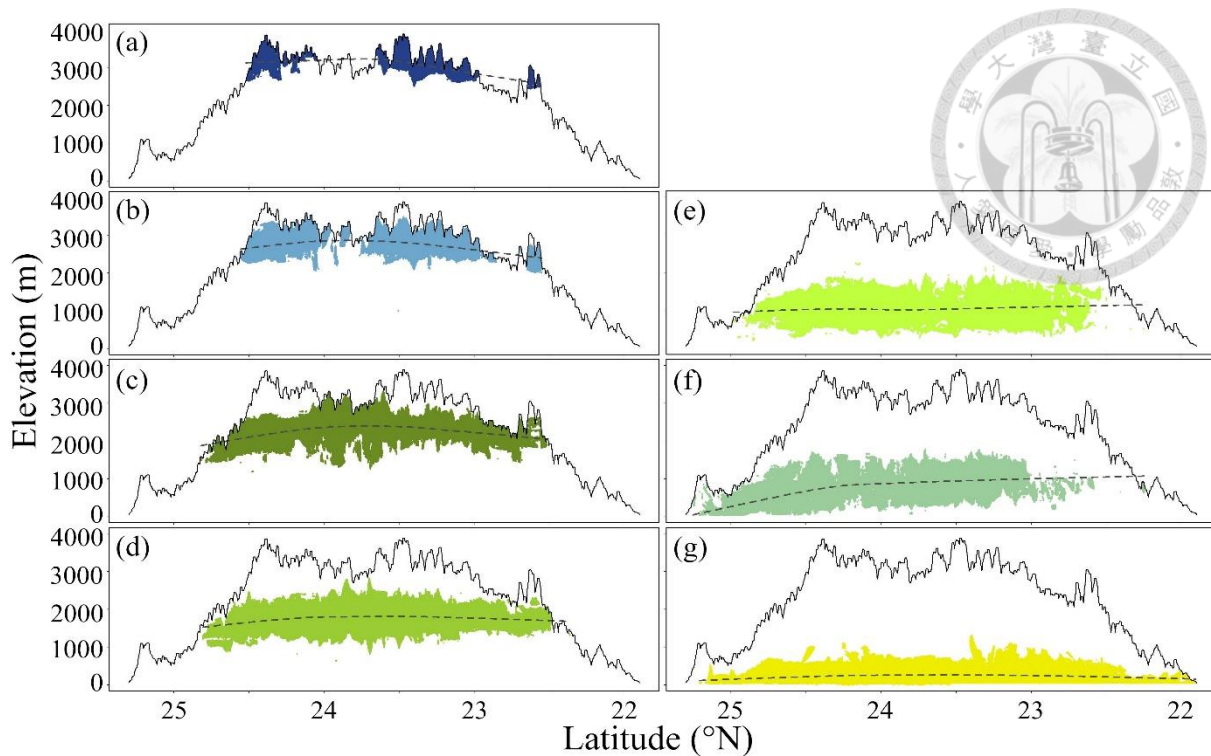


Fig. 3.7. Simulated distributions of seven selected zonal forest types on the elevational profile. (a) *Juniperus* woodland and scrub; (b) *Abies-Tsuga* forest; (c) *Chamaecyparis* cloud forest; (d) *Quercus* cloud forest; (e) *Machilus-Castanopsis* forest; (f) *Phoebe-Machilus* forest; (g) *Ficus-Machilus* forest.

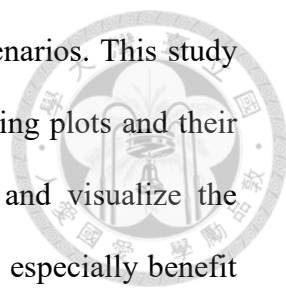
Applications of the RF model

In recent decades, climate data have become available from various sources published in fine-scale resolutions for ecological studies (Hannaway et al., 2005; Hijmans et al., 2005; Harris et al., 2014). The results of several studies in Europe (Hengl et al., 2018), North America (Rehfeldt et al., 2012; Wang et al., 2012), and mainland China (Zhang et al., 2015; Wang et al., 2016b) suggest that RF modeling is one of the optimal approaches for niche modeling and species distribution prediction, when sufficient presence and absence data exist (Zhang et al., 2015; Hengl et al., 2018). Fine-resolution predictions are particularly suitable for local interpretation and decision-making applications. Most ecological niche modeling studies have employed published global or regional climate databases, which represent the finest spatial resolutions of arc-

seconds or kilometers, but they are still too coarse to provide detailed information regarding mountainous and topographically diverse areas.

Besides, Species from adjacent zones may occur and coexist along the border of a given zone due to their close climatic suitability and ecological requirements. Because of the mixed, intermediate, and specific ecological characteristics of ecotones, they have been reported as important species-rich areas for influencing local and regional biodiversity patterns (Neilson, 1993; Martin et al., 2007). Inhabitants of ecotones are often near their physical limits and competitive tolerance, which means they may be sensitive to fluctuations and changes of environmental factors, and they are usually regarded as early indicators of the effects of climate change (Neilson, 1993; Risser, 1995; Wasson et al., 2013). The monitoring of migration patterns and compositional change in ecotones is one of the primary approaches for tracing the effects of climate change. For example, the range shift and demographical change of mountain forests often correspond with directional climatic change (Beniston, 2003; Beckage et al., 2008; Evans and Brown, 2017).

Taiwan is a relatively small continental island, where the interactions of humid monsoons, frequent typhoons, and dramatic topographical differences result in its diverse habitats and climatic conditions. The rainfall is enough for forest establishment over the whole island; however, factors including (1) the significant temperature gradient along elevational extent (Su, 1984b), (2) differences in seasonal precipitation (Su, 1985), and (3) mixed floras from tropical Asia and temperate Asia due to the island's historical and geographical context (Hsieh et al., 1994), co-contribute to the diverse forests harboring plants from tropical, temperate, and even subarctic regions. We suggest that potential vegetation maps in high resolution can be powerful aids to serve as drafts for stand classification, guides for optimal land use, and fundamental



models for projecting vegetation change under global warming scenarios. This study provides a statistical procedure integrating locations of field sampling plots and their corresponding climate variable estimates to calculate, simulate, and visualize the potential distribution of climatic-related forests. These applications especially benefit regions with complicated landscape mosaics with highly differentiated vegetation communities, such as Taiwan. When detailed and precise training data applied, eg. the updated climate historical observations, future climate change scenarios, or supplemented information from more field plots, this procedure is reproducible and can be used to update the predicted forest map for prompt use in resource management.

Last, we acknowledge that this study and its findings have several limitations. Azonal forests, whose occurrence and mortality are largely affected by non-climatic factors such as disturbances, succession, hydrologic regimes, and edaphic conditions, were not examined in detail. Although climate plays an important role in the distribution of zonal forests, there are still mechanical processes—such as competition, dispersal ability, and biotic or abiotic interactions—that are not considered by the statistical model in this study. Clearly, correlational modeling approaches can provide effective indications regarding ecological niches and potential distributions of organisms for the use in large-scale resource management, but non-climatic variables and mechanical processes should also be considered while conducting planning and management of natural resources at local scales.

AUTHOR CONTRIBUTIONS

HYL and JMH conceived the research idea and led the writing; CFL, TYC, and CFH contributed the data and vegetation classification; HYL performed the statistical

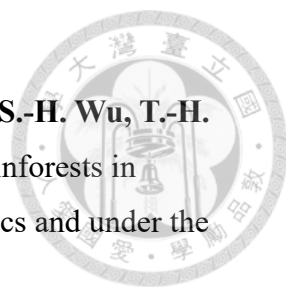
analyses with contributions from GW and TW; all authors discussed the results and commented on the manuscript.



LITERATURE CITED

- Attorre, F., M. Alfò, M. Sanctis, B. Francesconi, R. Valenti, M. Vitale and F. Bruno.** 2011. Evaluating the effects of climate change on tree species abundance and distribution in the Italian peninsula. *Applied Vegetation Science* **14**: 242–255. <https://doi.org/10.1111/j.1654-109X.2010.01114.x>
- Bailey, R. G.** 1983. Delineation of ecosystem regions. *Environmental Management* **7**: 365–373. <https://doi.org/10.1007/BF01866919>
- Barnes, B. V., D. R. Zak, S. R. Denton and S. H. Spurr.** 1997. *Forest Ecology*. 4th Edition, John Wiley & Sons, Inc., New York, 774 pp.
- Beckage, B., B. Osborne, D. G. Gavin, C. Pucko, T. Siccama and T. Perkins.** 2008. A rapid upward shift of a forest ecotone during 40 years of warming in the Green Mountains of Vermont. *PNAS* **105**: 4197–4202. <https://doi.org/10.1073/pnas.0708921105>
- Beniston, M.** 2003. Climatic change in mountain regions: a review of possible impacts. *Climatic Change* **59**: 5–31. <https://doi.org/10.1023/A:1024458411589>
- Breiman, L.** 2001. Random forests. *Machine learning* **45**: 5–32. <https://doi.org/10.1023/A:1010933404324>
- Brinkmann, K., A. Patzelt, E. Schlecht and A. Buerkert.** 2011. Use of environmental predictors for vegetation mapping in semi-arid mountain rangelands and the determination of conservation hotspots. *Applied Vegetation Science* **14**: 17–30. <https://doi.org/10.1111/j.1654-109X.2010.01097.x>
- Chang, L.-M.** 1974. Ecological studies on the vegetation of eastern coastal area of Taiwan. *Quarterly Journal of Chinese Forestry* **7**: 115–131. [In Chinese.]
- Chao, W.-C., K.-J. Chao, G.-Z. M. Song and C.-F. Hsieh.** 2007. Species composition and structure of the lowland subtropical rainforest at Lanjenchi,

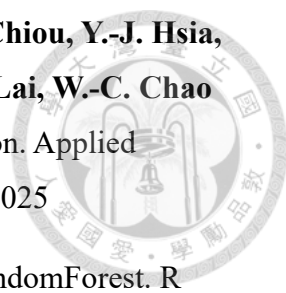
southern Taiwan. *Taiwania* **52**: 253–269.

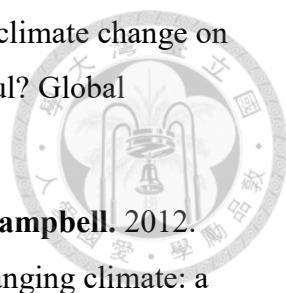
- 
- Chao, W.-C., G.-Z. M. Song, K.-J. Chao, C.-C. Liao, S.-W. Fan, S.-H. Wu, T.-H. Hsieh, I.-F. Sun, Y.-L. Kuo and C.-F. Hsieh.** 2010. Lowland rainforests in southern Taiwan and Lanyu, at the northern border of Paleotropics and under the influence of monsoon wind. *Plant Ecology* **210**: 1–17.
- Chen, C., A. Liaw and L. Breiman.** 2004. Using random forest to learn imbalanced data. University of California, Berkeley. Retrieved from <https://statistics.berkeley.edu/sites/default/files/tech-reports/666.pdf>
- Chiou, C.-R., G.-Z. M. Song, J.-H. Chien, C.-F. Hsieh, J.-C. Wang, M.-Y. Chen, H.-Y. Liu, C.-L. Yeh, Y.-J. Hsia and T.-Y. Chen.** 2010. Altitudinal distribution patterns of plant species in Taiwan are mainly determined by the northeast monsoon rather than the heat retention mechanism of Massenerhebung. *Botanical Studies* **51**: 89–97.
- Chiu, C.-A., T.-Y. Chen, C.-C. Wang, C.-R. Chiou, Y.-J. Lai and C.-Y. Tsai.** 2013. Using BIOMOD2 to model the species distribution of *Fagus hayatae*. *Quarterly Journal of Forest Research* **35**: 253–272. [In Chinese with English summary.]
- Evans, P. and C. D. Brown.** 2017. The boreal-temperate forest ecotone response to climate change. *Environmental Reviews* **25**: 423–431. <https://doi.org/10.1139/er-2017-0009>
- Fang, J.-Y., Y.-C. Song, H.-Y. Liu and S.-L. Piao.** 2002. Vegetation-climate relationship and its application in the division of vegetation zone in China. *Acta Botanica Sinica* **44**: 1105–1122.
- Genuer, R., J. M. Poggi and C. Tuleau-Malot.** 2015. VSURF: an R package for variable selection using random forests. *The R Journal* **7(2)**: 19–33.
- Hannaway, D. B., C. Daly, W. X. Cao, W. H. Luo, Y. R. Wei, W. L. Zhang, A. G. Xu, C. A. Lu, X. Z. Shi and L. X. Li.** 2005. Forage species suitability mapping for China using topographic, climatic and soils spatial data and quantitative plant tolerances. *Agricultural Science in China* **4(9)**: 660–667.
- Hansen, A. J. and L. B. Phillips.** 2015. Which tree species and biome types are most vulnerable to climate change in the US Northern Rocky Mountains? *Forest*

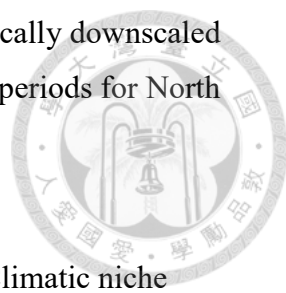
Ecology and Management **338**: 68–83.
<https://doi.org/10.1016/j.foreco.2014.11.008>



- Harris, I., P. D. Jones, T. J. Osborn and D. H. Lister.** 2014. Updated high-resolution grids of monthly climatic observations-the CRU TS 3.10 Dataset. *International Journal of Climatology* **34**: 623–642.
<https://doi.org/10.1002/joc.3711>
- Hengl, T., M. G. Walsh, J. Sanderman, I. Wheeler, S. P. Harrison and I. C. Prentice.** 2018. Global mapping of potential natural vegetation: an assessment of Machine Learning algorithms for estimating land potential. *PeerJ* **6**: e5457.
<https://doi.org/10.7717/peerj.5457>
- Hijmans, R. J., S. E. Cameron, J. L. Parra, P. G. Jones and A. Jarvis.** 2005. Very high resolution interpolated climate surface for global land areas. *International Journal of Climatology* **25**: 1965–1978. <https://doi.org/10.1002/joc.1276>
- Holdridge, L. R.** 1947. Determination of world plant formations from simple climatic data. *Science* **105**: 367–368. <https://doi.org/10.1126/science.105.2727.367>
- Holland, M. M. and P. G. Risser.** 1991. Introduction: the role of landscape boundaries in the management and restoration of changing environments. In M.M. Holland, P.G. Risser & R.J. Naiman (Eds.), *Ecotone: the role of landscape boundaries in the management and restoration of changing environments* (pp. 1–7). Chapman & Hall, New York, New York, USA.
- Hsieh, C.-F., C.-F. Shen and K.-C. Yang.** 1994. Introduction to the flora of Taiwan, 3: floristics, phytogeography, and vegetation. In Huang & Editorial Committee of the Flora of Taiwan (Eds.), *Flora of Taiwan Second edition* (pp. 7–16). Editorial Committee of the Flora of Taiwan, Taipei.
- Hsu, H.-H., C. Chou, Y.-C. Wu, M.-M. Lu, C.-T. Chen and Y.-M. Chen.** 2011. *Climate Change in Taiwan: Scientific Report 2011 (Summary)*. National Science Council, Taipei, Taiwan.
- Klassen, H. A. and P. J. Burton.** 2015. Climatic characterization of forest zones across administrative boundaries improves conservation planning. *Applied Vegetation Science* **18**: 343–356. <https://doi.org/10.1111/avsc.12143>

- 
- Li, C.-F., M. Chytrý, D. Zelený, M.-Y. Chen, T.-Y. Chen, C.-R. Chiou, Y.-J. Hsia, H.-Y. Liu, S.-Z. Yang, C.-L. Yeh, J.-C. Wang, C.-F. Yu, Y.-J. Lai, W.-C. Chao and C.-F. Hsieh.** 2013. Classification of Taiwan forest vegetation. *Applied Vegetation Science* **16**: 698–719. <https://doi.org/10.1111/avsc.12025>
- Liaw, A. and M. Wiener.** 2002. Classification and regression by randomForest. *R news* **2(3)**: 18–22.
- Lin, C.-T., C.-F. Li, D. Zelený, M. Chytrý, Y. Nakamura, M.-Y. Chen, T.-Y. Chen, Y.-J. Hsia, C.-F. Hsieh, H.-Y. Liu, J.-C. Wang, S.-Z. Yang, C.-L. Yeh and C.-R. Chiou.** 2012. Classification of the high-mountain coniferous forests in Taiwan. *Folia Geobot* **47**: 373-401.
- Lin, C.-Y., S.-C.C. Lung, H.-R. Guo, P.-C. Wu and H.-J Su.** 2009. Climate variability of cold surge and its impact on the air quality of Taiwan. *Climatic Change* **94**: 457–471. <https://doi.org/10.1007/s10584-008-9495-9>
- Lin, H.-Y., J.-M. Hu, T.-Y. Chen, C.-F. Hsieh, G. Wang and T. Wang.** 2018. A dynamic downscaling approach to generate scale-free regional climate data in Taiwan. *Taiwania* **63**: 245–266. <https://doi.org/10.6165/tai.2018.63.251>
- Liu, T.-S. and H.-J Su.** 1972. Synecological survey on the summer-green forest of north Chia-Tien Mountains. *Bulletin of Taiwan Museum* **15**: 1–16. [In Chinese.]
- Martin, P. H., R. E. Sherman and T. J. Fahey.** 2007. Tropical montane forest ecotones: climate gradients, natural disturbance, and vegetation zonation in the Cordillera Central, Dominican Republic. *Journal of Biogeography* **34**: 1792–1806. <https://www.jstor.org/stable/4640645>
- Matsui, T., K. Nakao, M. Higa, I. Tsuyama, Y. Kominami, T. Yagihashi, D. Koide and N. Tanaka.** 2018. Potential impact of climate change on canopy tree species composition of cool-temperate forests in Japan using a multivariate classification tree model. *Ecological Research* **33**: 289–302. <https://doi.org/10.1007/s11284-018-1576-2>
- Neilson, R. P.** 1993. Transient ecotone response to climatic change: Some conceptual and modelling approaches. *Ecological Applications* **3**: 385–395. <https://doi.org/10.2307/1941907>

- 
- Pearson, R. G. and T. P. Dawson.** 2003. Predicting the impacts of climate change on the distribution of species: are bioclimate envelope models useful? *Global Ecology & Biogeography* **12**: 361–371.
- Rehfeldt, G. E., N. L. Crookston, C. Sáenz-Romero and E. M. Campbell.** 2012. North American vegetation model for land-use planning in a changing climate: a solution to large classification problems. *Ecological Applications* **22**: 119–141. <https://doi.org/10.1890/11-0495.1>
- Rehfeldt, G. E., N. L. Crookston, M. V. Warwell and J. S. Evans.** 2006. Empirical analyses of plant-climate relationships for the western United States. *International Journal of Plant Sciences* **167**: 1123–1150. <https://doi.org/10.1086/507711>
- Risser, P. G.** 1995. The status of the science examining ecotones. *BioScience* **45**: 318–325.
- Sasaki, S.** 1924. Vegetation zones of Sin-Kao Shan. Report of Formosan Natural History Society **69**: 1–54. [In Japanese.]
- Su, H.-J.** 1984a. Studies on the climate and vegetation types of the natural forests in Taiwan (I). Analysis of the variations in climatic factors. *Quarterly Journal of Chinese Forestry* **17**: 1–14.
- Su, H.-J.** 1984b. Studies on the climate and vegetation types of the natural forests in Taiwan (II). Altitudinal vegetation zones in relation to temperature gradient. *Quarterly Journal of Chinese Forestry* **17**: 57–73.
- Su, H.-J.** 1985. Studies on the climate and vegetation types of the natural forests in Taiwan (III). A scheme of geographical climatic regions. *Quarterly Journal of Chinese Forestry* **18**: 33–44.
- Suzuki, T.** 1938. Associations of Laurilignosa in the watershed of Tong-Hou stream. *Japanese Journal of Ecology* **4**: 197–314. [In Japanese.]
- Wang, T., E. M. Campbell, G. A. O'Neill and S. N. Aitken.** 2012. Projecting future distributions of ecosystem climate niches: uncertainties and management applications. *Forest Ecology and Management* **279**: 128–140. <https://doi.org/10.1016/j.foreco.2012.05.034>

- 
- Wang, T., A. Hamann, D. Spittlehouse and C. Carroll.** 2016a. Locally downscaled and spatially customizable climate data for historical and future periods for North America. *PLoS ONE* **11(6)**: e0156720.
<https://doi.org/10.1371/journal.pone.0156720>
- Wang, T., G. Wang, J. Innes, C. Nitschke and H. Kang.** 2016b. Climatic niche models and their consensus projections for future climates for four major forest tree species in the Asia-Pacific region. *Forest Ecology and Management* **360**: 357–366. <https://doi.org/10.1016/j.foreco.2015.08.004>
- Wang, T., G. Wang, J. Innes, B. Seely and B. Chen.** 2017. ClimateAP: an application for dynamic local downscaling of historical and future climate data in Asia Pacific. *Frontiers of Agricultural Science and Engineering* **4**: 448–458.
<https://doi.org/10.15302/J-FASE-2017172>
- Wasson, K., A. Woolfolk and C. Fresquez.** 2013. Ecotones as indicators of changing environmental conditions: rapid migration of salt marsh-upland boundaries. *Estuaries and Coasts* **36**: 654–664. <https://doi.org/10.1007/s12237-013-9601-8>
- Weng, S.-P. and C.-T. Yang.** 2012. The construction of monthly rainfall and temperature dataset with 1km gridded resolution over Taiwan area (1960-2009) and its application to climate projection in the near future (2015-2039). *Atmospheric Sciences* **40**: 349–369. [In Chinese with English summary.]
- Whittaker, R. H.** 1975. *Communities and Ecosystems*. MacMillan Publishing, New York, USA.
- Zhang, L., S. Liu, P. Sun, T. Wang, G. Wang, X. Zhang and L. Wang.** 2015. Consensus forecasting of species distributions: the effects of niche model performance and niche properties. *PLoS ONE* **10(3)**: e0120056.
<https://doi.org/10.1371/journal.pone.0120056>
- Zhu, H., C. Yong, S. Zhou, H. Wang and L. Yan.** 2015. Vegetation, floristic composition and species diversity in a tropical mountain nature reserve in southern Yunnan, SW China, with implications for conservation. *Tropical Conservation Science* **8**: 528–546. <https://doi.org/10.1177/194008291500800216>

SUPPORTING INFORMATION

Appendix S1. Visualization of RF predictions at Snow Mountain region. Please find the sample movie by this link:

<https://www.youtube.com/watch?v=NaR76WVDp30>



Chapter 4




How much does climate change alter the distribution of forests across a great altitudinal gradient on a subtropical island?

Chapter 4 is a manuscript co-authored by Huan-Yu Lin, Jer-Ming Hu, Tze-Ying Chen, Chang-Fu Hsieh, Yu-Shiang Tung, Yung-Ming Chen, and Tongli Wang. The authors preserve the right to submit the texts, figures, and tables to a scientific journal.

Abstract

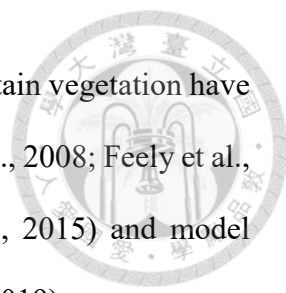
The impact of climate change on mountain forest ecosystems, involving potential range shifts, the progressive replacement of vegetation belts, and the local extinction of rare species, has particularly been concerned by ecologists. Taiwan is a high-mountain island with large altitudinal variations and diverse forest types driven by climate. In this study, we used the scale-free climate variable estimates and an established machine-learning approach to project the distributional changes of 13 climate-driven mountain forest types under selected global warming scenarios. The results demonstrated a consistent trend of the drastic habitat contractions of subalpine *Juniperus* woodland and the deciduous *Fagus* broadleaved forests (mostly disappear under moderate scenarios and disappear under high-emission scenarios). The projections also revealed that tropical montane cloud forest and tropical winter monsoon forest may be highly vulnerable under the extreme warm-humid or warm-dry climatic conditions because of the dramatic change in water availability. For the purpose of mitigating the risk of climate change to the vulnerable forest types, adaptive conservation strategies were suggested independently, in accordance with the environmental characteristics specific to each forest type.



KEY WORDS: Climate change impact, East Asia, Ecological niche modeling, Tropical montane forest, Subtropical montane forest, Random Forest, Taiwan.

INTRODUCTION

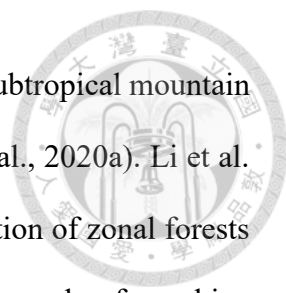
The mountain forest ecosystem is one of the most important storehouses of biodiversity, home to endemic and rare species, and an essential part of the globe (Lomolino, 2001; Beniston, 2003). Most mountain areas are experiencing serious ecological and environmental degradation, and the impact of climate change is an issue of the greatest concern (Beniston 2003). Mountains present the sharpest gradient in continental areas, including rapid change in climatic parameters over a very short distance, particularly temperature and precipitation. Lapse rate, the gradual decrease in air temperature with elevation by a rate of 5–7°C/km in the troposphere (Barry and Chorley, 2009), is the main factor that forms the rapid and directional temperature gradient along mountain slopes, creating diverse habitats of different vegetation types distributed within relatively small areas (Spehn et al., 2011). Thus, mountain ecosystems provide ideal materials to model vegetation-climate relationships and to predict response of vegetation to climate change. Vegetation types at mountain tops may be particularly vulnerable to climate change, imposing a serious challenge to genetic conservation and forest resource management. A first approximation of the response of mountain forests to a warming climate is the redistribution of organisms in the nearby altitudes to find optimal thermal conditions similar to their current habitats (Peters and Darling, 1985; Chen et al., 2011). According to this assumption, the expected impacts of climate change in the mountain biota would be the contraction of the coolest climatic zone at the top, which accompanies the upward shift and progressive replacement of vegetation belts (Pauli et al., 2012; Lenoir and Svenning,



2015; Morueta-Holme et al., 2015). In reality, upward shifts of mountain vegetation have been widely reported among both historical observations (Lenoir et al., 2008; Feely et al., 2011; Jump et al., 2012; Pauli et al., 2012; Morueta-Holme et al., 2015) and model projections (Costion et al., 2015; Matsui et al., 2018; Lin and Chiu, 2019).

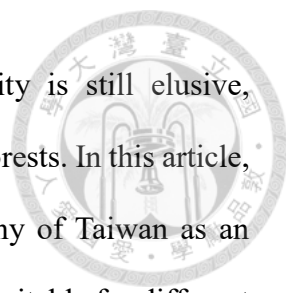
Research on terrestrial range shifts has been far more frequent in the Northern Hemisphere, chiefly within the latitudes 30–60°N, than in the Southern Hemisphere (Lenoir and Svenning, 2015). The currently available data for plant range shift studies are strongly biased toward boreal, temperate, and Mediterranean latitudes (Jump et al., 2009). Tropical and subtropical forests harbor most of the terrestrial biodiversity on the Earth (Myers et al., 2000), however, research efforts implemented to assess the potential change of forest distributions from tropics to subtropics are limited (Krishnaswamy et al., 2014). There are increasing evidences supporting the assumption that tropical forest biota is highly vulnerable to climate change (Corlett, 2011; Barlow et al., 2018). For example, biotic vulnerability may be enhanced by the low intrinsic climatic variability and the increased niche specialization of warm-adapted species (Feely et al., 2011; Perez et al., 2016), the complex interactions of heat and moisture (Pouteau et al., 2018), and the uncertainty in future precipitation or aridity projections (Tain et al., 2019), instead of a progressive upward or poleward march of species.

Taiwan is a subtropical island located on the west edge of the Pacific Ocean with a warm-humid climate brought by the East Asian monsoon. Steep mountains and huge climate variabilities create a pronounced forest zonation with changes in altitude. This forest zonation was firstly documented by Sasaki (1924) and Su (1984), and has been further classified into six altitudinal vegetation zones (Su, 1984) and 21 forest types in detail (Li et al., 2013). The forest zonation includes both the altitudinal zonation from subalpine to



montane cloud forests, followed by the latitudinal differentiation of subtropical mountain forests in the north and tropical montane forests in the south (Lin et al., 2020a). Li et al. (2013) suggested that the main factors responsible for the differentiation of zonal forests are temperature and moisture. Subsequently, a climate-based approach of machine learning was established to model this geographical distribution of zonal forest vegetation in Taiwan (Lin et al., 2020a); it was found that over 90% of the total variation among zonal vegetation types could be explained by climate variables and a fine-resolution vegetation map was obtained (Appendix S1). Although Taiwan is a small island with a minor latitudinal range extent, its diverse and distinct forest zonation along the steep and extensive elevational gradients provide ideal materials for exploring the potential impacts of climate change on forest distributions and range shifts.

Continuous instrumental measurement of climate parameters in Taiwan began in 1896. Data collected from six meteorological stations (Fig. 4.1) shows a significant warming trend. The mean annual temperature increased by 1.4°C in the past century, which is higher than the global warming rate of 0.07°C per decade (IPCC, 2013). In 1980–2009, the observed warming trend has accelerated at a rate of 0.29°C per decade with a faster increase in winter (Hsu et al., 2011). The century-long linear trend of precipitation change is not evident, whereas the number of raining days has decreased by 4 days per decade in the past 100 years and 6 days per decade in the past 30 years, with the fastest decreasing rate in summer (Hsu and Chen, 2002; Hung and Kao, 2010). The observed amplitude of warming is severe in Taiwan, however, the impact of climate change on mountain forests was only studied in particular communities or species, such as reports for the retreat of subalpine and upper-montane coniferous forests based on historical occurrences (Jump et al., 2012) and future projections (Lin et al., 2014), and the climatic niche modeling and projection for several broad-leaved tree species (Nakao et al., 2014; Lin and Chiu, 2019).



An intact assessment on the range shifts and habitat vulnerability is still elusive, especially for the widespread tropical and subtropical broad-leaved forests. In this article, we used the diverse climatic conditions and complicated topography of Taiwan as an example to predict potential impact of climate change on the habitat suitable for different forest types under different climate change scenarios. The goals of this study were to: (1) reveal the range shifts and the change of habitat suitability for forest types at different altitude, (2) identify the uncertainty of climatic niche modeling for each forest type under the selected climate change scenarios, and (3) assess the vulnerability of each mountain forest type under the influence of climate change.

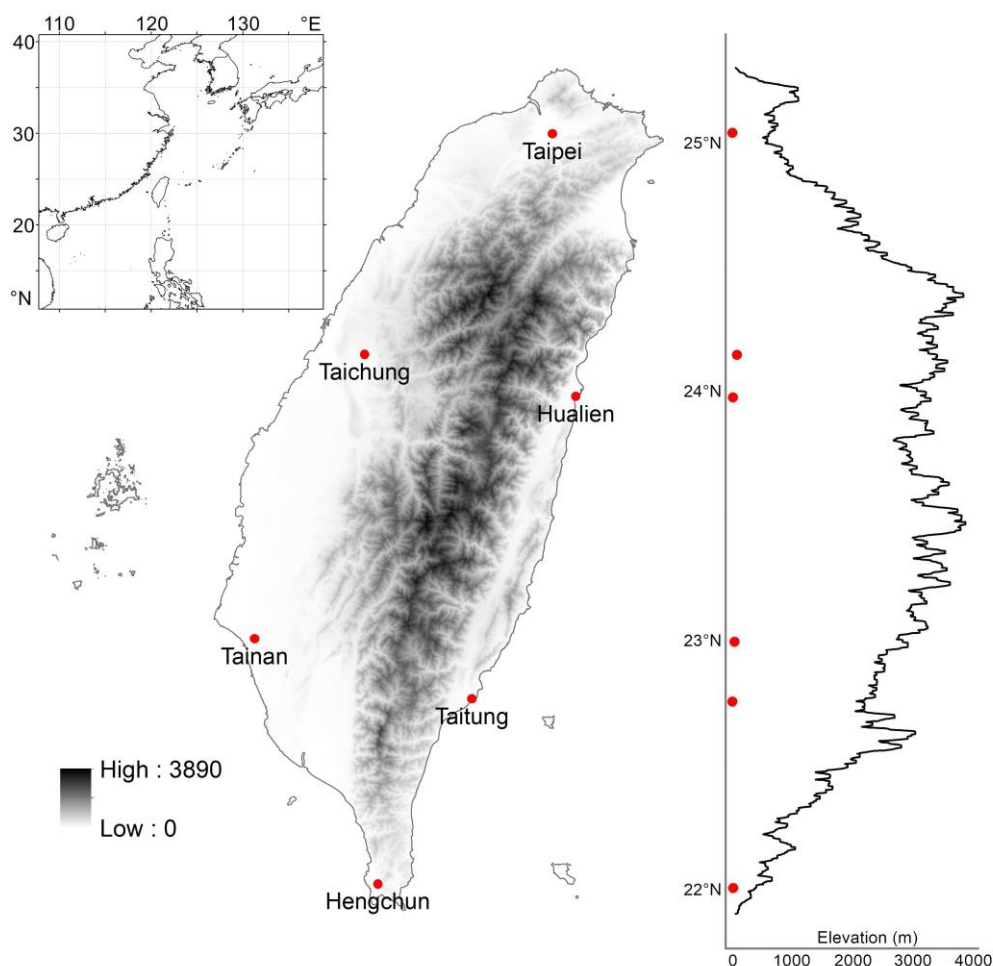


Fig. 4.1. Location and topography of Taiwan island. The red solid dots indicate the localities of six meteorological stations with continuous instrumental measurement of climate parameters longer than 100 years.

MATERIALS AND METHODS

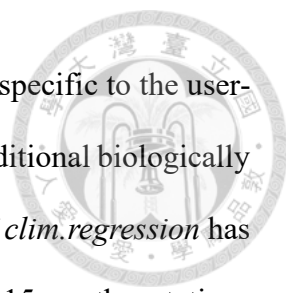


Study area

Forests cover 58% of the territorial area of Taiwan, and ca. 73% of the land is occupied by hills and mountains with more than 200 peaks over 3,000m asl (Fig. 4.1). Taiwan was uplifted as an island during the Miocene epoch, which has connected with the Asia mainland via the land bridge at least four times, and was permanently separated at the end of the last glacial period approximately 10,000 years ago (Shen, 1994). For geographical and historical reasons, Taiwan has mixed floristic components from adjacent areas. Among the >4200 known native vascular species, except for the 1052 endemic species (accounts for 22.9% of the total flora) (Lin et al., 2020b), Taiwan displayed a high floristic affinity with eastern Asia (33.40%, Japan included) and tropical Asia (27.17%) (Hsieh 2002).

Climate data

Gridded climate data at the resolution of 5km×5km were provided by Taiwan Climate Change Projection and Information Platform (TCCIP) (Weng and Yang, 2012). This dataset covers the main island of Taiwan and spans the historical period from 1960 to 2012 and projections of three future stages (2016–2035, 2046–2065, 2081–2100) based on 47 general circulation models (GCMs), with four sets of primary climate variables: monthly precipitation (PPT1 to PPT12), monthly minimum temperature (T_{min1} to T_{min12}), monthly mean temperature (T_{ave1} to T_{ave12}), and monthly maximum temperature (T_{max1} to T_{max12}). Due to the demand for fine-scale climate data to depict the ecological and environmental conditions that fit the diverse topography in the mountains, a downscaling process namely *clim.regression* (Lin et al., 2018), was applied to generate scale-free climate data based on the source of TCCIP's 5-km gridded climate



surfaces. *Clim.regression* can generate 73 climate variable estimates specific to the user-defined points of interest, including primary climatic variables and additional biologically relevant derivatives for historical and future periods. The accuracy of *clim.regression* has been evaluated by comparisons with historical observations from the 15 weather stations over various altitudinal zones. It displayed prediction errors of 0.56°C, 0.79°C, 0.80°C, and 36.26mm in *Tave*, *Tmin*, *Tmax*, and PPT (in mean absolute error, MAE), respectively, showing a considerable improvement (54.6%–66.7%) over the original TCCIP data (Lin et al., 2018).

General circulation models (GCMs) are essential for projecting future climate, however, it is not realistic to apply all GCM datasets when conducting analysis. Lin and Tung (2017) established a procedure for selecting GCM datasets for a region based on the weighted-average ranking method and demerit point system to rank the GCM performance. They suggested that six AR5 GCM datasets are suitable for use in Taiwan (Fig. 4.2). In this paper, uncertainty in future climate was incorporated through consensus from 12 climate change scenarios—including these six selected GCMs and two representative concentration pathways (RCPs), RCP 4.5 and RCP 8.5.

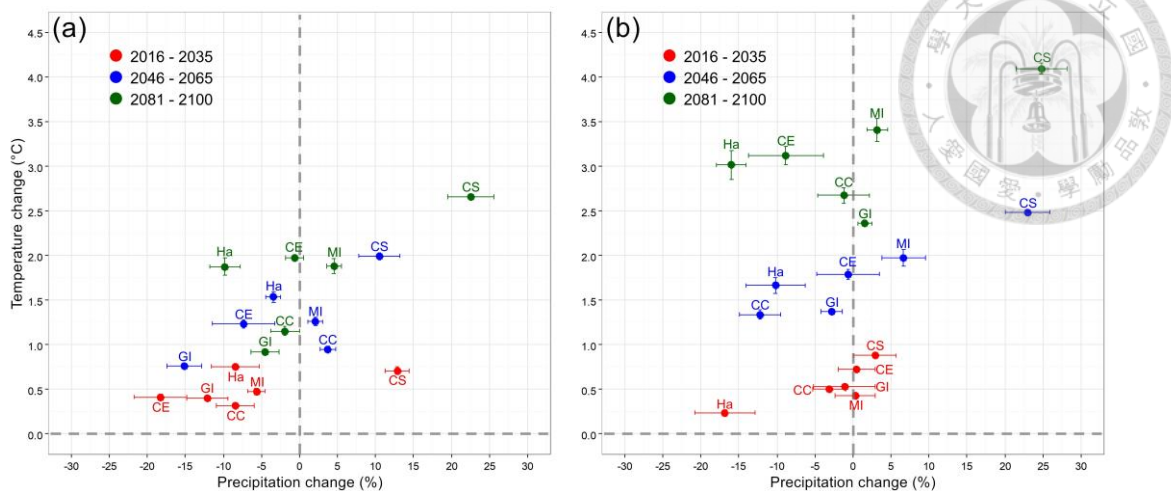


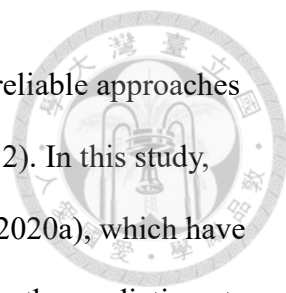
Fig. 4.2. Relative changes of projected MAT and MAP among six selected GCMs under (a) RCP 4.5 and (b) RCP 8.5 scenarios. The solid dot represents the average changes of MAT and MAP over the whole island of Taiwan, the horizontal and vertical bars demonstrate the standard deviation of the MAT and MAP values. Abbreviations: CC, CCSM4; CE, CESM1-AM5; CS, CSIRO-Mk3-6-0; GI, GISS-E2-R; Ha, HadGEM2-AO; and MI, MIROC5.

Vegetation data

Taiwan’s national vegetation survey was accomplished in 2008. The natural forests were classified into 21 types according to composition data from 8,804 plots. It was reported that 13 of the 21 forest types are driven by climate, including 11 zonal forest types, plus two other azonal forest types affected by monsoons (Li et al., 2013). A total of 3824 plots belonging to the 13 climate-related forest types were used to model the spatial distribution of these climate-dependent forest types, based on 57 climate variable estimates for the baseline period (1986–2005) (Lin et al., 2020a). The predicted current distribution of forest types (Appendix S1) and the built ecological niche models provide the basis for projecting their future changes in this study (Table 4.1).

Statistical analysis

The R version (Liaw and Wiener, 2002) of the random forest (RF) algorithm (Breiman, 2001) was utilized to model the relationship between the occurrence of a forest type and



its related climatic variables. RF is considered to be one of the most reliable approaches for ecological niche modeling (Rehfeldt et al., 2006; Wang et al., 2012). In this study, we adopted the RF ecological niche models developed by Lin et al. (2020a), which have been evaluated with an average mismatch rate of 6.59% by comparing the prediction at locations of all forest-type-classified plots. Predictions of the 13 RF models were assembled for delineating potential forest distributions under climatic conditions of the baseline period and of various future scenarios.

For projections of spatial distributions of suitable climate habitat for each forest type, 100m×100m gridded climate surfaces, which cover regions above 100m asl in Taiwan (2.7 million hectares in total), were generated by *clim.regression* with the same set of 57 climate variable estimates. A total of 6 GCMs (Table 4.2), 2 RCPs (RCP 4.5 and RCP 8.5), and 3 future stages (2016–2035, 2046–2065, and 2081–2100) were considered. These gridded climate surfaces were then fed to RF models for producing climatic suitability of each forest type over the study area.

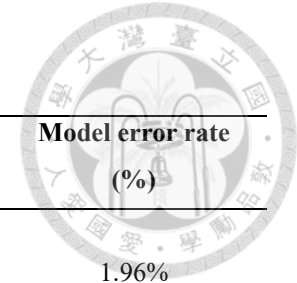


Table 4.1. The 13 climate-related forest types and field plots incorporated for establishing climatic niche models.

Forest type	Number of plots	Mean annual temperature (°C) ¹	Mean annual precipitation (mm) ²	Model error rate (%)
High-mountain coniferous woodlands and forests				
<i>Juniperus</i> woodland and scrub	102	4.54 (1.64)	2,367.38 (412.60)	1.96%
<i>Abies–Tsuga</i> forest	89	8.64 (1.76)	2,646.43 (430.15)	7.87%
Subtropical mountain zonal forests				
<i>Chamaecyparis</i> cloud forest	543	11.58 (1.50)	2,699.89 (386.74)	5.89%
<i>Fagus</i> cloud forest	55	12.54 (1.44)	3,389.41 (682.97)	3.64%
<i>Quercus</i> cloud forest	1058	13.66 (1.42)	2,681.79 (362.20)	6.24%
<i>Machilus–Castanopsis</i> forest	359	17.15 (1.66)	2,651.72 (475.05)	14.21%
<i>Phoebe–Machilus</i> forest	410	18.82 (1.73)	3,104.20 (725.52)	10.98%
<i>Ficus–Machilus</i> forest	145	21.27 (1.10)	2,390.37 (418.56)	2.08%
Tropical mountain zonal forests				
<i>Pasania–Elaeocarpus</i> cloud forest	57	16.03 (1.44)	2,523.81 (169.34)	3.51%
<i>Drypetes–Helicia</i> forest	425	18.41 (1.86)	2,623.93 (468.60)	3.53%
<i>Dysoxylum–Machilus</i> forest	27	21.89 (1.56)	2,362.70 (406.55)	7.69%
Tropical mountain azonal forest				
<i>Illicium–Cyclobalanopsis</i> winter monsoon forest	40	19.51 (1.98)	2,630.43 (160.91)	17.50%
Subtropical mountain azonal forest				
<i>Pyrenaria–Machilus</i> winter monsoon forest	514	18.49 (2.21)	3,695.86 (695.10)	3.54%

^{1, 2)} Brackets represent the standard deviation (SD) of climatic parameters from localities where this forest type was sampled.



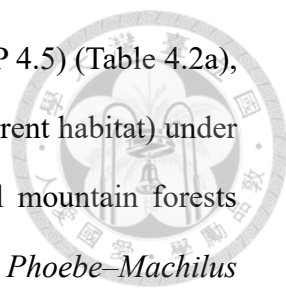
RESULTS

Future climate in Taiwan

TCCIP's 5km × 5km climate surfaces demonstrate identical trends of rising temperatures among the six selected climate change scenarios in Taiwan. Under a high emission scenario of RCP 8.5 among the selected GCMs, the increase in MAT by the end of the 21st century can be as high as 2.36–4.09°C, with an average increase of 3.11°C relative to the reference period. For a medium stabilization scenario such as RCP 4.5, an average increase in MAT of 1.74°C was predicted with the range of 0.92–2.66°C. However, projections of future precipitation conditions are highly variable. Some GCMs predict an evident increase in MAP, for example, the simulation of CSIRO-Mk3-6-0 under RCP 8.5 indicates a 24.79% increase in annual rainfall; by comparison, simulation of HadGEM2-AO under RCP 8.5 reveals a significant decrease in annual rainfall (-15.97%) relative to the baseline period (Fig. 4.2 and Appendix S2). Detailed inspection of the projected climate data shows that the temperature increase is slightly higher in northern Taiwan and the mountains of the whole island. For central and southern Taiwan, the models project a greater contrast in rainfall between the dry (October to April) and wet (May to September) seasons, leading to a drier winter and spring coupled with more extreme rainfall in the summer and autumn.

Projected geographic changes in climatic niche for future periods

The climatic niche projections based on the six selected GCMs, regardless of emission scenarios, consistently revealed a decline in area of suitable habitats for high-mountain forests (*Juniperus* woodland and scrub, and *Abies-Tsuga* forest) and three subtropical mountain zonal forests (*Chamaecyparis* cloud forest, *Fagus* cloud forest, and *Quercus* cloud forest) (Fig. 4.3 a–e; Fig. 4.4 a–e). Two rare forest types, the *Fagus* cloud forest and the *Juniperus* woodland and scrub, may suffer the most severe impact with 92.90%

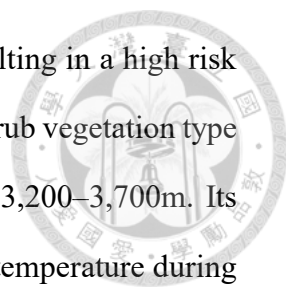


and 83.92% habitat loss under a medium stabilization scenario (RCP 4.5) (Table 4.2a), or almost lose their habitats (account for 99.23% and 97.42% of current habitat) under a high emission scenario (RCP 8.5) (Table 4.2b). For subtropical mountain forests located in lower elevations, such as *Machilus–Castanopsis* forest, *Phoebe–Machilus* forest, and *Ficus–Machilus* forest, the predicted area of suitable habitats is relatively stable under moderate predictive uncertainties (Fig. 4.3 f–h; Fig. 4.4 f–h).

It is noteworthy that the uncertainty of model predictions becomes larger in tropical mountain zonal forests and monsoon forests (Fig. 4.3 i–m; Fig. 4.4 i–m). In most warming scenarios, our results revealed a moderate trend of habitat expansion in tropical forest types (Table 4.2), eg. the *Pasania–Elaeocarpus* cloud forest (in RCP 8.5), the *Dysoxylum–Machilus* forest (in RCP 4.5 and RCP 8.5), and the *Illicium–Cyclobalanopsis* winter monsoon forest (in RCP 4.5 and RCP 8.5). However, models projected a crash of specific tropical mountain forests under some particular scenarios. The *Pasania–Elaeocarpus* cloud forest is a rare community at 1,200–1,600m asl. in the south of Central Mountain Range, which is subject to frequent cloud covers, a relative dryness in winter and spring, and strong winds due to the lack of topographic shading. Climatic conditions from two GCMs, the HadGEM2-AO and CSIRO-Mk3-6-0, may not provide a physical environment suitable for this forest type anymore, possibly leading to the crash of tropical cloud forest (only 0.20–4.46% suitable habitat left till 2081–2100) (Table 4.2). The *Illicium–Cyclobalanopsis* winter monsoon forest may face a fate similar to *Pasania–Elaeocarpus* cloud forest under the climatic condition represented by CSIRO-Mk3-6-0 scenario, which results in a dramatic habitat loss (only 18.73–25.17% suitable habitat left till 2081–2100).

Projected elevational changes for forest types

According to the ensemble of climatic niche projections from six selected GCMs and two emission scenarios, two forest types, the *Juniperus* woodland and scrub and the



Fagus cloud forest, may suffer a strong limit for upslope shift, resulting in a high risk of extinction (Fig. 4.5 a–b; Fig. 4.6 a–b). *Juniperus* woodland and scrub vegetation type in Taiwan occurs at the highest altitudes, inhabiting elevations of 3,200–3,700m. Its distribution range is significantly related to the maximum monthly temperature during growing season (Lin et al., 2020a). Because of the lack of a higher and cooler habitat in which to retreat, a decline of the *Juniperus* community is unavoidable under the predicted climate change. *Fagus* cloud forest, a forest type dominated by the glacier relict species in Taiwan, *Fagus hayatae*, is a rare community isolated on a few mountaintops and ridges (1,400–2,100m) in northern Taiwan. Due to the lack of corridor linking higher mountain regions, and also the scarce of its required physical environment—low winter temperature with ample rainfall and frequent cloud cover, our model consistently predicts an ongoing contraction and local extinction at elevations near its present habitat (Fig. 4.5 d; Fig. 4.6 d). The upward range shift and habitat contraction of high-mountain forest types are illustrated in 3-D maps (Fig. 4.7).

Among the four tropical forest types, the *Pasania–Elaeocarpus* cloud forest may suffer the highest stress along its elevational range (Fig. 4.5 i–l; Fig. 4.6 i–l). *Pasania–Elaeocarpus* cloud forest is a cool-adapted tropical vegetation type, usually inhabiting the windward ridge with a wind-chilling environment, dominated by sclerophyllous broadleaved tree species with low canopy height and a very high individual tree density. This forest type can be sparsely distributed at elevations as low as 300–500m if the habitat is sufficiently exposed to strong winter monsoons to provide a relatively cool environment. According to this climatic and geographic requirement, the model predicts the *Pasania–Elaeocarpus* altitudinal center to be at 1,200–1,500m (Table 4.3), but the forest type has a long tail extending to the low-elevation end (stage P in Fig. 4.5 i). The model ensembles demonstrate a possible upward shift for the central community of *Pasania–Elaeocarpus* cloud forest, however, the low-elevation populations may be

extremely vulnerable to warming, possibly resulting in extinction in the middle of this century (2046–2065).

Except for the above-mentioned vulnerable forest types, the model ensembles revealed that suitable habitat for most middle-elevation forest types may keep shifting upward at the pace of 230 to 450m under RCP 4.5 scenario (Fig. 4.5 b, c, e, f, g, j), or at the pace of 400 to 745m under RCP 8.5 scenario (Fig. 4.6 b, c, e, f, g, j). For low-elevation forest types and monsoon forests, the upslope migration of suitable habitat is relatively insignificant, and the distribution of their low-end populations are usually maintained (Fig. 4.5 h, k, l, m; Fig. 4.6 h, k, l, m).

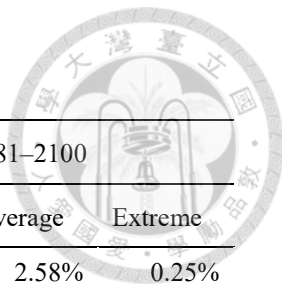


Table 4.2. The current area of potential habitats of the 13 climate-related forest types, and possible changes under two climate change scenarios.

a. RCP 4.5

Forest type	Baseline area (ha)	2016–2035			2046–2065			2081–2100		
		Moderate	Average	Extreme	Moderate	Average	Extreme	Moderate	Average	Extreme
<i>Juniperus</i>	29,134	62.54%	49.41%	36.00%	40.47%	26.53%	8.73%	34.28%	16.08%	2.24%
<i>Abies–Tsuga</i>	114,151	91.93%	81.75%	69.30%	80.83%	63.74%	40.41%	79.50%	50.42%	25.90%
<i>Chamaecyparis</i>	250,006	83.37%	79.48%	73.95%	74.49%	59.81%	51.29%	67.80%	53.96%	46.00%
<i>Fagus</i>	15,433	52.59%	41.93%	31.44%	30.37%	15.08%	5.50%	13.97%	7.10%	2.06%
<i>Quercus</i>	358,009	105.21%	99.69%	90.97%	104.72%	95.56%	86.97%	110.09%	89.60%	75.41%
<i>Machilus–Castanopsis</i>	326,277	114.08%	98.45%	89.77%	104.43%	99.39%	94.81%	117.69%	91.41%	78.62%
<i>Phoebe–Machilus</i>	318,017	127.55%	98.51%	87.17%	101.90%	86.38%	65.22%	120.76%	91.65%	71.71%
<i>Ficus–Machilus</i>	694,606	116.38%	99.17%	77.02%	118.93%	108.07%	97.87%	137.69%	110.75%	81.06%
<i>Pasania–Elaeocarpus</i>	8,750	406.33%	197.49%	69.12%	350.51%	166.44%	2.75%	158.63%	69.34%	0.20%
<i>Drypetes–Helicia</i>	143,575	162.78%	118.29%	62.27%	137.07%	106.68%	69.57%	152.02%	71.16%	23.83%
<i>Dysoxylum–Machilus</i>	240,205	247.09%	146.75%	80.89%	207.45%	171.43%	114.18%	270.85%	213.81%	120.78%
<i>Illicium–Cyclobalanopsis</i>	27,314	273.07%	125.27%	30.33%	288.90%	181.28%	17.60%	358.43%	202.79%	18.73%
<i>Pyrenaria–Machilus</i>	182,806	96.27%	83.07%	79.01%	113.45%	91.03%	74.15%	123.48%	93.65%	72.76%

b. RCP 8.5



Forest type	Baseline area (ha)	2016–2035			2046–2065			2081–2100		
		Moderate	Average	Extreme	Moderate	Average	Extreme	Moderate	Average	Extreme
<i>Juniperus</i>	29,134	68.00%	52.63%	44.01%	28.81%	14.61%	3.16%	8.29%	2.58%	0.25%
<i>Abies–Tsuga</i>	114,151	94.36%	83.20%	77.02%	71.48%	50.59%	28.36%	41.29%	19.72%	6.28%
<i>Chamaecyparis</i>	250,006	94.43%	85.41%	78.45%	59.90%	54.10%	43.77%	43.16%	33.57%	22.19%
<i>Fagus</i>	15,433	49.15%	41.23%	33.85%	9.76%	6.05%	2.48%	2.79%	0.87%	0.06%
<i>Quercus</i>	358,009	104.54%	95.56%	79.46%	97.84%	86.67%	74.79%	80.13%	64.24%	56.17%
<i>Machilus–Castanopsis</i>	326,277	102.89%	89.94%	74.48%	95.62%	82.97%	74.31%	96.19%	73.01%	44.82%
<i>Phoebe–Machilus</i>	318,017	105.57%	96.55%	90.35%	111.58%	99.08%	84.05%	142.64%	104.77%	82.28%
<i>Ficus–Machilus</i>	694,606	106.43%	95.22%	89.82%	111.69%	96.12%	80.84%	136.79%	111.70%	79.97%
<i>Pasania–Elaeocarpus</i>	8,750	553.19%	223.15%	93.33%	492.28%	196.28%	0.11%	444.42%	172.89%	4.46%
<i>Drypetes–Helicia</i>	143,575	166.72%	134.08%	96.82%	128.06%	93.26%	9.31%	153.08%	88.80%	8.62%
<i>Dysoxylum–Machilus</i>	240,205	194.64%	156.15%	113.16%	328.70%	261.09%	197.42%	401.84%	309.42%	251.54%
<i>Illicium–Cyclobalanopsis</i>	27,314	301.88%	188.86%	64.34%	379.45%	180.56%	38.17%	483.89%	240.82%	25.17%
<i>Pyrenaria–Machilus</i>	182,806	94.54%	81.47%	60.79%	123.69%	83.05%	67.95%	88.98%	60.87%	18.38%

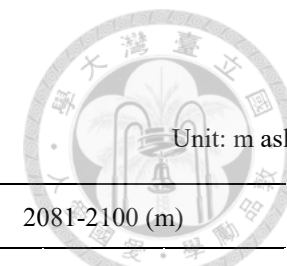


Table 4.3. Current elevational distribution of the 13 climate-related forest types, and possible changes under two climate change scenarios.

a. RCP 4.5

Forest type	Baseline elevation (m)			2016-2035			2046-2065			2081-2100		
	25% Qu.	Median	75% Qu.	25% Qu.	Median	75% Qu.	25% Qu.	Median	75% Qu.	25% Qu.	Median	75% Qu.
<i>Juniperus</i>	2,941	3,098	3,250	3,008	3,183	3,347	3,069	3,242	3,406	3,099	3,271	3,426
<i>Abies-Tsuga</i>	2,586	2,755	2,947	2,680	2,847	3,031	2,761	2,928	3,102	2,814	2,986	3,154
<i>Chamaecyparis</i>	2,100	2,284	2,474	2,232	2,411	2,601	2,345	2,532	2,714	2,407	2,596	2,782
<i>Fagus</i>	1,230	1,514	1,690	1,233	1,626	1,815	1,292	1,763	1,915	1,306	1,428	1,936
<i>Quercus</i>	1,574	1,763	1,952	1,697	1,891	2,086	1,834	2,029	2,238	1,906	2,103	2,319
<i>Machilus-Castanopsis</i>	799	1,032	1,266	947	1,194	1,428	1,093	1,341	1,580	1,213	1,455	1,696
<i>Phoebe-Machilus</i>	397	706	1,007	389	686	1,016	572	898	1,239	717	1,079	1,393
<i>Ficus-Machilus</i>	112	207	355	127	242	425	129	247	454	136	270	517
<i>Pasania-Elaeocarpus</i>	1,184	1,365	1,526	991	1,582	1,814	962	1,679	1,894	1,350	1,699	1,865
<i>Drypetes-Helicia</i>	553	776	1,040	702	950	1,227	842	1,071	1,325	981	1,227	1,487
<i>Dysoxylum-Machilus</i>	91	153	315	94	171	339	106	220	478	115	245	521
<i>Illicium-Cyclobalanopsis</i>	258	401	542	335	525	778	376	590	852	346	587	893
<i>Pyrenaria-Machilus</i>	260	486	837	261	487	841	232	450	772	252	465	784

b. RCP 8.5



Forest type	Baseline elevation (m)			2016-2035			2046-2065 (m)			2081-2100 (m)		
	25% Qu.	Median	75% Qu.	25% Qu.	Median	75% Qu.	25% Qu.	Median	75% Qu.	25% Qu.	Median	75% Qu.
<i>Juniperus</i>	2,941	3,098	3,250	3,000	3,181	3,338	3,122	3,292	3,446	3,223	3,366	3,522
<i>Abies-Tsuga</i>	2,586	2,755	2,947	2,676	2,842	3,026	2,831	2,993	3,158	2,999	3,158	3,313
<i>Chamaecyparis</i>	2,100	2,284	2,474	2,202	2,393	2,584	2,420	2,603	2,782	2,653	2,826	2,995
<i>Fagus</i>	1,230	1,514	1,690	1,206	1,546	1,765	1,254	1,337	1,527	1,316	1,379	1,426
<i>Quercus</i>	1,574	1,763	1,952	1,698	1,885	2,076	1,924	2,110	2,316	2,170	2,360	2,571
<i>Machilus-Castanopsis</i>	799	1,032	1,266	970	1,212	1,440	1,237	1,478	1,705	1,543	1,777	1,993
<i>Phoebe-Machilus</i>	397	706	1,007	373	675	1,038	676	1,042	1,383	891	1,297	1,654
<i>Ficus-Machilus</i>	112	207	355	132	247	431	145	291	552	157	334	676
<i>Pasania-Elaeocarpus</i>	1,184	1,365	1,526	1,000	1,532	1,748	1,494	1,782	1,993	1,747	2,000	2,221
<i>Drypetes-Helicia</i>	553	776	1,040	704	943	1,205	967	1,202	1,450	1,288	1,513	1,749
<i>Dysoxylum-Machilus</i>	91	153	315	94	166	329	110	221	459	127	280	586
<i>Illicium-Cyclobalanopsis</i>	258	401	542	338	545	805	331	599	907	424	783	1,133
<i>Pyrenaria-Machilus</i>	260	486	837	252	467	794	245	448	772	246	455	754

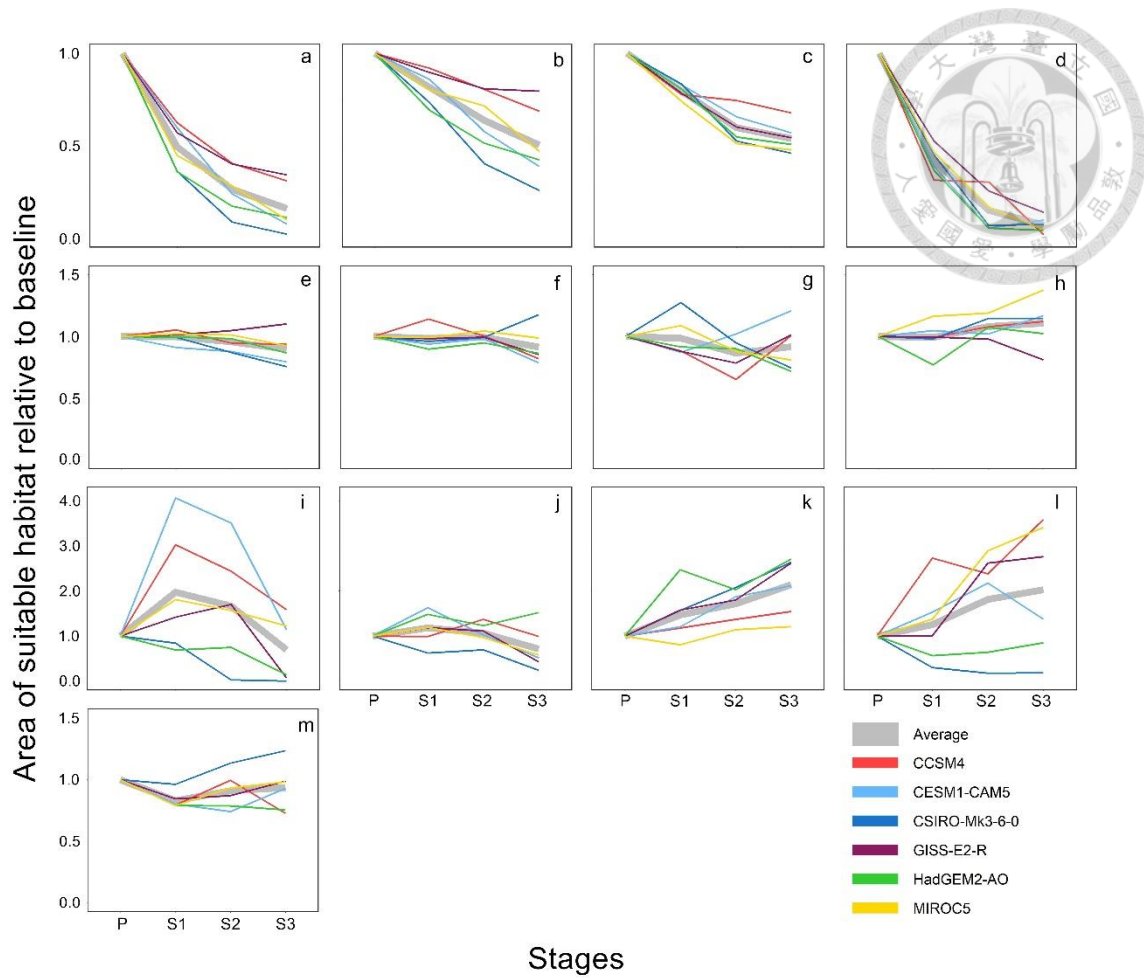


Fig. 4.3. Change in the area of potential habitat of each forest type under RCP 4.5 emission scenarios relative to the baseline. Stage: P, present; S1, 2016–2035; S2, 2046–2065; and S3, 2081–2100. Forest types: a, *Juniperus* woodland and scrub; b, *Abies-Tsuga* forest; c, *Chamaecyparis* cloud forest; d, *Fagus* cloud forest; e, *Quercus* cloud forest; f, *Machilus-Castanopsis* forest; g, *Phoebe-Machilus* forest; h, *Ficus-Machilus* forest; i, *Pasania-Elaeocarpus* cloud forest; j, *Drypetes-Helicia* forest; k, *Dysoxylum-Machilus* forest; l, *Illicium-Cyclobalanopsis* winter monsoon forest; and m, *Pyrenaria-Machilus* winter monsoon forest.

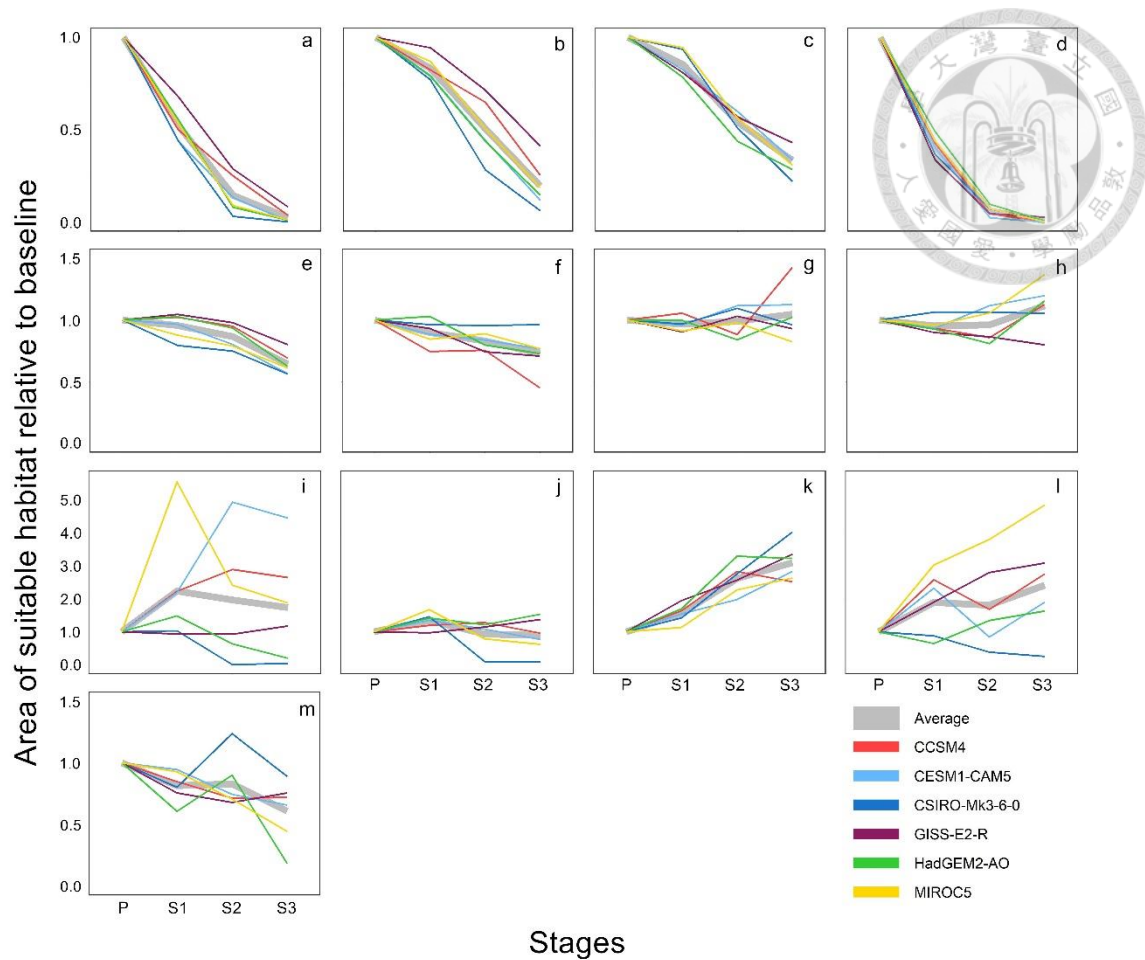


Fig. 4.4. Change in the area of potential habitat of each forest type under RCP 8.5 emission scenarios relative to the baseline. Abbreviations of legend are the same as Fig. 4.3.

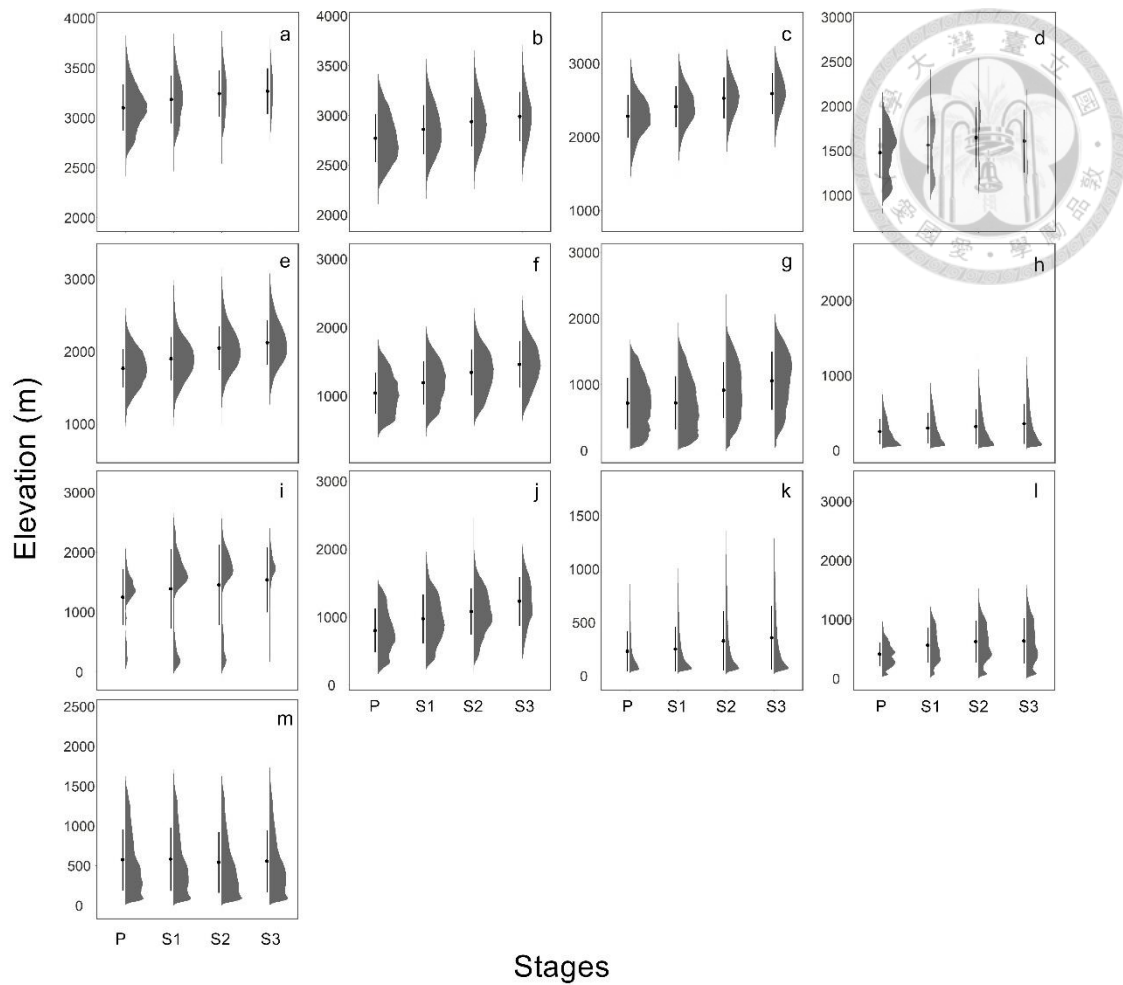


Fig. 4.5. Altitudinal change in the potential distribution of each forest type under RCP 4.5 emission scenarios. Shaded area under the curve represents the area of potential habitat of each stage relative to the baseline. The vertical bar represents the standard deviation of elevational range, whereas the solid circle represents its mean. Abbreviations of legend are the same as Fig. 4.3.

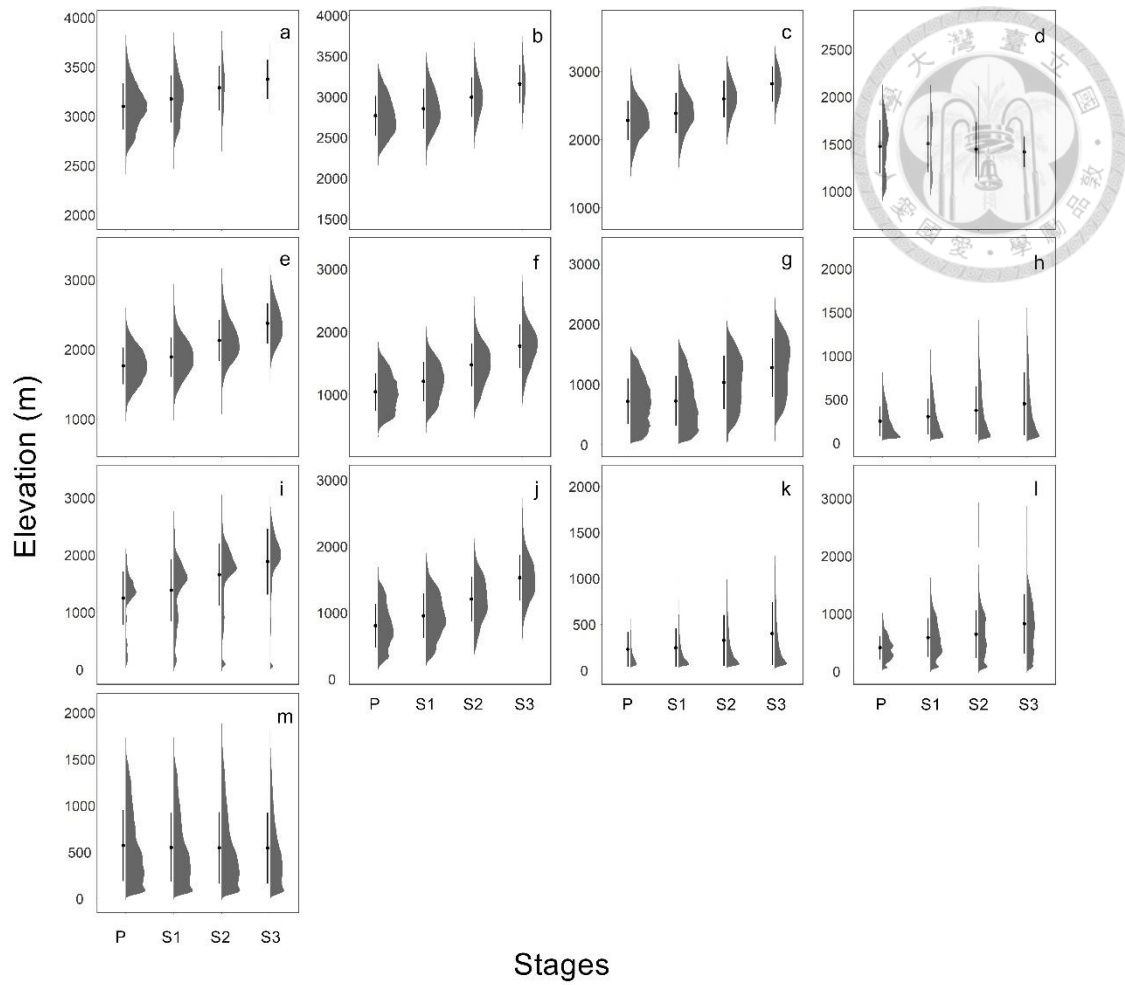


Fig. 4.6. Altitudinal change in the potential distribution of each forest type under RCP 8.5 emission scenarios. Abbreviations and the legends are the same as Fig. 4.5.

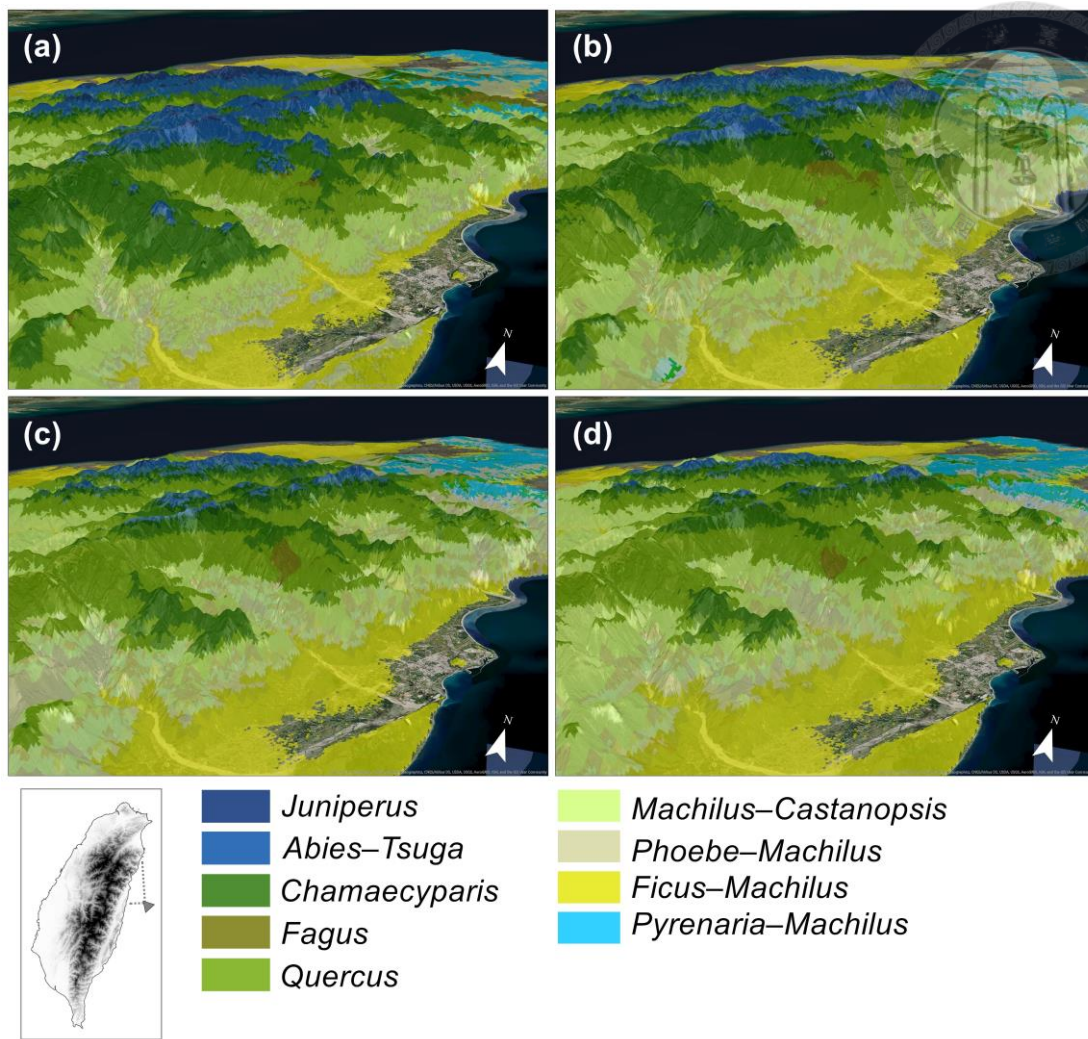


Fig. 4.7. 3-D illustrations of the predicted upward range shift in vegetation belts in north Taiwan relative to the reference period (a), by 2016–2035 (b), 2046–2065 (c), and 2081–2100 (d), based on the climate projection of the CSIRO-Mk3-6-0 model with RCP 4.5 scenario. The triangle and dotted lines indicate the scene view of 3-D maps.

DISCUSSION

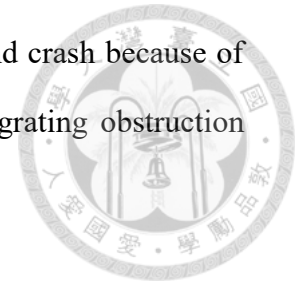
Projected changes in the distribution of forest types

This study projected geographical and elevational changes in suitable habitats of the 13 climate-related forest types (including 2 high-mountain types, 7 subtropical types, and 4 tropical types) under future climates. The projected impact of climate change varied substantially among forest types. Specific characteristics of the projections are discussed below.

a. High-mountain forests

High-mountain forests, communities primarily constrained by direct and indirect effects of low temperatures, radiation, wind, or insufficient water availability (Körner and Larcher, 1988), and the topographical isolation, are ecotypes known to be vulnerable to climate change with evident extent contraction, competitive weakness, and a high risk of local extinction (Pauli et al., 2012; Costion et al., 2015; Morueta-Holme et al., 2015; Freeman et al., 2018). In this study, a consistent pattern of habitat contraction and topographical barrier of upward migration for high-mountain forests were revealed among all of the selected climate change scenarios. Taiwan is an island with sufficient annual rainfall. Our previous study has revealed that the distribution of high-mountain forests on this island is significantly related to the maximum monthly temperature at the start of the growing season (March to June), rather than precipitation (Lin et al., 2020a). The projected habitat contraction of high-mountain forests was positively correlated to the increase in temperature. The extreme warming scenarios, eg. CSIRO-Mk3-6-0 (CS) and CESM1-AM5 (CE), were projected to result in more habitat losses than moderate scenarios, such as GISS-E2-R (GI) and CCSM4 (CC). Our results also displayed that mountaintop represents a strong limitation on the upward migration of high-mountain vegetation. The *Juniperus* woodland and scrub is the highest vegetation

type in Taiwan, thus, its elevational extent will probably retract and crash because of the push of its lower-neighboring *Abies-Tsuga* forest and the migrating obstruction from mountaintops and ridgetops.

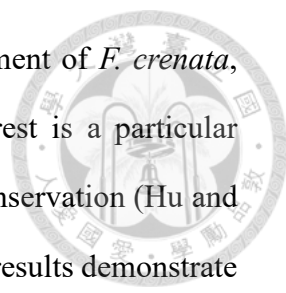


b. Subtropical montane forests

Most subtropical montane forest types we studied consistently followed the march conceptual model that Lenoir and Svenning (2015) presented. However, the survival of a few cloud forest communities may be severely threatened by a changing climate.

Fagus hayatae is a tree species distributed in mainland China and migrated to Taiwan during the LGM via land bridges (Shu and Wang, 2012). It occurs only limited to a few isolated fragments on ridgetops and formed a pure deciduous broad-leaved forest (1,340–2,000m altitude) in northern and northeastern Taiwan while the temperature increased after the ice age (Huang & Editorial Committee of the Flora of Taiwan, 1996). It is a tree species restricted to unique climatic conditions of low temperature and plentiful precipitation in winter (Lin et al., 2020a). Our simulations revealed that their current communities will drastically decline in the coming decades due to the lack of suitable habitats and corridors to migrate (Appendix S3), which may completely follow the crash conceptual model that Lenoir and Svenning (2015) suggested.

The habitat contraction of *Fagus* cloud forests is not a phenomenon observed solely in Taiwan. Téllez-Valdés et al. (2006) have reported the fragmentation and drastic distribution contraction of *Fagus* cloud forests (composed by *Fagus grandifolia* var. *mexicana*) in Mexico, where it represents the southernmost known boundary of the genus of *Fagus* in the Northern Hemisphere. A similar pattern was also reported in Japan where only 11.4% of current beech-dominant forest type (composed by *Fagus crenata*) remains stable till 2081–2100. These forests are mainly distributed at high elevations in snowy areas on the side close to Sea of Japan. The northwards or upwards

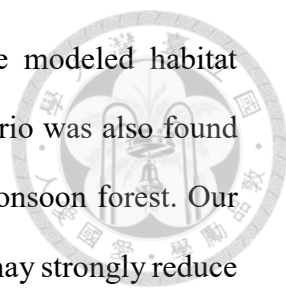


range expansions of *Quercus* spp., leading to the possible replacement of *F. crenata*, needs to be carefully monitored (Matsui et al., 2018). Cloud forest is a particular ecosystem harboring unique and valuable biodiversity worthy of conservation (Hu and Riveros-Iregui, 2016; Schulz et al., 2017; Pouteau et al., 2018). Our results demonstrate the vulnerability and sensitivity of *Fagus* cloud forest to the warming climate on the subtropical island of Taiwan, and we believe that adapted conservation strategies should be undertaken in the coming years.

c. Tropical montane forests

Based on the averaged projections from six selected GCMs, our results generally indicate a maintained or expanded distribution of tropical montane forests (Fig. 4.5 i–l; Fig. 4.6 i–l). However, the predictive uncertainties in tropical montane forest types are significantly larger than in high-mountain and subtropical forest types. Furthermore, our results indicate the probability of the collapse of specific tropical forest communities under particular climate change scenarios.

We found that climatic conditions of a few scenarios may lead to the drastic contraction of specific tropical forest types, such as the predicted collapse of *Pasania–Elaeocarpus* tropical cloud forest under the scenarios of CSIRO-Mk3-6-0 (CS) and HadGEM2-AO (Ha). *Pasania–Elaeocarpus* forest is a rare community occupying the southernmost peak above 2,000m asl of the Central Mountain Range, which is adapted to strong wind, frequent cloud cover, and a relative dryness during the spring (February–April) (Li et al., 2013; Lin et al., 2020a). The two adverse GCMs to the survival of *Pasania–Elaeocarpus* forest represent scenarios of extreme precipitation changes. For example, CSIRO-Mk3-6-0 is a warm-humid scenario that illustrates a 20–28% increase in annual precipitation till 2080–2100 and brings heavier rainfall in summer that leads to a more evident difference in water availability between dry and wet season. On the contrary, HadGEM2-AO is a warm-dry scenario that may reduce precipitation by 8–18% in

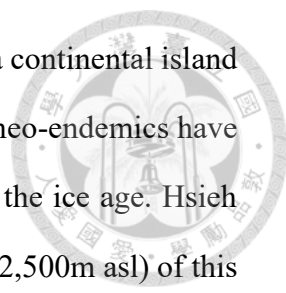


2080–2100 and result in a longer dryness in south Taiwan. The modeled habitat contraction of tropical forests under an extreme warm-humid scenario was also found in *Drypetes–Helicia* forest and *Illicium–Cyclobalanopsis* winter monsoon forest. Our results indicate that if an extreme change in precipitation occurs, it may strongly reduce the suitability of tropical cloud forest. Changes in precipitation have more of an effect than changes in temperature.

Range shifts of tropical tree species have been reported in recent decade (Feeley et al., 2011; Feeley, 2012; Feeley et al., 2013; Morueta-Holme et al., 2015), and there are increasing numbers of studies supporting the hypothesis that tropical mountain ecosystems are likely to experience considerable change in the near future, such as the lifting of cloud base (Still et al., 1999; Hu and Riveros-Iregui, 2016) and temperature-induced moisture stress (Pounds et al., 1999; Krishnaswamy et al., 2013). Among the climatic threats to tropical ecosystems, drought is the condition receiving most attention. It not only refers to the shortage or unevenness of precipitation, but also the physiological water stress induced by higher temperature and greater transpiration rates. Water availability plays a more crucial role than temperature variables in the existence of tropical forests, however, the accuracy and precision of precipitation projections are limited and these predictions are usually accompanied by a high level of uncertainty. Our results suggest large changes in the range extent of tropical cloud and monsoon forest types, including the possibility of extinctions. In spite of the limitations in accuracy and precision of these predictions, we should not ignore the possibility of specific ecosystem collapse.

Adapted strategy for forest management

Uncertainty in the projection for future climate is probably the greatest challenge in assessing the impact of climate change on the distribution of forests. In this study, however, all emission scenarios bring a drastic habitat contraction of high-mountain



vegetation and the deciduous *Fagus* broad-leaved forest. Taiwan is a continental island harboring many plant species originating from East Asia and many neo-endemics have been evolved due to the topographical isolation of mountains after the ice age. Hsieh (2002) has calculated an endemic rate of >50% at high elevations (>2,500m asl) of this island. This rate of endemism indicates a high conservation value of the high-mountain ecosystem in Taiwan, and further implies that the precious plant biodiversity may be threatened by the competition stress from its low-boundary neighbors due to the rising temperature. For high-mountain ecosystems, there will be no more cold habitat to sustain in the future, and *ex-situ* conservation for the endemic and small-population plant species, such as the collection for germplasm, and assisted regeneration in anthropogenic facilities, should be implemented to mitigate the urgent risk from climate change (Shoo et al., 2013). *Fagus* forest would be limited and isolated by topographical barriers without corridors for retreat. Mitigation actions for this forest type might include assistance in migration and colonization, such as transplanting seedlings and saplings to climatically suitable areas near its native habitat. These actions would help retain their field populations (Shoo et al., 2013).

In contrast to the consistent projection on the changes of high-mountain and subtropical montane forest types, projected changes of tropical montane forests are highly variable and uncertain. This study revealed that under the extreme humid or dry scenarios, the current extent of tropical montane cloud forest and tropical winter monsoon forest may be dramatically reduced. These results provide a scientific basis for the management and preservation for rare and localized forest types such as the tropical montane cloud forest in southern Taiwan. We suggest long-term field monitoring to establish trends in extreme thermal and rainfall events and to depict the actual vegetation composition and changes in areal extent of tropical montane forests in the coming decades. If the change of forests follows the worse track that we modeled, adaptive management should be

launched as needed, including refuge preservation, movement path security, and colonization assistance.



AUTHOR CONTRIBUTIONS

All authors conceived the research idea. HYL, JMH and TW led the writing; TYC and CFH contributed the vegetation data; YST and YMC contributed the data of climate change scenarios; HYL performed the statistical analyses with contributions from TW; all authors discussed the results and commented on the manuscript.

LITERATURE CITED

- Barlow, J., F. França, T. A. Gardner, C. C. Hicks, G. D. Lennox, E. Berenguer, L. Castello, E. P. Economo, J. Ferreira, B. Guénard, C. G. Leal, V. Isaac, A. C. Lees, C. L. Parr, S. K. Wilson, P. J. Young and N. A. J. Graham.** 2018. The future of hyper diverse tropical ecosystems. *Nature* **559**: 517–526.
<https://doi.org/10.1038/s41586-018-0301-1>
- Barry, R. G. and R. J. Chorley.** 2009. *Atmosphere, Weather and Climate*, 9th edition, Routledge, London, 536 pp.
- Beniston, M.** 2003. Climatic change in mountain regions: a review of possible impacts. *Climatic Change* **59**: 5–31. <https://doi.org/10.1023/A:1024458411589>
- Breiman, L.** 2001. Random forests. *Machine learning* **45**: 5–32.
<https://doi.org/10.1023/A:1010933404324>
- Chen, I.-C., J. K. Hill, R. Ohlemüller, D. B. Roy and C. D. Thomas.** 2011. Rapid range shifts of species associated with high levels of climate warming. *Science* **333**: 1024–1026.
- Corlett, R. T.** 2011. Impacts of warming on tropical lowland rainforests. *Trends in Ecology and Evolution* **26**: 606–613.
- Costion, C. M., L. Simpson, P. L. Pert, M. M. Carlsen and W. J. Kress.** 2015. Will tropical mountaintop plant species survive climate change? Identifying key knowledge gaps using species distribution modelling in Australia. *Biological*

Conservation **191**: 322–330.

Feeley, K. J. 2012. Distributional migrations, expansions, and contractions of tropical plant species as revealed in dated herbarium records. *Global Change Biology* **18**: 1335–1341. <https://doi.org/10.1111/j.1365-2486.2011.02602.x>

Feeley, K. J., J. Hurtado, S. Saatchi, M. R. Silman and D. B. Clark. 2013. Compositional shifts in Costa Rican forests due to climate-driven species migrations. *Global change biology* **19**: 3472–3480.

Feeley, K. J., M. R. Silman, M. B. Bush, W. Farfan, K. G. Cabrera, Y. Malhi, P. Meir, N. S. Revilla, M. N. R. Quisiyupanqui, and S. Saatchi. 2011. Upslope migration of Andean trees. *Journal of Biogeography* **38**: 783–791.

Freeman, B. G., J. A. Lee-Yaw, J. M. Sunday and A. L. Hargreaves. 2018. Expanding, shifting and shrinking: The impact of global warming on species' elevational distributions. *Global Ecology and Biogeography* **27**: 1268–1276. <https://doi.org/10.1111/geb.12774>

Hsieh, C.-F. 2002. Composition, endemism and phytogeographical affinities of the Taiwan flora. *Taiwania* **47**: 298–310.


Hsu, H.-H. and C.-T. Chen. 2002. Observed and projected climate change in Taiwan. *Meteorology and Atmospheric Physics* **79**: 87–104.

Hsu, H.-H., C. Chou, Y.-C. Wu, M.-M. Lu, C.-T. Chen and Y.-M. Chen. 2011. Climate Change in Taiwan: Scientific Report 2011 (Summary). National Science Council, Taipei, Taiwan.

Hu, J. and D. A. Riveros-Iregui. 2016. Life in the clouds: are tropical montane cloud forests responding to changes in climate? *Oecologia* **180**: 1061–1073. <https://doi.org/10.1007/s00442-015-3533-x>

Huang, T.-C. and Editorial Committee of the Flora of Taiwan (eds.). 1996. Flora of Taiwan, 2. 2nd. Editorial Committee of the Flora of Taiwan, Taipei, Taiwan.

Hung, C.-W. and P.-K. Kao. 2010. Weakening of the winter monsoon and abrupt increase of winter rainfalls over northern Taiwan and southern China in the early 1980s. *Journal of Climate* **23**: 2357–2367. <https://doi.org/10.1175/2009JCLI3182.1>

- 
- IPCC.** 2013. Climate Change 2013: The Physical Science Basis. Contribution of Working Group I to the Fifth Assessment Report of the Intergovernmental Panel on Climate Change [Stocker, T.F., D. Qin, G.-K. Plattner, M. Tignor, S.K. Allen, J. Boschung, A. Nauels, Y. Xia, V. Bex and P.M. Midgley (eds.)]. Cambridge University Press, Cambridge, United Kingdom and New York, NY, USA, 1535 pp. <https://doi.org/10.1017/CBO9781107415324>
- Jump, A. S., T.-J. Hunag and C.-H. Chou.** 2012. Rapid altitudinal migration of mountain plants in Taiwan and its implications for high altitude biodiversity. *Ecography* **35**: 204–210.
- Jump, A. S., C. Mátyás and J. Peñuelas.** 2009. The altitude-for-latitude disparity in the range retractions of woody species. *Trends in Ecology and Evolution* **24**: 694–701. <https://doi.org/10.1016/j.tree.2009.06.007>
- Körner, C. and W. Larcher.** 1988. Plant life in cold climates. *Symposia of the Society for Experimental Biology*, 01 Jan 1988, **42**: 25–57.
- Krishnaswamy, J., R. John and S. Joseph.** 2014. Consistent response of vegetation dynamics to recent climate change in tropical mountain regions. *Global Change Biology* **20**: 203–215. <https://doi.org/10.1111/gcb.12362>
- Lenoir, J., J. C. Gégout, P. A. Marquet, P. Ruffray and H. Brisse.** 2008. A significant upward shift in plant species optimum elevation during the 20th century. *Science* **320**: 1768–1771.
- Lenoir, J. and J.-C. Svenning.** 2015. Climate-related range shifts—a global multidimensional synthesis and new research directions. *Ecography* **38**: 15–28.
- Lomolino, M. V.** 2001. Elevation gradients of species-density: historical and prospective views. *Global Ecology and Biogeography* **10**: 3–13.
- Li, C.-F., M. Chytrý, D. Zelený, M.-Y. Chen, T.-Y. Chen, C.-R. Chiou, Y.-J. Hsia, H.-Y. Liu, S.-Z. Yang, C.-L. Yeh, J.-C. Wang, C.-F. Yu, Y.-J. Lai, W.-C. Chao and C.-F. Hsieh.** 2013. Classification of Taiwan forest vegetation. *Applied Vegetation Science* **16**: 698–719. <https://doi.org/10.1111/avsc.12025>
- Liaw, A. and M. Wiener.** 2002. Classification and regression by randomForest. *R news* **2(3)**: 18–22.
- Lin, C.-T. and C.-A. Chiu.** 2019. The relic *Trochodendron aralioides* Siebold &

Zucc. (Trochodendraceae) in Taiwan: Ensemble distribution modeling and climate change impacts. *Forests* **10(1)**: 7. <https://doi.org/10.3390/f10010007>

Lin, C.-Y. and Tung, C.-P. 2017. Procedure for selecting GCM datasets for climate risk assessment. *Terr. Atmos. Ocean. Sci.* **28**: 43–55.

[https://doi.org/10.3319/TAO.2016.06.14.01\(CCA\)](https://doi.org/10.3319/TAO.2016.06.14.01(CCA))

Lin, H.-Y., J.-M. Hu, T.-Y. Chen, C.-F. Hsieh, G. Wang and T. Wang. 2018. A dynamic downscaling approach to generate scale-free regional climate data in Taiwan. *Taiwania* **63**: 245–266. <https://doi.org/10.6165/tai.2018.63.251>

Lin, H.-Y., C.-F. Li, T.-Y. Chen, C.-F. Hsieh, G. Wang, T. Wang and J.-M. Hu. 2020a. Climate-based approach for modeling the distribution of montane forest vegetation in Taiwan. *Applied Vegetation Science* **31**: in press. <https://doi.org/10.1111/AVSC.12485>

Lin, H.-Y., Y.-H. Tseng, C.-F. Hsieh and J.-M. Hu. 2020b. Geographical distribution of dioecy and its ecological correlates based on fine-scaled species distribution data from a subtropical island. *Ecological Research* **35**: 170–181.

<https://doi.org/10.1111/1440-1703.12068>

Lin, W.-C., Y.-P. Lin, W.-Y. Lien, Y.-C. Wang, C.-T. Lin, C.-R. Chiou, J. Anthony and N. D. Crossman. 2014. Expansion of protected areas under climate change: An example of mountainous tree species in Taiwan. *Forests* **2014(5)**: 2882–2904.

Matsui, T., K. Nakao, M. Higa, I. Tsuyama, Y. Kominami, T. Yagihashi, D. Koide and N. Tanaka. 2018. Potential impact of climate change on canopy tree species composition of cool-temperate forests in Japan using a multivariate classification tree model. *Ecological Research* **33**: 289–302. <https://doi.org/10.1007/s11284-018-1576-2>

Morueta-Holme, N., K. Engemann, P. Sandoval-Acuña, J. D. Jonas, R. M. Segnitz and J.-C. Svenning. 2015. Strong upslope shifts in Chimborazo's vegetation over two centuries since Humboldt. *PNAS* **112**: 12741–12745.

Myers, N., R. A. Mittermeier, C. G. Mittermeier, G. A. B. Fonseca and J. Kent. 2000. Biodiversity hotspots for conservation priorities. *Nature* **403**: 853–858.

Nakao, K., M. Higa, I. Tsuyama, C.-T. Lin, S.-T. Sun, J.-R. Lin, C.-R. Chiou, T.-Y. Chen, T. Matsui and N. Tanaka. 2014. Changes in the potential habitats of 10

dominant evergreen broad-leaved tree species in the Taiwan-Japan archipelago. *Plant Ecology* **215**: 639–650.

- Pauli, H., M. Gottfried, S. Dullinger, O. Abdaladze, M. Akhalkatsi, J. L. B. Alonso, G. Coldea, J. Dick, B. Erschbamer, R. F. Calzado, D. Ghosn, J. I. Holten, R. Kanka, G. Kazakis, J. Kollár, P. Larsson, P. Moiseev, D. Moiseev, U. Molau, J. M. Mesa, L. Nagy, G. Pelino, M. Puşcaş, G. Rossi, A. Stanisci, A. O. Syverhuset, J.-P. Theurillat, M. Tomaselli, P. Unterluggauer, L. Villar, P. Vittoz and G. Grabherr.** 2012. Recent plant diversity changes on Europe's mountain summits. *Science* **336**: 353–355.
- Perez, T. M., J. T. Stroud and K. J. Feeley.** 2016. Thermal trouble in the tropics. *Science* **351**: 1392–1393.
- Peters, R. L. and J. D. S. Darling.** 1985. The greenhouse effect and nature reserves. *BioScience* **35**: 707–717.
- Pounds, J. A., M. P. L. Fogden and J. H. Campbell.** 1999. Biological response to climate change on a tropical mountain. *Nature* **398**: 611–615.
- Pouteau, R., T. W. Giambelluca, C. Ah-Peng and J.-Y. Meyer.** 2018. Will climate change shift the lower ecotone of tropical montane cloud forests upwards on islands? *Journal of Biogeography* **45**: 1326–1333.
<https://doi.org/10.1111/jbi.13228>
- Rehfeldt, G. E., N. L. Crookston, M. V. Warwell and J. S. Evans.** 2006. Empirical analyses of plant-climate relationships for the western United States. *International Journal of Plant Sciences* **167**: 1123–1150. <https://doi.org/10.1086/507711>
- Sasaki, S.** 1924. Vegetation zones of Sin-Kao Shan. Report of Formosan Natural History Society **69**: 1–54. [In Japanese.]
- Schulz, H. M., C.-F. Li, B. Thies, S.-C. Chang and J. Bendix.** 2017. Mapping the montane cloud forest of Taiwan using 12 year MODIS-derived ground fog frequency data. *PLoS ONE* **12(2)**: e0172663.
<https://doi.org/10.1371/journal.pone.0172663>
- Shen, C.-F.** 1994. Introduction to the flora of Taiwan, 2: geotectonic evolution, paleogeography, and the origin of the flora. In Huang & Editorial Committee of the Flora of Taiwan (Eds.), *Flora of Taiwan Second edition* (pp. 3–7). Editorial

Committee of the Flora of Taiwan, Taipei.

Shoo, L. P., A. A. Hoffmann, S. Garnett, R. L. Pressey, Y. M. Williams, M. Taylor, L. Falconi, C. J. Yates, J. K. Scott, D. Alagador and S. E. Williams. 2013.

Making decisions to conserve species under climate change. *Climatic Change* **119**: 239–246. <https://doi.org/10.1007/s10584-013-0699-2>

Shu, J.-W. and W.-M. Wang. 2012. A unique Middle Pleistocene beech (*Fagus*)-rich deciduous broad-leaved forest in the Yangtze Delta Plain, East China: Its climatic and stratigraphic implication. *Journal of Asian Earth Sciences* **56**: 180–190.

Spehn, E. M., K. Rudmann-Maurer and C. Körner. 2011. Mountain biodiversity. *Plant Ecology & Diversity* **4**: 301–302.

<https://doi.org/10.1080/17550874.2012.698660>

Still, C. J., P. N. Foster and S. H. Schneider. 1999. Simulating the effects of climate change on tropical montane cloud forests. *Nature* **398**: 608–610.

Su, H.-J. 1984. Studies on the climate and vegetation types of the natural forests in Taiwan (II). Altitudinal vegetation zones in relation to temperature gradient. *Quarterly Journal of Chinese Forestry* **17**: 57–73.

Téllez-Valdés, O., P. Dávila and P. Lira. 2006. The effects of climate change on the long-term conservation of *Fagus grandifolia* var. *mexicana*, an important species of the Cloud Forest in Eastern Mexico. *Biodiversity and Conservation* **15**: 1095–1107.

Tian, F., B. Dong, J. Robson, R. Sutton and S. Tett. 2019. Projected near term changes in the East Asian summer monsoon and its uncertainty. *Environmental Research Letters* **14**: 084038. <https://doi.org/10.1088/1748-9326/ab28a6>

Wang, T., E. M. Campbell, G. A. O'Neill and S. N. Aitken. 2012. Projecting future distributions of ecosystem climate niches: uncertainties and management applications. *Forest Ecology and Management* **279**: 128–140. <https://doi.org/10.1016/j.foreco.2012.05.034>

Weng, S.-P. and C.-T. Yang. 2012. The construction of monthly rainfall and temperature dataset with 1km gridded resolution over Taiwan area (1960-2009) and its application to climate projection in the near future (2015-2039). *Atmospheric Sciences* **40**: 349–369. [In Chinese with English summary.]



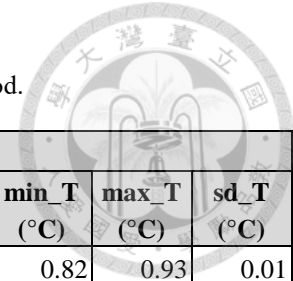
SUPPORTING INFORMATION

Appendix S1. Visualization of the predicted distribution of 13 forest types over Taiwan island based on the baseline climate data. Please find the sample movie using this link:

<https://www.youtube.com/watch?v=KBwRSSwmUYg>

Appendix S2. The projected changes in MAP and MAT using selected GCMs and emission scenarios for future stages relative to the baseline period.

Appendix S3. A visualized simulation of *Fagus hayatae* for the possible local extinction near its currently largest habitat, Tung Shan. Please find the sample movie using this link: <https://www.youtube.com/watch?v=hBSIc8AL4yI>



Appendix S2. The projected changes in MAP and MAT using selected GCMs and emission scenarios for future stages relative to the baseline period.

		RCP 4.5								RCP 8.5							
		MAP (%)	min_P (%)	max_P (%)	sd_P (%)	MAT (°C)	min_T (°C)	max_T (°C)	sd_T (°C)	MAP (%)	min_P (%)	max_P (%)	sd_P (%)	MAT (°C)	min_T (°C)	max_T (°C)	sd_T (°C)
2016 - 2035	CSIRO-Mk3-6-0	12.87	9.37	18.36	1.59	0.71	0.58	0.77	0.04	2.91	-3.49	7.46	2.74	0.88	0.82	0.93	0.01
	HadGEM2-AO	-8.42	-14.98	-3.39	3.16	0.76	0.63	0.82	0.03	-16.86	-26.71	-8.84	3.93	0.24	0.08	0.31	0.04
	CESM1-CAM5	-18.25	-25.86	-10.84	3.46	0.42	0.31	0.48	0.03	0.48	-3.64	5.24	2.46	0.73	0.61	0.77	0.02
	MIROC5	-5.65	-8.42	-2.43	1.12	0.48	0.31	0.56	0.04	0.30	-4.17	5.45	2.61	0.43	0.28	0.49	0.03
	CCSM4	-8.41	-13.21	-2.38	2.50	0.32	0.20	0.40	0.03	-3.15	-7.97	2.06	2.19	0.50	0.37	0.56	0.03
	GISS-E2-R	-12.10	-17.78	-7.80	2.71	0.40	0.28	0.44	0.02	-1.12	-6.54	9.46	4.02	0.53	0.40	0.58	0.03
	Average	-6.66	-11.81	-1.41	2.42	0.51	0.39	0.58	0.03	-2.91	-8.75	3.47	2.99	0.55	0.43	0.61	0.03
2046 - 2065	CSIRO-Mk3-6-0	10.50	3.66	15.69	2.69	2.00	1.91	2.05	0.04	23.00	17.65	29.81	2.92	2.49	2.41	2.53	0.02
	HadGEM2-AO	-3.43	-6.42	-0.15	1.00	1.53	1.34	1.62	0.06	-10.20	-17.35	-3.34	3.88	1.66	1.40	1.78	0.09
	CESM1-CAM5	-7.35	-16.12	0.95	4.13	1.24	1.13	1.33	0.05	-0.65	-9.62	5.75	4.10	1.79	1.65	1.90	0.06
	MIROC5	2.11	-1.65	4.24	1.00	1.26	1.13	1.33	0.05	6.66	1.57	13.71	2.88	1.97	1.79	2.11	0.09
	CCSM4	3.75	1.70	7.73	1.05	0.95	0.84	1.02	0.04	-12.23	-17.02	-6.48	2.66	1.34	1.20	1.44	0.05
	GISS-E2-R	-15.19	-20.45	-9.12	2.27	0.76	0.65	0.81	0.02	-2.81	-4.82	0.46	1.43	1.37	1.26	1.42	0.02
	Average	-1.60	-6.55	3.23	2.02	1.29	1.17	1.36	0.04	0.63	-4.93	6.65	2.98	1.77	1.62	1.86	0.05
2081 - 2100	CSIRO-Mk3-6-0	22.58	16.61	27.98	3.04	2.66	2.57	2.70	0.02	24.79	17.51	31.19	3.37	4.09	3.96	4.19	0.06
	HadGEM2-AO	-9.81	-15.43	-6.95	2.03	1.88	1.57	1.99	0.10	-15.97	-20.78	-12.33	1.95	3.02	2.59	3.23	0.16
	CESM1-CAM5	-0.62	-2.88	1.68	1.18	1.97	1.87	2.07	0.04	-8.84	-17.95	0.47	4.95	3.12	2.88	3.28	0.10
	MIROC5	4.54	1.97	8.04	1.00	1.88	1.71	2.03	0.08	3.21	0.06	7.35	1.34	3.41	3.15	3.61	0.13
	CCSM4	-1.92	-6.48	1.81	1.91	1.15	1.01	1.27	0.05	-1.23	-7.87	5.49	3.39	2.67	2.47	2.81	0.09
	GISS-E2-R	-4.54	-7.66	2.32	1.88	0.92	0.78	1.00	0.04	1.55	-1.33	5.23	0.92	2.36	2.25	2.42	0.04
	Average	1.70	-2.31	5.81	1.84	1.74	1.59	1.84	0.05	0.59	-5.06	6.23	2.65	3.11	2.88	3.26	0.10

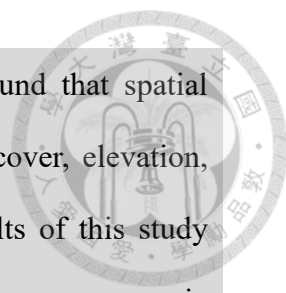
Chapter 5

Geographical distribution of dioecy and its ecological correlates based on fine-scaled species distribution data from a subtropical island

This chapter is a published paper in Ecological Research 35(1): 170–181, 2020, co-authored by Huan-Yu Lin, Yu-Hsin Tseng, Chang-Fu Hsieh, and Jer-Ming Hu. This article is an application of Taiwanese Vascular Plant Distribution Database and clim.regression model in the use of ecological studies.

Abstract

Dioecy is a rather rare sexual expression system guarantees outcrossing to avoid the deleterious effects of inbreeding. The incidence of dioecy varied among local floras and suggested inclining to tropical and oceanic environments, but its eco-correlates received little research attention. In this paper, we explore geographical patterns and variations in sexual expression systems of angiosperms in mountainous environments of Taiwan, a subtropical island in East Asia. A comprehensive geo-database of vegetation inventories and herbarium specimens were used to identify eco-correlates causing variations in the horizontal geographical extent and along a large elevational gradient of more than 3,500m. We found the average incidence of dioecy in the flora of Taiwan to be 8.2%, but it exhibits geographical variations from islets in the Taiwan Strait to the Pacific Ocean. Detailed studies on the main island of Taiwan revealed that the incidence of dioecy varied among land cover types and elevational zones. An apparent two-step decreasing pattern of dioecy percentages with elevation was found, with the highest proportion in the lowlands (0–600m; 23.96%), followed by middle elevations (600–2,700m; 20.87%) and subalpine

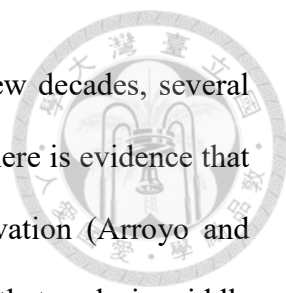


regions (2,700–3,900m; with a range of 11.38% to 0%). We found that spatial variations of dioecy were associated with eco-correlates of land cover, elevation, woodiness, species richness, and mean annual temperature. Results of this study partially support Bawa's hypothesis of a higher incidence of dioecy on oceanic islands, and is consistent with Baker and Cox's observations of richer dioecious species on high-mountain islands in the tropics and subtropics.

KEY WORDS: Elevational gradient, Dioecy, Sexual expression system, Subtropics, Taiwan.

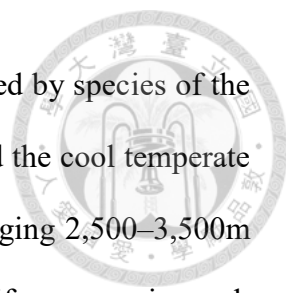
INTRODUCTION

Dioecy is a rather rare breeding system in plants that guarantees outcrossing to avoid the deleterious effects of inbreeding. The global incidence of dioecy among angiosperms is estimated to be 6% (Renner and Ricklefs, 1995), and its presence can vary among local floras. Some researchers found higher proportions of dioecious species in tropical floras (22.0–40.0% by Bawa and Opler, 1975; 30.6% in Venezuela by Sobrevila and Arroyo, 1982) than in temperate floras such as the British Isles, North Carolina, southern California and South Australia (less than 4.0% by Bawa, 1980). In addition, oceanic islands were suggested as being hotspots of dioecy (Bawa, 1982; Baker and Cox, 1984). For example, Hawaii (27.7% by Bawa, 1982; 14.7% by Sakai et al., 1995), New Zealand (12.0–13.0% by Godley, 1979), Tonga (16.0% by Yuncker, 1959, in Baker and Cox, 1984), and Samoa (17.0% by Setchell, 1924, in Baker and Cox, 1984) are the most dioecy-rich islands in the world. Baker and Cox (1984) reported that the maximum elevation plays an important role in the percentage of dioecy on islands. However, variations in the incidences of dioecy among elevation, vegetation types, and possible ecological



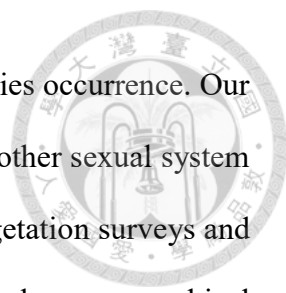
correlates have received little research attention. During the past few decades, several studies focused on the relationship between dioecy and elevation. There is evidence that the percentage of dioecious species increases with increasing elevation (Arroyo and Squeo, 1990), or dioecy and elevation exhibit a unimodal relationship that peaks in middle elevations (Vamosi and Queenborough, 2010). It is known that dioecy is also correlated with several life-form attributes such as woodiness (Bawa, 1980; Bullock, 1985; Sakai et al., 1995; Webb et al., 1999); small, inconspicuous, or greenish flowers (Bawa, 1980; Fox, 1985); fleshy fruits (Bawa, 1980; Givnish, 1980; Webb et al., 1999); unspecialized pollinators (Bawa and Opler, 1975; Baker and Cox, 1984); and a young successional stage (Réjou-Méchain and Cheptou, 2015).

Taiwan is a continental island on the western edge of the Pacific Ocean; it is located approximately 200km east of the Asian mainland and 360km north of Luzon Island, the Philippines (Hsieh and Shen, 1994). More than 73% of the land is occupied by hills and mountains, and the Central Mountain Range reaches nearly 4,000m above sea level. The main landmass of Taiwan was formed as an island during the Miocene epoch, but is generally believed to have been connected to the Asian mainland during the four glacial periods of the late Quaternary, with the final connection occurring at the end of the last glacial period approximately 10,000 years ago (Shen, 1994). The dynamic environment of the island creates diverse topography and habitats harboring more than 4,200 vascular plant species (with approximately 3,500 species being angiosperms), of which 1,052 (22.9%) are endemic to Taiwan. A total of 60.7% of the island is covered by forests, in which 79% is natural (<https://www.forest.gov.tw/EN/0002664>) and shows a clear vertical zonation caused by elevational variations in climate conditions (Su, 1984). Hills below 500m are considered subtropical to tropical environments and are occupied by *Ficus*–*Machilus* forests. Areas at 500–1,500m, corresponding to the subtropical climate zone,



are occupied by broadleaf evergreen forests and are mainly dominated by species of the Lauraceae and Fagaceae. Mountains at 1,500–2,500m are considered the cool temperate vegetation zone, usually dominated by *Quercus* species. Forests ranging 2,500–3,500m are comparable to the cold temperate zone and are dominated by coniferous species such as *Tsuga*, *Picea*, and *Abies*. Areas above 3,500m are considered subarctic environments that approach the timber line of Taiwan (Hsieh et al., 1994).

A tropical climate (Baker, 1959; Bawa and Opler, 1975; Baker and Cox, 1984) and island habitats (Baker and Cox, 1984; Sakai et al., 1995) have long been speculated to be correlated with the presence of dioecy. Taiwan contains plant species that migrated from temperate Asia via a land bridge during the Last Glacial Maximum (LGM); however, this island also harbors abundant tropical species conveyed by ocean currents and animals. Because of the transition between temperate- and tropical-originating floras and the obvious elevational climatic variations that exist in Taiwan, we can reasonably assume that sexual expression systems should gradually vary along geographical and elevational gradients. In our previous study, we documented the incidence of dioecy in Taiwan using species lists and taxonomic revisions from the second edition of the Flora of Taiwan (Huang and Editorial Committee of the Flora of Taiwan, 1993, 1996, 1998, 2000, 2003). We found that the overall percentage of dioecious species was approximately 8%, but the percentage varied among different forests and climatic zones in selected plots. We also found that dioecy probably tended to decrease with elevation (Tseng et al., 2008) based on data from seven selected forest plots at different elevations. However, descriptive data of the flora were only preliminary in that research on breeding systems; further detailed and advanced studies are required to elucidate correlations between dioecy and ecological factors. In this study, we applied a geographic information system (GIS) to accurately integrate geo-referenced data from extensive plot-based vegetation surveys and



herbarium specimen collections with ecological factors for each species occurrence. Our main objectives were to: (1) determine the incidences of dioecy and other sexual system for more than 3500 angiosperms based on data of newly updated vegetation surveys and herbarium specimens; and (2) explore changes in dioecy percentages along geographical and elevational gradients and their possible ecological correlates.

MATERIALS AND METHODS

Data source

We collected distribution data of angiosperms, including 379,962 specimen records from four main herbaria (TAI, TAIF, HAST, and TNM) and 991,455 occurrences from two national biological resource inventory projects in Taiwan (Fig. 5.1). Specimen metadata from the herbaria included the following content: scientific name, collection date, locality, collectors, collector number, and identifiers. Specimens with collection locality descriptions but without geographical coordinates were assigned coordinates by consulting place name databases and archival and online maps. The two national biological resource inventory projects were the National Vegetation Mapping implemented in 2003–2008 and the Survey of Invasive Alien Plants implemented in 2009–2012. In the National Vegetation Mapping project, 3,564 plots (400m² in size) were established and surveyed in national forest districts throughout Taiwan. In the Survey of Invasive Alien Plants project, another 3,566 plots (125 m²) were established at low elevations and on the plains. In accordance with criteria set forth by the vegetation survey team, each plot was categorized into one of eight land cover types: bamboo forest (BAM), cropland (CL), grassland (GL), natural forest (NF), plantation (PL), roadside (RS), shrub land (SL), and *Yushania* grassland (YUS). For each plot, the following parameters were measured: geographical coordinates, abiotic environmental factors (elevation, slope, and

aspect), and biotic factors (species, diameter at breast height for woody plants, and coverage of herbaceous plants and seedlings). Ultimately, 1,364,490 occurrence records were compiled into our GIS database, including 187 families, 1,216 genera, and 3,537 angiosperm taxa.

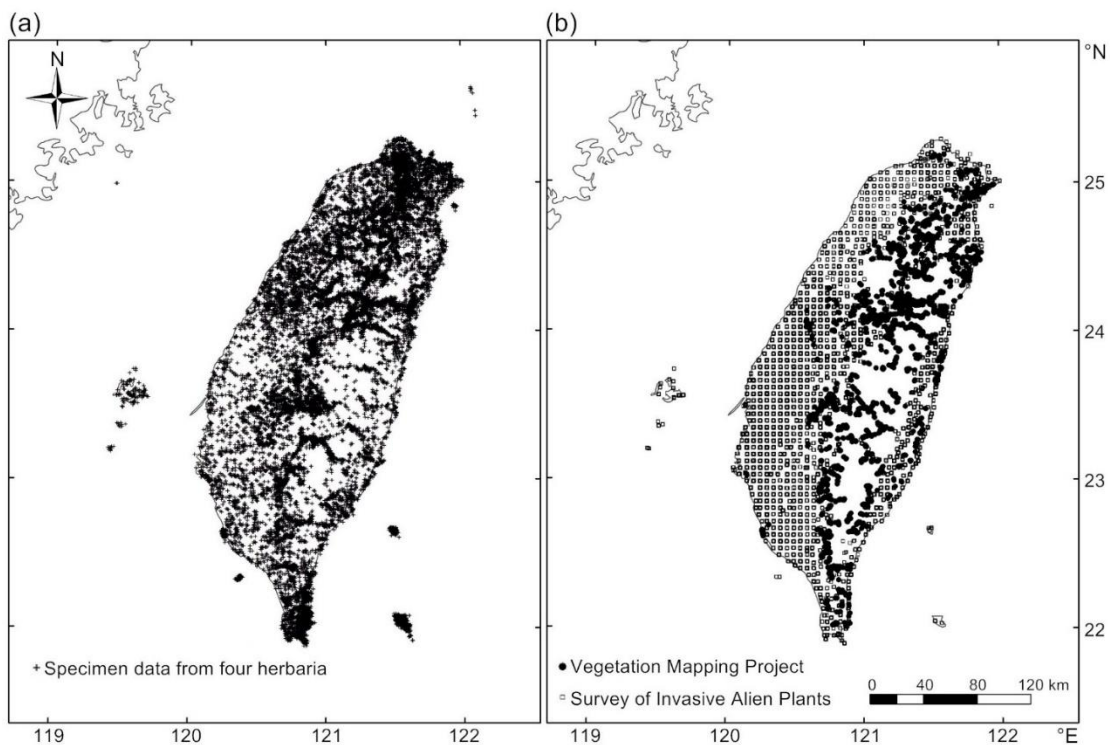
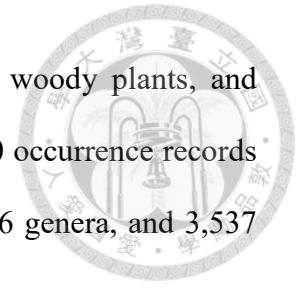
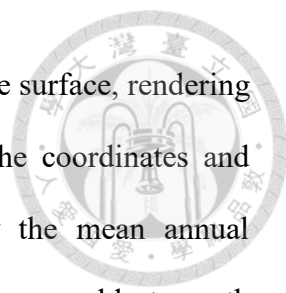


Fig. 5.1. (a) Distribution of specimen data from four main herbaria of Taiwan. (b) Plots of the National Vegetation Mapping Project (solid circles) and Survey of Invasive Alien Plants (open squares).

Estimates of climatic variables for field survey plots

Because of difficulties in measuring climatic variables in each plot, we utilized *clim.regression*, a climate downscaling program based on algorithms of bilinear interpolation and dynamic elevation adjustment (Wang et al., 2016; Wang et al., 2017; Lin et al., 2018), to downscale the 5-km-gridded climate data produced by the Taiwan

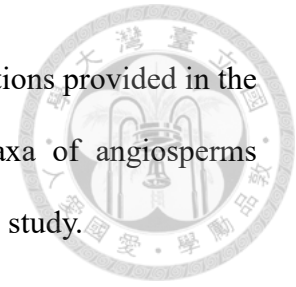


Climate Change Projection and Information Platform into a scale-free surface, rendering it more suitable and accurate for ecological research. Based on the coordinates and elevation of each plot, five climatic variable estimates, namely the mean annual temperature (MAT), mean warmest month temperature (MWMT), mean coldest month temperature (MCMT), temperature difference between the MWMT and MCMT (TD), and mean annual precipitation (MAP), were obtained.

Identification of sexual systems

Tseng et al. (2008) documented sexual expression systems of the flora of Taiwan, including 181 families, 1,120 genera, and 3,052 native species. Following Tseng et al.'s report, plant sexual systems were divided into four categories in this study: monoecious, dioecious, hermaphroditic, and "polygamous and others". Species described as "monoecious or dioecious" in the Flora of Taiwan were considered monoecious because dioecious records sometimes reflect the dichogamous expression of unisexual flowers. Species listed as "dioecious or rarely monoecious" or "functionally dioecious" were considered to be dioecious. Species were recorded as hermaphroditic if they had bisexual flowers. Species recognized as "polygamous and others" included andromonoecious, gynomonoecious, androdioecious, polygamodioecious, polygamousmonoecious, dioecious or hermaphroditic, dioecious or polygamous, monoecious or polygamous, dioecious or hermaphroditic or polygamous, dioecious or monoecious or polygamous, and species without detailed sexual system information. In Tseng et al.'s study, species with more than one variety, subspecies, or forma were considered one record to reduce double counts at the infraspecific level. However, ecological niches and geographical distributions may differ among varieties and subspecies; to reveal spatial and ecological identities of sexual expression systems, we narrowed our data down to the infraspecific

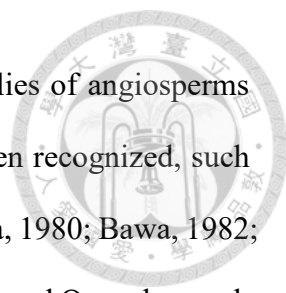
level based on definitions provided in previous research and descriptions provided in the Flora of Taiwan. Finally, sexual expression systems of 3,537 taxa of angiosperms belonging to 187 families and 1,216 genera were documented in this study.



Data analysis

Taiwan is located on the southeastern edge of Eurasia Plate and is surrounded by islets that originated from different geological events. The Taiwanese flora also displays a transition from the Eastern Asiatic Region to the Malesian Region due to its geographical and historical context (Takhtajan, 1978). To express geographical patterns of sexual systems, geo-referenced specimens and inventory data were used to calculate the relative representation of sexual expression systems (dioecious, monoecious, hermaphroditic, and “polygamous and others”) among Taiwan and its associated islets (Fig. 5.2).

In order to exclude imprecise ecological factors from ambiguous localities of specimen metadata, we extracted data from two national biological resource inventory projects which contained accurate GPS coordinates and plot parameters to conduct further analyses (Fig. 5.1b). An analysis of variance (ANOVA) and Tukey’s honest significant difference (HSD) post-hoc test were used to examine differences in the percentage of dioecy among land cover types and elevational zones. A linear regression was conducted to explore relationships between dioecy and elevation. However, in order to verify the difference among land cover types, the regression analysis was carried out for each land cover type separately. To assess the detailed elevational patterns of dioecy of natural vegetation, plots of the four natural land cover types (NF, SL, GL, and YUS) were extracted and categorized into 13 elevational groups of 300-m contour intervals for local polynomial regression function (LOESS) analysis to reveal the overall variation in dioecy with the change in elevation.



Dioecy is unevenly distributed among regions, life forms, and families of angiosperms (Bawa, 1980). Many biotic and abiotic correlates of dioecy have been recognized, such as woody communities (Bawa, 1980), tropical floras on islands (Bawa, 1980; Bawa, 1982; Baker and Cox, 1984), species richness, phylogenetic diversity (Vamosi and Queenborough, 2010), and mesic habitats in lowlands and lowland-montane regions (Sakai et al., 1995). Most of the factors are highly entangled, and correlations cannot be easily separated, especially when using vegetation data from field surveys. For this reason, a principal component analysis (PCA) was conducted to explore possible variables related to sexual expression systems. Proportion of sexual expression systems of each surveyed plot was used as input data and first analyzed by the PCA, and then groups of biotic variables (number of species; the rate of endemic species; proportion of tree, shrub, herbaceous, and climber species; proportion of native, naturalized, and cultivated species of each plot) and abiotic variables (elevation, slope, and aspect from field measurement and MAT, MAP, and TD from the output of *clim.regression*) were added separately as passive variables and projected on the ordination plot. All data processing and analyses were performed with ESRI ArcGIS 10.5 and R 3.3.1 software (R Core Team, 2016).

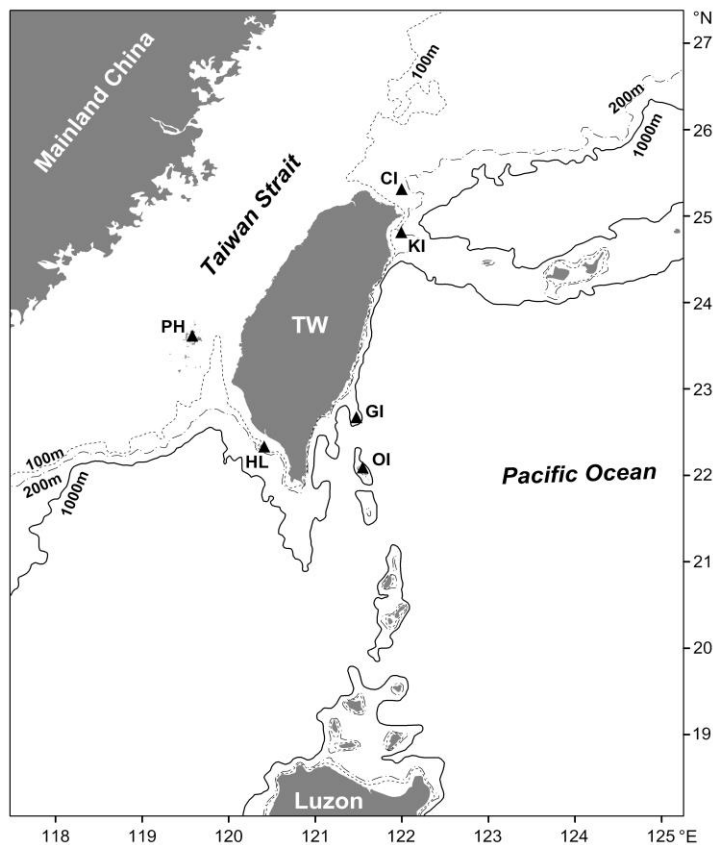


Fig. 5.2. Location of Taiwan and its associated islets. For abbreviations of localities and proportions of plant sexual expression systems of each islet see Table 5.1.

RESULTS

Distribution patterns of sexual systems in Taiwan and its associated islands

According to our compiled database based on specimens and inventory surveys, 290 (8.20%), 379 (10.72%), 2582 (73.00%), and 246 (6.96%) of 3,537 taxa were dioecious, monoecious, hermaphroditic and “polygamous and others”, respectively. The remnant 40 taxa (1.12%) are lack of sexual expression information.

The percentage of dioecy considerably varied among Taiwan proper and its associated islets. The dioecy percentage of the main island of Taiwan was 8.07%. Richer assemblages of dioecious species were discovered on three volcanic islands of Kueishan Island (KI), Orchid Island (OI), and Green Island (GI), representing 13.4%, 11.3%, and 10.6% of the overall proportions, respectively. All three of these islets which were richer in dioecious species are located off the east coast of Taiwan and are isolated by ocean

waters deeper than 200m. Other islets located to the west in the Taiwan Strait, with sea depths shallower than 200m, exhibited lower proportions of dioecy, ranging 3.8–6.7%, (Fig. 5.2, Table 5.1).

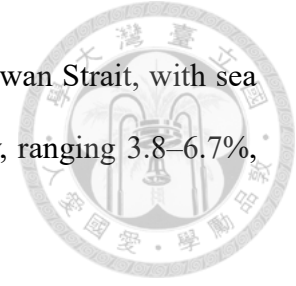


Table 5.1. Number of taxa and proportions of sexual expression systems of angiosperms in the flora of Taiwan and associated islands.

Region	Area (km ²)	Number of angiosperms	Sexual system			
			Dioecy	Monoecy	Hermaphrodite	Polygamy & Others
Kueishan Island (KI)	2.84	372	50 13.44%	37 9.95%	247 66.40%	38 10.22%
Orchid Island (OI)	48.39	957	108 11.29%	115 12.02%	649 67.82%	85 8.88%
Green Island (GI)	15.09	529	56 10.59%	61 11.53%	359 67.86%	53 10.02%
Taiwan (TW)	35,582.62	3,484	281 8.07%	371 10.65%	2,548 73.13%	284 8.15%
Hsiao Lyukyu (HL)	6.80	360	24 6.67%	41 11.39%	257 71.39%	38 10.56%
Penghu (PH)	126.86	303	13 4.29%	33 10.89%	226 74.59%	31 10.23%
Cotton Islet (CI)	0.12	158	6 3.80%	8 5.06%	119 75.32%	25 15.82%
Total	35,782.72	3,537	290 8.20%	379 10.72%	2,582 73.00%	286 8.09%

Table 5.2. ANOVA (a) and Tukey's HSD test (b) for dioecy percentage among different land cover types.

(a)

	df	SS	MS	F	p
Land cover types	7	38.56	5.508	1097	< 0.001
Residuals	5,849	29.37	0.005		

df, degrees of freedom; SS, sum-of-squares; MS, mean squares.

(b)

Land cover type	No. of plots	Average dioecy (%)	SD (%)	Tukey's HSD test (conf. level = 0.95)
Natural forests (NF)	3,240	20.81%	7.81%	d
Plantations (PL)	323	17.28%	9.30%	c
Bamboo forests (BAM)	150	17.01%	8.82%	c
Shrub lands (SL)	53	15.41%	15.51%	c
Roadsides (RS)	1,131	4.26%	4.56%	b
Grasslands (GL)	75	4.30%	7.26%	ab
<i>Yushania</i> grasslands (YUS)	79	2.16%	5.72%	ab
Croplands (CL)	806	2.56%	4.21%	a

(1) SD, standard deviation.

(2) a, b, c, or d is group divided by Tukey's HSD test. The means in the same group are not different significantly by the test.

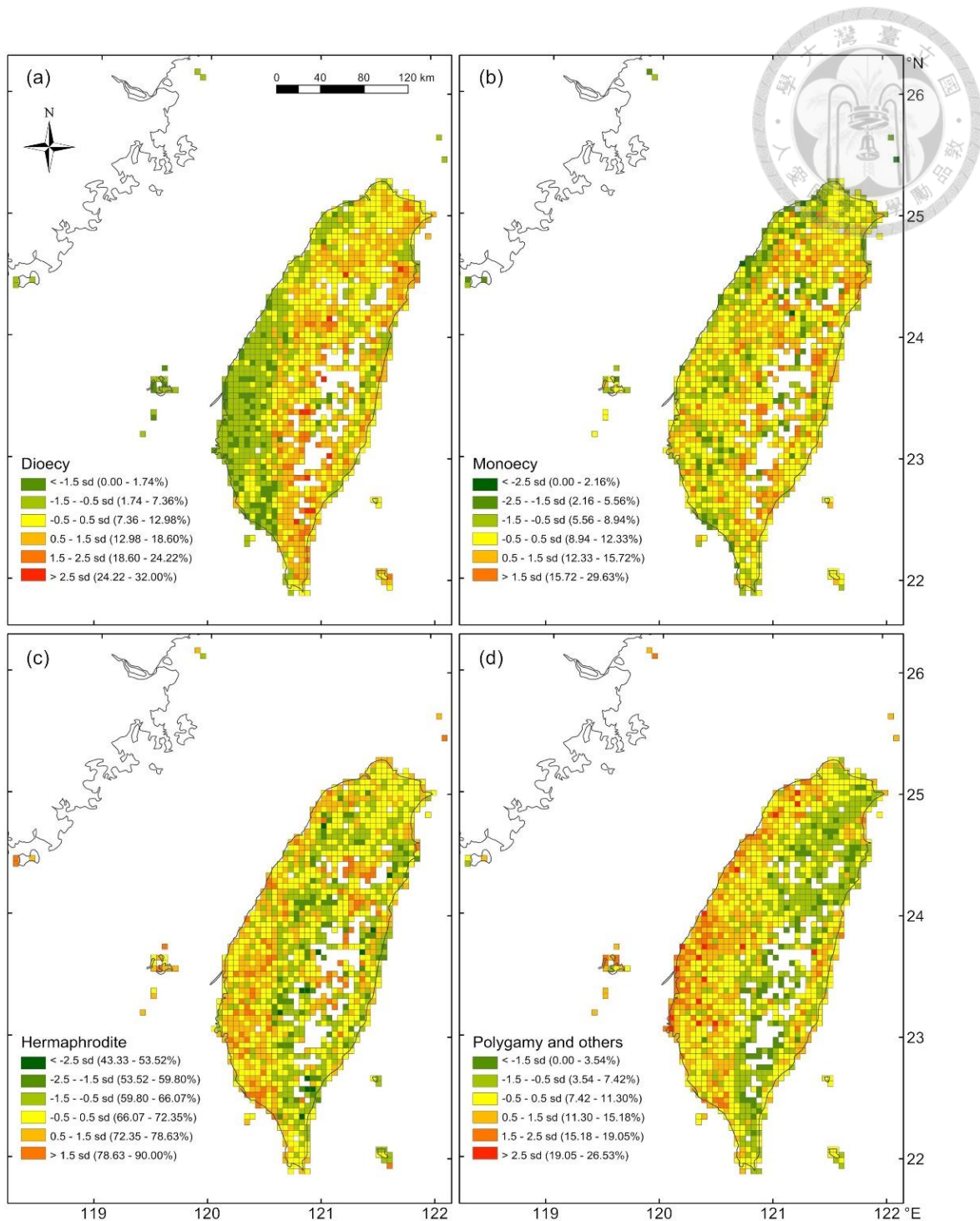
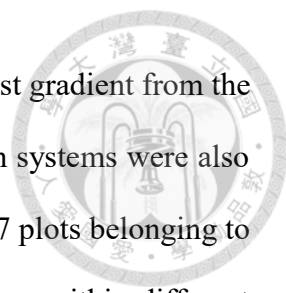


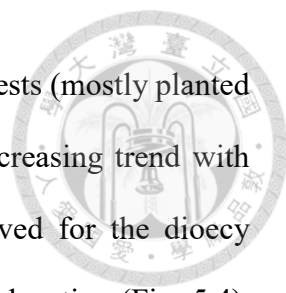
Fig. 5.3. Distribution map of sexual expression systems of Taiwan and its associated islands. (a) Dioecy; (b) monoecy; (c) hermaphrodite; (d) polygamy and others. We divided the main island of Taiwan and its neighboring islets into 1,629 continuous 5km × 5km grids, which were overlaid with angiosperm occurrence data to calculate the proportions of breeding systems for each grid. To avoid dramatic changes in the proportion caused by a lack of data, grids that contained fewer than 50 species occurrence records were excluded. We also excluded grids that covered a terrestrial area of less than 1.25km² (5% of the grid area) to prevent the distribution pattern from being abbreviated. Finally, 1,395 grids, accounting for 85.63% of Taiwan's total land area, were included in the maps.



In addition to the increasing incidence of dioecy through a west-to-east gradient from the Taiwan Strait to the Pacific Ocean, distributions of sexual expression systems were also highly variable among local habitats of Taiwan. Field data from 5,857 plots belonging to eight land cover types were used to evaluate the incidences of dioecy within different environmental surroundings. The average incidence of dioecy in Taiwan was 8.20%, however, results of the ANOVA indicated that it was significantly inconsistent among land cover types (Table 5.2a, $F = 1,097, p < 0.001$). The result of Tukey's HSD test further grouped land cover types into three categories based on their dioecy proportion. Natural forests (NF) were the most dioecy-rich community with an average incidence of 20.81%. Dioecious species were also common in woody-dominant communities, including plantations (PL), bamboo forests (BAM), and shrub lands (SL), with proportions ranging 15.41–17.28%, which were relatively lower compared to natural forests. The lowest incidences of dioecy were found in disturbed, early successional, and non-woody vegetation, such as roadsides (RS), grasslands (GL), *Yushania* grasslands (YUS), and croplands (CL), with proportions ranging 2.56–4.26% (Table 5.2b). The mapped distribution of sexual expression systems also exhibited high spatial heterogeneity. Hotspots of dioecy usually occurred in mountainous areas, whereas the western plains and islets in the Taiwan Strait were mostly dioecious-poor and dominated by polygamous and hermaphroditic species (Fig. 5.3).

Elevational patterns of dioecy and their ecological correlates

Results of the linear regression analysis revealed that the dioecy percentage significantly decreased with increasing elevation ($m < 0, p < 0.001$) for each of the four natural land cover types of natural forests (NF), shrub lands (SL), grasslands (GL), and *Yushania* grasslands (YUS). Contrary results were obtained for anthropogenic vegetation and



human-exploited areas. The incidence of dioecy for both bamboo forests (mostly planted on the main island of Taiwan) and croplands (CL) exhibited an increasing trend with elevation ($m > 0$, $p < 0.001$), but no consistent trend was observed for the dioecy proportion of plantation forests (PL) or roadside (RS) habitats with elevation (Fig. 5.4). Several authors mentioned that the percentage of out-breeding or dioecious species in natural forests displayed a decreasing (Jacquemyn et al., 2005; Tseng et al, 2008) or unimodal relationship (Vamosi and Queenborough, 2010) with elevation. Our data supported the declining incidence of dioecy with elevation; however, this pattern was only found for natural vegetation types and not for anthropogenic or disturbed habitats.

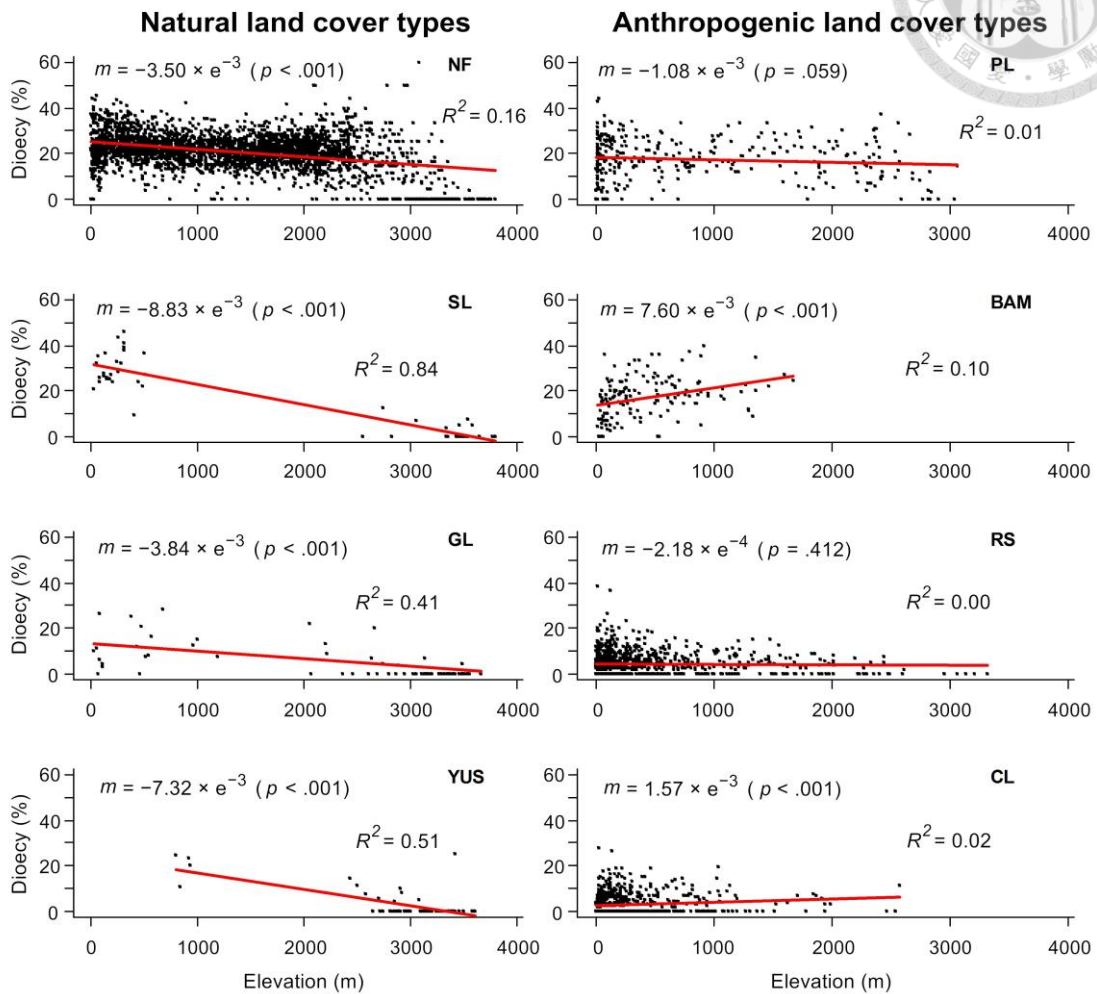


Fig. 5.4. Results of a linear regression analysis between elevation and the proportion of dioecy for each of eight land cover types. Natural land cover types are in the left column (NF, natural forests; SL, shrub lands; GL, grassland; and YUS, *Yushania* grasslands), and anthropogenic land cover types are in the right column (PL, plantations; BAM, bamboo forests; RS, roadsides; and CL, croplands). The slope of the regression line is represented by m .

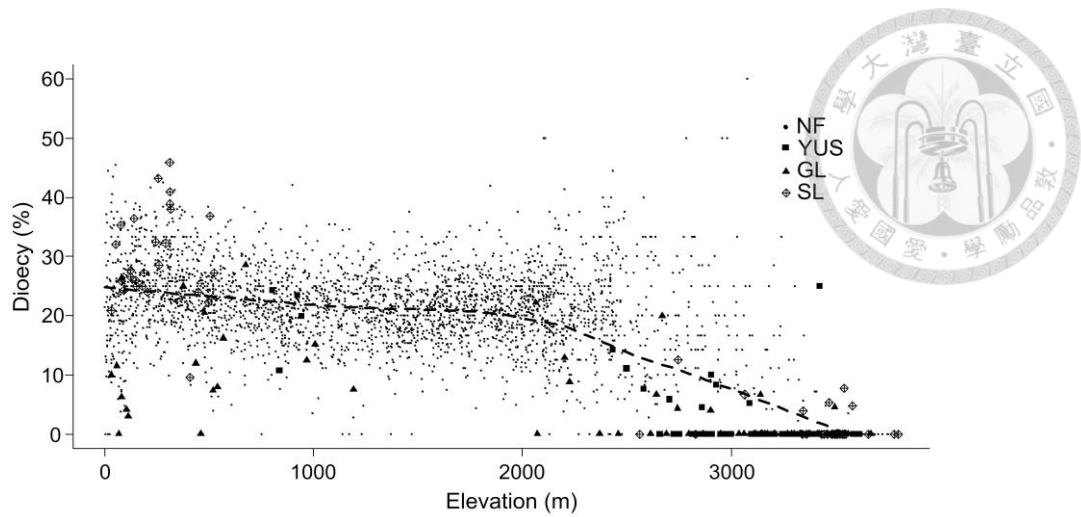


Fig. 5.5. Relationship between the percentage of dioecy and elevation for natural vegetation (NF, natural forests; YUS, *Yushania* grasslands; GL, grassland; and SL, shrub lands). The fitted curve is a local polynomial regression.

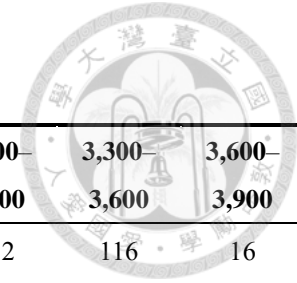


Table 5.3. Tukey's HSD test for dioecy of natural vegetation among different elevational groups.

Elevation (m)	0–300	300–600	600–900	900–1,200	1,200–1,500	1,500–1,800	1,800–2,100	2,100–2,400	2,400–2,700	2,700–3,000	3,000–3,300	3,300–3,600	3,600–3,900
No. of plots	429	421	336	275	336	370	407	326	157	126	132	116	16
Average dioecy (%)	23.87%	24.10%	21.88%	21.15%	20.55%	21.26%	21.31%	20.67%	19.29%	11.38%	4.74%	1.25%	0.00%
Standard deviation	7.92%	6.11%	5.52%	5.67%	5.27%	5.03%	5.35%	7.49%	10.21%	12.05%	9.31%	4.07%	0.00%
Tukey's HSD test (conf. level = 0.95)	f	f	e	de	de	de	de	de	d	c	a	b	ab

a, b, c, d, e or f is group divided by Tukey's HSD test. The means in the same group are not different significantly by the test.

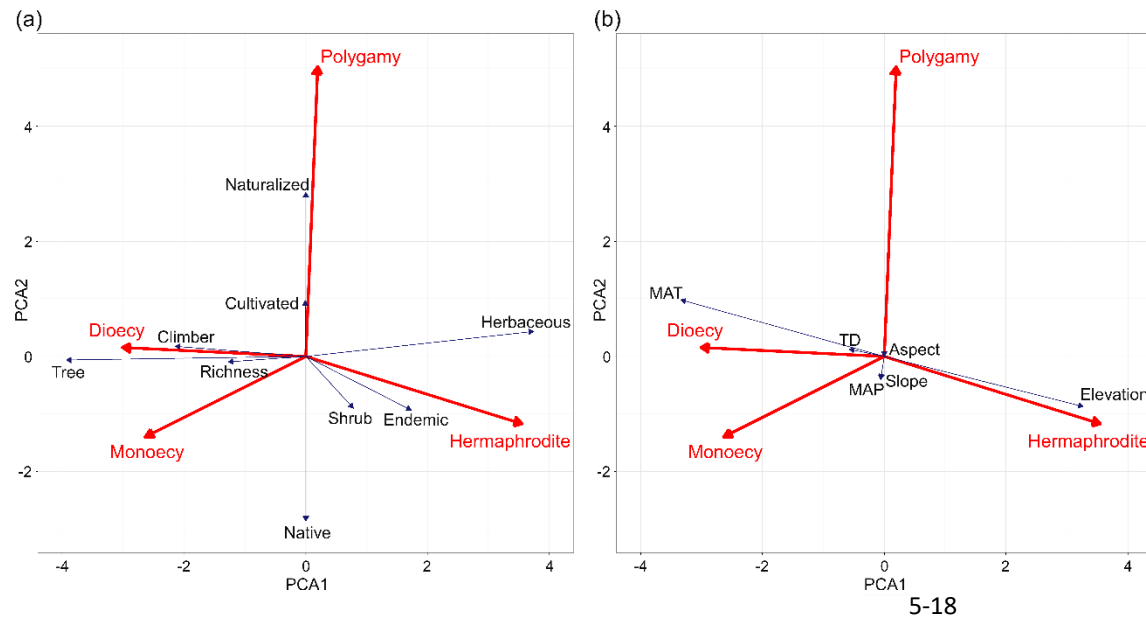
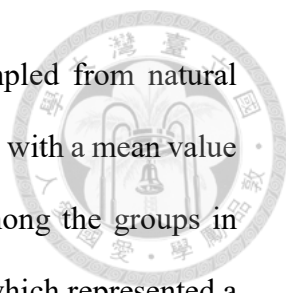
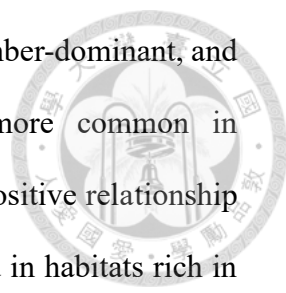


Fig. 5.6. Biplots of the principal component analysis (PCA) showing relationships between sexual expression systems and (a) biotic and (b) abiotic correlates. The variables are indicated by vectors pointing in the direction of maximum variation. Long vectors indicate strong trends, and the angle between pairs of vectors approximates the correlation between the respective variables. Each vector points in the direction of increase for a given variable, and its length indicates the relative importance of that variable in the dataset.



Results of Tukey's HSD test (Table 5.3) indicated that plots sampled from natural vegetation below 600m had a significantly higher dioecy percentage, with a mean value of 23.96%. No statistically significant difference was detected among the groups in middle elevations (at 600–2,400m, with a mean value of 21.14%), which represented a slightly decreased incidence of dioecy than that at low elevations. The dioecy percentage significantly declined in elevational groups above 2,400m, and no dioecious species were found in any subalpine plots (at $\geq 3,600$ m). The LOESS regression demonstrated that the relationship between dioecy and elevation in natural habitats could be split into two segments with a breakpoint at approximately 2,200m (Fig. 5.5). The segment below 2,200m showed a moderate decreasing trend for the dioecy proportion; whereas it became distinctly steeper above the breakpoint. In high-elevation plots above 2,500m, zero values of dioecy were common, especially for *Yushania* grasslands (YUS) and grasslands (GL).

Results of the PCA showed that the first two principal components (axes) together accounted for 80.65% of the total variance in the sexual expression dataset. The first component was primarily related in one extreme (negative values) with high proportions of dioecious and monoecious species, and at the opposite extreme (positive values) with high proportions of hermaphroditic species (Fig. 5.6). The second component represented a sharp contrast between polygamous species and those with other sexual expressions. Plots near the top tended to have a high proportion of polygamy, and this was strongly independent of the occurrence of dioecious and hermaphroditic species along the first component. Biotic variables of each plot, including the proportions of life forms (trees, climbers, shrubs, and herbs), proportions of origins (native, naturalized, and cultivated), species richness, and the rate of endemic species were orthogonally projected onto the first two principal components (Fig. 5.6a).

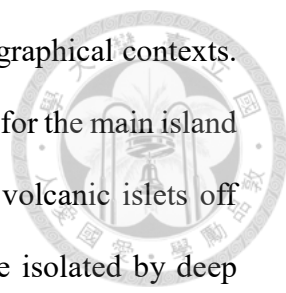


This illustrated that dioecy was significantly related to tree- and climber-dominant, and species-rich communities; in contrast, hermaphrodites were more common in herbaceous-dominant communities, and they also demonstrated a positive relationship with the rate of endemism. Polygamous species were usually found in habitats rich in naturalized and cultivated species. Fig. 5.6b displays the orthogonal projection of abiotic factors. Only two variables, MAT and elevation, were correlated with the composition of sexual expression systems, especially for the presence of dioecious and hermaphroditic species. This result revealed that dioecious species may prefer low-elevation regions with a warm climate, while hermaphroditic species exhibited higher dominance in subalpine areas with lower annual temperatures. The remaining abiotic factors (TD, MAP, slope, and aspect) seemed to have little effect on the distributions of sexual expression systems.

DISCUSSION

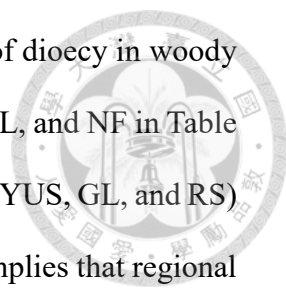
The horizontal distribution of dioecy — from continental to oceanic

The continental and oceanic distributions of dioecism and its latitudinal pattern have long been the subject of biogeographical research. Most studies relied on regional floristic checklists (e.g., Baker and Cox, 1984; Sakai et al., 1995; Tseng et al., 2008), but analyses examining dioecy and its geographical patterns based on complete and detailed inventory data are lacking. A review (Sakai and Weller, 1999) of geographic patterns of dioecism noted that dioecy is mainly related to island habitats (Baker, 1967; Bawa, 1980; Baker and Cox, 1984; Sakai et al., 1995) and tropical climates (Bawa, 1980; Givnish, 1980). Baker and Cox (1984) reported a strong correlation between the level of dioecy on islands and proximity to the equator as well as the maximum elevation of the island. Based on these perspectives, the level of dioecism in Taiwan should be higher than those of continents and should display a transitional characteristic



between continental and oceanic floras due to its historical and geographical contexts. Our study documented that the average incidence of dioecy is 8.07% for the main island of Taiwan, and also discovered high dioecy percentages for three volcanic islets off eastern Taiwan (KI, OI, and GI, ranging 10.6–13.4%), which were isolated by deep ocean waters since their formation. Dioecy-poor floras were observed in islets west of Taiwan in the Taiwan Strait (CI, PH, and HL, ranging 3.80–6.67%), which were connected to the Asian mainland and Taiwan by the continental shelf during the LGM. The increasing trend of dioecy along islets from the Taiwan Strait toward the Pacific Ocean, which corresponds to the transition between continental and oceanic geographical contexts, might be a phenomenon supporting Bawa's hypothesis (Bawa 1980, 1982), which refers to a higher proportion of dioecy for tropical and oceanic insular floras.

In addition to the geographical reasons we stated, habitat type could be another factor affecting the composition of sexual systems of local floras. Sakai et al. (1995) explored the biogeographical and ecological correlates of dioecy in Hawaii. They found that dioecious species were rich in lowland and lowland-montane habitats but poor in coastal, coastal-lowland, and montane-subalpine habitats. In addition, tropical and subtropical forests are often reported to have higher incidences of dioecy than the regional average, such as subtropical evergreen broadleaf forests of Yunnan, China (24%, woody angiosperms only) (Chen and Li, 2008a), azonal tropical forests in Yunnan (25.1%) (Chen and Li, 2008b), tropical montane forests of Costa Rica (30.5%) (Vamosi and Queenborough, 2010), and Neotropical forests in the Volta Velha Reserve, Brazil (28%) (Vamosi, 2006). In Taiwan, Tseng et al. (2008) first reported the average proportion of dioecy to be 7.9%; however, they also identified higher dioecy percentages (11.9–23.9%) for seven selected forest sites. In this study, data from



numerous field plots were utilized to confirm the high proportions of dioecy in woody communities, and a range of 15.41–20.81% was found (SL, BAM, PL, and NF in Table 5.2b). In contrast, we also proved that non-woody communities (CL, YUS, GL, and RS) are poorer in dioecy than the average of the total flora. This result implies that regional incidences of sexual expression systems might not serve as the only indicator in breeding system studies, and varieties among habitats and local floras (e.g., montane broadleaf forests and subalpine coniferous forests) also need to be considered.

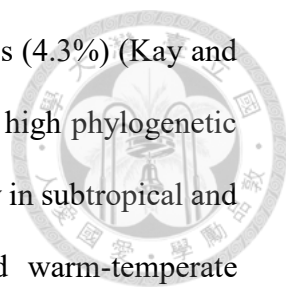
The elevational distribution of dioecy — from lowlands to the subalpine zone

Variations in dioecy with changes in elevation are the other issue with which researchers are concerned but which have received comparatively little attention. Vamosi and Queenborough (2010) used inventory data from 15 permanent 1-ha plots, that ranged from 30 to 2,600m, to explore relationships between the proportion of dioecy and elevation in tropical montane forests of Costa Rica. That study reported a unimodal relationship with a peak at 750m, and a positive association with species richness. They suggested that the coincident decline in pollinator abundances with elevation may be one of the reasons, but could not provide further evidence in support of the underlying hypothesis. Another relevant study was an investigation of the change in orchid breeding systems with elevation on Réunion Island by Jacquemyn et al. (2005). Relatively high proportions of animal-pollinated orchids were found in low- to mid-elevation zones (below the sector of 1601–2,000m), whereas a reverse trend was observed at higher elevations (> 2,000m) with almost no outcrossing orchid species observed. They proffered two explanations for the observed patterns of elevational variation in the orchid breeding systems: a decline of pollinators, mainly predominated by long-tongued moths and flies, with elevation; and harsher more-disturbed habitats above 2,000m where pollinator activities may have been more unpredictable than those

in stable forest environments at low- to mid-elevation regions.

Our study discovered high dioecy proportions in low- and mid-elevation areas in Taiwan, which exhibited a declining and two-step linear pattern toward the subalpine zone with a distinct transition at elevations of 2,200–2,400m. Results of the PCA also demonstrated clear associations of dioecy with elevation, warm temperatures, and woodiness. However, the two variables, MAT and elevation, are highly negative correlated because of the effect of lapse rate. Due to the multicollinearity problem between temperature and elevation, even though the patterns we revealed are closer to Jacquemyn's observations on Réunion, however, the causal effects of decreasing dioecy or out-crossings along elevational and temperature gradients are still obscure and could not precisely be explained by the present approach. The estimation of causal relationships by detailed field sampling and statistical modeling would be an issue worthy for further studies.

This paper demonstrated that tropical and subtropical zones of Taiwan were the most dioecy-rich regions, with proportions of 20–24%, values which are concordant with those found in azonal tropical forests (25.1%) (Chen and Li, 2008a) and subtropical evergreen broadleaf forests (24%, woody angiosperms only) (Chen and Li, 2008b) of southwestern China at a similar latitude. Lowland forests in Taiwan are mainly dominated by *Ficus* (37 species in total, 27 of 37 of which are dioecious), and commonly contain dioecious-rich genera such as *Smilax* (19/19 of which are dioecious), *Diospyros* (10/10 of which are dioecious), and *Mallotus* (5/6 of which are dioecious). This may be the main reason supporting the highest incidences of dioecy in tropical and subtropical zones of Taiwan. However, the temperate vegetation of Taiwan displays dioecy proportions of 19.29–21.26%, which are completely incongruent with those in other temperate continental areas such as Ohio (11.0%) (Braun, 1950 in Bawa and Opler,



1975), California (3.5%) (Freeman et al., 1980), and the British Isles (4.3%) (Kay and Stevens, 1986). We speculated that floras composed of plants with high phylogenetic affinities might, at least, partially explained the high levels of dioecy in subtropical and warm-temperate montane forests. For example, subtropical and warm-temperate montane forests in Taiwan commonly contain widespread genera such as *Ilex* (all 24 species of which are dioecious), *Dioscorea* (14/16 of which are dioecious), *Litsea* (14/14 of which are dioecious), *Eurya* (12/12 of which are dioecious), *Neolitsea* (12/12 of which are dioecious), *Lindera* (7/7 of which are dioecious), and *Elatostema* (6/15 of which are dioecious), which contribute to and support the high incidences of dioecy.

In this study, the average incidence of dioecy in coniferous and subalpine zones in Taiwan was 4.34%, which approximates those in subarctic and arctic territories such as Alaska (5.8% and 3.9%) (Fox, 1985) and Iceland (3.0%) (Baker and Cox, 1984). The dramatic decrease in dioecy at elevations above 2,400m coincided with the lower bound of coniferous forests in Taiwan. We speculated that the decrease in dioecious species could be associated with the transition from broadleaf forests to coniferous forests as well as the simplified floristic compositions found at higher elevations.

Pollination by small generalist insects is one of the most important characteristics of dioecy (Bawa and Opler, 1975; Bawa, 1980; Sobrevilla and Arroyo, 1982). Some studies reviewed the richness of terrestrial insect species along elevational gradients (Hodkinson, 2005). Most such studies, which were conducted at 0–2,000m, revealed a decreasing pattern of insect richness with elevation (Hanski, 1983, in Indonesia; Wolda, 1987, in Panama; McCoy, 1990, in the southeastern United States; Perillo et al., 2017, in tropical Brazil), or discovered a pattern that peaks at mid-elevations (Gagne, 1979, in Hawaii; McCoy, 1990, in the southeastern United States; Lefebvre et al., 2018, in the southern Alps, France). Insects are the main pollinators of flowering plants in general,

regardless of whether they are generalists or specialists (Jacquemyn et al., 2005), thus it is reasonable to suspect that our finding on the decline in dioecy may be partially correlated with the change of insect pollinators along the elevational gradient. Nevertheless, pollinators in Taiwan have been insufficiently surveyed to support our assumptions, more investigations on the relationship between plant sexual expressions and pollinators would be a future subject.

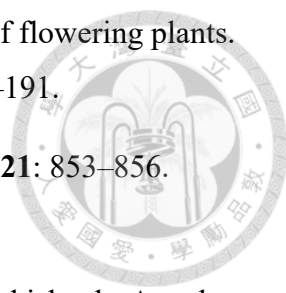
Overall, natural vegetation in the low- to mid-elevation regions of Taiwan showed higher proportions of dioecious species than the average global proportion, and demonstrated a decreasing trend toward the subalpine zone. This might be associated with the island context, and responses to a warm climate, woody floras, and the richness of insect pollinators on an elevational gradient. Although the intact species distribution database that we used in this paper was helpful in studying geo-patterns of breeding systems, better knowledge and investigations of patterns of pollinator richness, phylogenetic affinities of components of the local floras, and further ecological studies are required to verify the causalities.

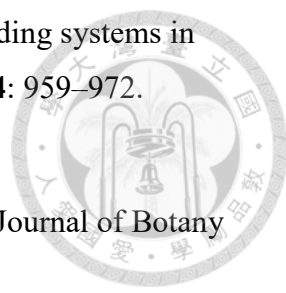
AUTHOR CONTRIBUTIONS


JMH conceived the idea; HYL carried out analyses and led the writing; YHT and CFH contributed data of angiosperm's sexual expressions and geographical occurrence; all authors commented on the manuscript.

LITERATURE CITED

Arroyo, M. T. K. and F. A. Squeo. 1990. Relationship between plant breeding systems and pollination. In S. Kawana (Ed.), *Biological approaches and evolutionary trends in plants* (pp. 205–227). Academic Press, London.

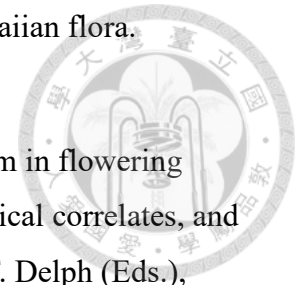
- 
- Baker, H. G.** 1959. Reproductive methods as factors in speciation of flowering plants. *Cold Spring Harbor Symposia on Quantitative Biology* **24**: 177–191.
- Baker, H. G.** 1967. Support for Baker's law — as a rule. *Evolution* **21**: 853–856.
<https://doi.org/10.2307/2406780>
- Baker, H. G. and P. A. Cox.** 1984. Further thoughts on dioecism and islands. *Annals of the Missouri Botanical Garden* **71**: 244–253. <https://doi.org/10.2307/2399068>
- Bawa, K. S.** 1980. Evolution of dioecy in flowering plants. *Annual Review of Ecology and Systematics* **11**: 15–39. <https://doi.org/10.1146/annurev.es.11.110180.000311>
- Bawa, K. S.** 1982. Outcrossing and the incidence of dioecism in island floras. *The American Naturalist* **119**: 866–871.
- Bawa, K. S. and P. A. Opler.** 1975. Dioecy in tropical forest trees. *Evolution* **29**: 167–179. <https://doi.org/10.2307/2407150>
- Bullock, S. H.** 1985. Breeding systems in the flora of a tropical deciduous forest in Mexico. *Biotropica* **17**: 287–301. <https://doi.org/10.2307/2388591>
- Chen, X.-S. and Q.-J. Li.** 2008a. Patterns of plant sexual systems in subtropical evergreen broad-leaved forests in Ailao Mountains, SW China. *Journal of Plant Ecology* **1**: 179–185. <https://doi.org/10.1093/jpe/rtn019>
- Chen, X.-S. and Q.-J. Li.** (2008b). Sexual systems and ecological correlates in an azonal tropical forest, SW China. *Biotropica* **40**: 160–167.
<https://doi.org/10.1111/j.1744-7429.2007.00364.x>
- Freeman, D. C., K. T. Harper and W. K. Ostler.** 1980. Ecology of plant dioecy in the intermountain region of western North America and California. *Oecologia* **44**: 410–417. <https://doi.org/10.1007/BF00545246>
- Fox, J. F.** 1985. Incidence of dioecy in relation to growth form, pollination and dispersal. *Oecologia* **67**: 244–249. <https://doi.org/10.1007/BF00384293>
- Gagne, W. C.** 1979. Canopy-associated arthropods in *Acacia koa* and *Metrosideros* tree communities along an altitudinal transect on Hawaii Island. *Pacific Insects* **21**: 56–82.

- 
- Givnish, T. J.** 1980. Ecological constraints on the evolution of breeding systems in seed plants: dioecy and dispersal in Gymnosperms. *Evolution* **34**: 959–972.
<https://doi.org/10.2307/2408001>
- Godley, E. J.** 1979. Flower biology in New Zealand. *New Zealand Journal of Botany* **17**: 441–466. <https://doi.org/10.1080/0028825X.1979.10432564>
- Hanski, I.** 1983. Distributional ecology and abundance of dung and carrion feeding beetles Scarabaeidae in tropical rain forests in Sarawak, Malaysia. *Acta Zoologica Fennica* **167**: 1–45.
- Hodkinson, I. D.** 2005. Terrestrial insects along elevation gradients: species and community responses to altitude. *Biological Reviews* **80**: 489–513.
<https://doi.org/10.1017/S1464793105006767>
- Hsieh, C.-F. and C.-F. Shen.** 1994. Introduction to the flora of Taiwan, 1: geography, geology, climate, and soils. In Huang & Editorial Committee of the Flora of Taiwan (Eds.), *Flora of Taiwan Second edition* (pp. 1–3). Editorial Committee of the Flora of Taiwan, Taipei.
- Hsieh, C.-F., C.-F. Shen and K.-C. Yang.** 1994. Introduction to the flora of Taiwan, 3: floristics, phytogeography, and vegetation. In Huang & Editorial Committee of the Flora of Taiwan (Eds.), *Flora of Taiwan Second edition* (pp. 7–16). Editorial Committee of the Flora of Taiwan, Taipei.
- Huang, T.-C. and Editorial Committee of the Flora of Taiwan (eds.).** 1993. *Flora of Taiwan*, 3. 2nd. Editorial Committee of the Flora of Taiwan, Taipei, Taiwan.
- Huang, T.-C. and Editorial Committee of the Flora of Taiwan (eds.).** 1996. *Flora of Taiwan*, 2. 2nd. Editorial Committee of the Flora of Taiwan, Taipei, Taiwan.
- Huang, T.-C. and Editorial Committee of the Flora of Taiwan (eds.).** 1998. *Flora of Taiwan*, 4. 2nd. Editorial Committee of the Flora of Taiwan, Taipei, Taiwan.
- Huang, T.-C. and Editorial Committee of the Flora of Taiwan (eds.).** 2000. *Flora of Taiwan*, 5. 2nd. Editorial Committee of the Flora of Taiwan, Taipei, Taiwan.
- Huang, T.-C. and Editorial Committee of the Flora of Taiwan (eds.).** 2003. *Flora of Taiwan*, 6. 2nd. Editorial Committee of the Flora of Taiwan, Taipei, Taiwan.

- 
- Jacquemyn, H., C. Micheneau, D. L. Roberts and T. Pailler.** 2005. Elevational gradients of species diversity, breeding system and floral traits of orchid species on Réunion Island. *Journal of Biogeography* **32**: 1751–1761.
<https://doi.org/10.1111/j.1365-2699.2005.01307.x>
- Kay, Q. O. N. and D. P. Stevens.** 1986. The frequency, distribution and reproductive biology of dioecious species in the native flora of Britain and Ireland. *Botanical Journal of the Linnean Society* **92**: 39–64. <https://doi.org/10.1111/j.1095-8339.1986.tb01426.x>
- Lefebvre, V., C. Villemant, C. Fontaine and C. Daugeron.** 2018. Altitudinal, temporal and trophic partitioning of flower-visitors in Alpine communities. *Scientific Reports* **8**: Article number: 4706. <https://doi.org/10.1038/s41598-018-23210-y>
- Lin, H.-Y., J.-M. Hu, T.-Y. Chen, C.-F. Hsieh, G. Wang and T. Wang.** 2018. A dynamic downscaling approach to generate scale-free regional climate data in Taiwan. *Taiwania* **63**: 251–266. <https://doi.org/10.6165/tai.2018.63.251>
- McCoy, E. D.** 1990. The distribution of insects along elevational gradients. *Oikos* **58**: 313–322. <https://doi.org/10.2307/3545222>
- Perillo, L. N., F. de S. Neves, Y. Antonini and R. P. Martins.** 2017. Compositional changes in bee and wasp communities along Neotropical mountain altitudinal gradient. *PLoS ONE* **12(7)**: e0182054.
<https://doi.org/10.1371/journal.pone.0182054>
- R Core Team.** 2016. R: A language and environment for statistical computing. R Foundation for Statistical Computing, Vienna, Austria. URL <https://www.R-project.org/>
- Réjou-Méchain, M. and P.-O. Cheptou.** 2015. High incidence of dioecy in young successional tropical forests. *Journal of Ecology* **103**: 725–732.
<https://doi.org/10.1111/1365-2745.12393>
- Renner, S. S. and R. E. Ricklefs.** 1995. Dioecy and its correlates in the flowering plants. *American Journal of Botany* **82**: 596–606. <https://doi.org/10.2307/2445418>
- Sakai, A. K., W. L. Wagner, D. M. Ferguson and D. R. Herbst.** 1995.

Biogeographical and ecological correlates of dioecy in the Hawaiian flora.

Ecology **76**: 2530–2543. <https://doi.org/10.2307/2265826>



Sakai A. K. and S. G. Weller. 1999. Gender and sexual dimorphism in flowering plants: A review of terminology, biogeographic patterns, ecological correlates, and phylogenetic approaches. In M. A. Geber, T. E. Dawson, & L. F. Delph (Eds.), *Gender and Sexual Dimorphism in Flowering Plants* (pp. 1–31). Springer, Berlin, Heidelberg. https://doi.org/10.1007/978-3-662-03908-3_1

Shen, C.-F. 1994. Introduction to the flora of Taiwan, 2: geotectonic evolution, paleogeography, and the origin of the flora. In Huang & Editorial Committee of the Flora of Taiwan (Eds.), *Flora of Taiwan Second edition* (pp. 3–7). Editorial Committee of the Flora of Taiwan, Taipei.

Sobrevila, C. and M. T. K. Arroyo. 1982. Breeding systems in a tropical montane cloud forest in Venezuela. *Biotropica* **10**: 221–230.
<https://doi.org/10.1007/BF02409895>

Su, H.-J. 1984. Studies on the climate and vegetation types of the natural forests in Taiwan (II). Altitudinal vegetation zones in relation to temperature gradient. *Quarterly Journal of Chinese Forestry* **17(4)**: 57-73.

Takhtajan, A. 1986. *Floristic Regions of the World*. University of California Press, Berkeley. [translated by T. J. Crovello & A. Cronquist]

Tseng, Y.-H., C.-F. Hsieh and J.-M. Hu. 2008. Incidences and ecological correlates of dioecious angiosperms in Taiwan and its outlying Orchid Island. *Botanical Studies* **49**: 261–276.

Vamosi, S. M. 2006. A reconsideration of the reproductive biology of the Atlantic forest in the Volta Velha Reserve. *Biodiversity and Conservation* **15**: 1417–1424.
<https://doi.org/10.1007/s10531-005-0308-4>

Vamosi, S. M. and S. A. Queenborough. 2010. Breeding systems and phylogenetic diversity of seed plants along a large-scale elevational gradient. *Journal of Biogeography* **37**: 465–476. <https://doi.org/10.1111/j.1365-2699.2009.02214.x>

Wang, T., A. Hamann, D. Spittlehouse and C. Carlos. 2016. Locally downscaled and spatially customizable climate data for historical and future periods for North

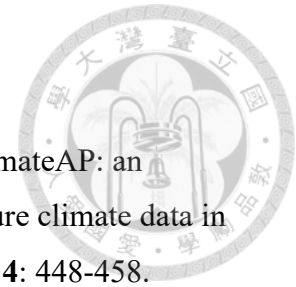
America. PLoS ONE **11(6)**: e0156720.

<https://doi.org/10.1371/journal.pone.0156720>

Wang, T., G. Wang, J. L. Innes, B. Seely and B. Chen. 2017. ClimateAP: an application for dynamic local downscaling of historical and future climate data in Asia Pacific. *Frontiers of Agricultural Science and Engineering* **4**: 448-458.
<https://doi.org/10.15302/J-FASE-2017172>

Webb, C. J., D. G. Lloyd and L. F. Delph. 1999. Gender dimorphism in indigenous New Zealand seed plants. *New Zealand Journal of Botany* **37**: 119–130.
<https://doi.org/10.1080/0028825X.1999.9512618>

Wolda, H. 1987. Altitude, habitat and tropical insect diversity. *Biological Journal of the Linnean Society* **30**: 313–323. <https://doi.org/10.1111/j.1095-8312.1987.tb00305.x>



Appendix S1. List of dioecious angiosperm species in Taiwan and its associated islets.

Family	Scientific name	Chinese name
Anacardiaceae	<i>Pistacia chinensis</i> Bunge	黃連木
Anacardiaceae	<i>Rhus javanica</i> L. var. <i>roxburghiana</i> (DC.) Rehd. & Wilson	羅氏鹽膚木
Anacardiaceae	<i>Rhus succedanea</i> L.	山漆
Anacardiaceae	<i>Rhus sylvestris</i> Sieb. & Zucc.	野漆樹
Aquifoliaceae	<i>Ilex arisanensis</i> Yamamoto	阿里山冬青
Aquifoliaceae	<i>Ilex asprella</i> (Hook. & Arn.) Champ.	燈稱花
Aquifoliaceae	<i>Ilex bioritsensis</i> Hayata	苗栗冬青
Aquifoliaceae	<i>Ilex cochinchinensis</i> (Lour.) Loes.	革葉冬青
Aquifoliaceae	<i>Ilex crenata</i> Thunb.	假黃楊
Aquifoliaceae	<i>Ilex ficoidea</i> Hemsl.	臺灣糊櫨
Aquifoliaceae	<i>Ilex formosana</i> Maxim.	糊櫨
Aquifoliaceae	<i>Ilex goshiensis</i> Hayata	圓葉冬青
Aquifoliaceae	<i>Ilex hayataiana</i> Loes.	早田氏冬青
Aquifoliaceae	<i>Ilex integra</i> Thunb.	全緣葉冬青
Aquifoliaceae	<i>Ilex kusanoi</i> Hayata	草野氏冬青
Aquifoliaceae	<i>Ilex lonicerifolia</i> Hayata var. <i>lonicerifolia</i>	忍冬葉冬青
Aquifoliaceae	<i>Ilex lonicerifolia</i> Hayata var. <i>matsudai</i> Yamamoto	松田氏冬青
Aquifoliaceae	<i>Ilex maximowicziana</i> Loes.	倒卵葉冬青
Aquifoliaceae	<i>Ilex micrococca</i> Maxim.	朱紅水木
Aquifoliaceae	<i>Ilex pedunculosa</i> Miq.	刻脈冬青
Aquifoliaceae	<i>Ilex pubescens</i> Hook. & Arn.	密毛假黃楊
Aquifoliaceae	<i>Ilex rarasanensis</i> Sasaki	拉拉山冬青
Aquifoliaceae	<i>Ilex rotunda</i> Thunb.	鐵冬青
Aquifoliaceae	<i>Ilex sugeroki</i> Maxim. var. <i>brevipedunculata</i> (Maxim.) S. Y. Hu	太平山冬青
Aquifoliaceae	<i>Ilex suzukii</i> S. Y. Hu	鈴木冬青
Aquifoliaceae	<i>Ilex tugitakayamensis</i> Sasaki	雪山冬青
Aquifoliaceae	<i>Ilex uraiensis</i> Mori & Yamamoto	烏來冬青
Aquifoliaceae	<i>Ilex yunnanensis</i> Fr. var. <i>parvifolia</i> (Hayata) S. Y. Hu	雲南冬青
Balanophoraceae	<i>Balanophora harlandi</i> Hook. f.	筆頭蛇菖
Balanophoraceae	<i>Balanophora laxiflora</i> Hemsl. ex Forbes & Hemsl.	穗花蛇菖
Cecropiaceae	<i>Poikilospermum acuminatum</i> (Trecul) Merr.	錐頭麻
Celastraceae	<i>Celastrus punctatus</i> Thunb.	光果南蛇藤
Chenopodiaceae	<i>Atriplex nummularia</i> Lindl.	臺灣濱藜
Cornaceae	<i>Aucuba chinensis</i> Benth.	桃葉珊瑚
Cornaceae	<i>Aucuba chinensis</i> Benth. var. <i>fongfangshanensis</i> Liao et al.	鳳凰山珊瑚

Family	Scientific name	Chinese name
Cornaceae	<i>Aucuba japonica</i> Thunb.	東瀛珊瑚
Cornaceae	<i>Helwingia japonica</i> (Thunb.) Dietr. subsp. <i>formosana</i> (Kanehira & Sasaki) Hara & Kurosawa	臺灣青莢葉
Cucurbitaceae	<i>Gynostemma pentaphyllum</i> (Thunb.) Makino	絞股藍
Cucurbitaceae	<i>Momordica cochinchinensis</i> (Lour.) Spreng.	木鱉子
Cucurbitaceae	<i>Neosalsomitra integrifoliola</i> (Cogn.) Hutch.	穿山龍
Cucurbitaceae	<i>Siraitia taiwaniana</i> (Hayata) C. Jeffrey ex Lu & Zhang	臺灣羅漢果
Cucurbitaceae	<i>Solena amplexicaulis</i> (Lam.) Gandhi	茅瓜
Cucurbitaceae	<i>Thladiantha nudiflora</i> Hemsl. ex Forbes. & Hemsl.	青牛膽
Cucurbitaceae	<i>Thladiantha punctata</i> Hayata	斑花青牛膽
Cucurbitaceae	<i>Trichosanthes quinquangulata</i> A. Gray.	蘭嶼括樓
Cucurbitaceae	<i>Zehneria mucronata</i> (Blume) Miq.	黑果馬蛟兒
Cyperaceae	<i>Carex kobomugi</i> Ohwi	海米
Daphniphyllaceae	<i>Daphniphyllum glaucescens</i> Blume subsp. <i>oldhamii</i> (Hemsl.) Huang var. <i>kengii</i> (Hurusawa) Huang	耿氏虎皮楠
Daphniphyllaceae	<i>Daphniphyllum glaucescens</i> Blume subsp. <i>oldhamii</i> (Hemsl.) Huang var. <i>lanyuese</i> Huang	蘭嶼虎皮楠
Daphniphyllaceae	<i>Daphniphyllum glaucescens</i> Blume subsp. <i>oldhamii</i> (Hemsl.) Huang var. <i>oldhamii</i> (Hemsl.) Huang	奧氏虎皮楠
Daphniphyllaceae	<i>Daphniphyllum himalaense</i> (Benth.) Muell.-Arg. subsp. <i>macropodum</i> (Miq.) Huang	薄葉虎皮楠
Dioscoreaceae	<i>Dioscorea benthamii</i> Prain & Burkill	田菁、大青薯
Dioscoreaceae	<i>Dioscorea bulbifera</i> L.	山芋
Dioscoreaceae	<i>Dioscorea codonopsifolia</i> Kamikoti	掌葉薯
Dioscoreaceae	<i>Dioscorea collettii</i> Hook. f.	華南薯蕷
Dioscoreaceae	<i>Dioscorea cumingii</i> Prain & Burkill	蘭嶼田薯
Dioscoreaceae	<i>Dioscorea doryphora</i> Hance	戟葉田薯
Dioscoreaceae	<i>Dioscorea esculenta</i> (Lour.) Burk. var. <i>spinuosa</i> R. Knuth	刺薯蕷
Dioscoreaceae	<i>Dioscorea hispida</i> Dennst.	大苦薯
Dioscoreaceae	<i>Dioscorea japonica</i> Thunb. var. <i>japonica</i>	薄葉野山藥
Dioscoreaceae	<i>Dioscorea japonica</i> Thunb. var. <i>oldhamii</i> R. Knuth	細葉野山藥
Dioscoreaceae	<i>Dioscorea japonica</i> Thunb. var. <i>pseudojaponica</i> (Hayata) Yamamoto	基隆野山藥
Dioscoreaceae	<i>Dioscorea kanoi</i> T. S. Liu & T. C. Huang	圓錐花薯蕷
Dioscoreaceae	<i>Dioscorea matsudai</i> Hayata	裏白葉薯榔
Dioscoreaceae	<i>Dioscorea persimilis</i> Prain & Burkill	假山藥薯
Ebenaceae	<i>Diospyros eriantha</i> Champ. ex Benth.	軟毛柿
Ebenaceae	<i>Diospyros ferrea</i> (Willd.) Bakhuizen	象牙樹
Ebenaceae	<i>Diospyros japonica</i> Sieb. & Zucc.	山柿

Family	Scientific name	Chinese name
Ebenaceae	<i>Diospyros kotoensis</i> Yamazaki	蘭嶼柿
Ebenaceae	<i>Diospyros maritima</i> Blume	黃心柿
Ebenaceae	<i>Diospyros morrisiana</i> Hance	山紅柿
Ebenaceae	<i>Diospyros oldhamii</i> Maxim.	俄氏柿
Ebenaceae	<i>Diospyros philippensis</i> (Desr.) Gurke	毛柿
Ebenaceae	<i>Diospyros rhombifolia</i> Hemsl.	菱葉柿
Ebenaceae	<i>Diospyros vaccinioides</i> Lindl.	楓港柿
Euphorbiaceae	<i>Acalypha suirenbiensis</i> Yamamoto	花蓮鐵莧
Euphorbiaceae	<i>Antidesma hiiranense</i> Hayata	南仁五月茶
Euphorbiaceae	<i>Antidesma japonicum</i> Sieb. & Zucc. var. <i>acutisepalum</i> (Hayata) Hurukawa	南投五月茶
Euphorbiaceae	<i>Antidesma japonicum</i> Sieb. & Zucc. var. <i>densiflorum</i> Hurusawa	密花五月茶
Euphorbiaceae	<i>Antidesma pentandrum</i> Merr. var. <i>barbatum</i> (Presl) Merr.	枯里珍
Euphorbiaceae	<i>Bischofia javanica</i> Blume	茄苳
Euphorbiaceae	<i>Claoxylon brachyandrum</i> Pax & Hoffm.	假鐵莧
Euphorbiaceae	<i>Drypetes karapinensis</i> (Hayata) Pax	交力坪鐵色
Euphorbiaceae	<i>Drypetes littoralis</i> (C. B. Rob.) Merr.	鐵色
Euphorbiaceae	<i>Excoecaria agallocha</i> L.	土沉香
Euphorbiaceae	<i>Flueggea suffruticosa</i> (Pellae) Baillon	白飯樹
Euphorbiaceae	<i>Flueggea virosa</i> (Roxb. ex Willd.) Voigt	密花白飯樹
Euphorbiaceae	<i>Gelonium aequoreum</i> Hance	白樹仔
Euphorbiaceae	<i>Liodendron formosanum</i> (Kanehira & Sasaki) Keng	臺灣假黃楊
Euphorbiaceae	<i>Macaranga sinensis</i> (Baill.) Muell.-Arg.	紅肉橙蘭
Euphorbiaceae	<i>Macaranga tanarius</i> (L.) Muell.-Arg.	血桐
Euphorbiaceae	<i>Mallotus japonicus</i> (Thunb.) Muell. -Arg.	野桐
Euphorbiaceae	<i>Mallotus paniculatus</i> (Lam.) Muell. -Arg. var. <i>formosanus</i> (Hayata) Hurusawa	臺灣白匏子
Euphorbiaceae	<i>Mallotus paniculatus</i> (Lam.) Muell. -Arg. var. <i>paniculatus</i>	白匏子
Euphorbiaceae	<i>Mallotus philippensis</i> (Lam.) Muell. -Arg.	粗糠柴
Euphorbiaceae	<i>Mallotus repandus</i> (Willd.) Muell. -Arg.	扛香藤
Euphorbiaceae	<i>Margaritaria indica</i> (Dalz.) Airy Shaw	紫黃
Euphorbiaceae	<i>Mercurialis leiocarpa</i> Sieb. & Zucc.	山殼
Flacourtiaceae	<i>Flacourtia rukam</i> Zoll & Merr.	羅庚果
Flacourtiaceae	<i>Idesia polycarpa</i> Maxim.	山桐子
Flacourtiaceae	<i>Xylosma congesta</i> (Lour.) Merr.	柞木
Gramineae	<i>Spinifex littoreus</i> (Burm. f.) Merr.	濱刺麥
Guttiferae	<i>Garcinia linii</i> C. E. Chang	蘭嶼福木
Guttiferae	<i>Garcinia multiflora</i> Champ.	福木
Guttiferae	<i>Garcinia subelliptica</i> Merrll	菲島福木

Family	Scientific name	Chinese name
Haloragaceae	<i>Myriophyllum propinquum</i> Cum	烏蘇里聚藻
Hydrocharitaceae	<i>Halophila ovalis</i> (R. Br.) Hook. f.	卵葉鹽藻
Hydrocharitaceae	<i>Hydrilla verticillata</i> (L. f.) Royle	水王孫
Hydrocharitaceae	<i>Thalassia hemprichii</i> (Ehrenb.) Aschers.	泰來藻
Hydrocharitaceae	<i>Vallisneria gigantea</i> Graebner	大苦草
Icacinaceae	<i>Gonocaryum calleryanum</i> (Baill.) Becc.	柿葉茶茱萸
Lauraceae	<i>Lindera aggregata</i> (Sims) Kosterm. f. <i>aggregata</i>	天臺烏藥
Lauraceae	<i>Lindera aggregata</i> (Sims) Kosterm. f. <i>playfairii</i> (Hemsl.) Liao	小葉烏藥
Lauraceae	<i>Lindera akoensis</i> Hayata	內芩子
Lauraceae	<i>Lindera communis</i> Hemsl.	香葉樹
Lauraceae	<i>Lindera erythrocarpa</i> Makino	鐵釘樹
Lauraceae	<i>Lindera glauca</i> (Sieb. & Zucc.) Bl.	白葉釣樟
Lauraceae	<i>Lindera megaphylla</i> Hemsl.	大香葉樹
Lauraceae	<i>Litsea acuminata</i> (Bl.) Kurata	長葉木薑子
Lauraceae	<i>Litsea acutivena</i> Hayata	銳脈木薑子
Lauraceae	<i>Litsea akoensis</i> Hayata var. <i>akoensis</i>	屏東木薑子
Lauraceae	<i>Litsea akoensis</i> Hayata var. <i>chitouchiaoensis</i> Liao	竹頭角木薑子
Lauraceae	<i>Litsea akoensis</i> Hayata var. <i>sasakii</i> (Kamikoti) Liao	狹葉木薑子
Lauraceae	<i>Litsea coreana</i> Levl.	鹿皮斑木薑子
Lauraceae	<i>Litsea cubeba</i> (Lour.) Persoon	山胡椒
Lauraceae	<i>Litsea elongata</i> (Wall. ex Nees) Benth. & Hook. f. var. <i>mushaensis</i> (Hayata) J. C. Liao	霧社木薑子
Lauraceae	<i>Litsea garciae</i> Vidal	蘭嶼木薑子
Lauraceae	<i>Litsea hypophaea</i> Hayata	黃肉樹
Lauraceae	<i>Litsea lii</i> Chang var. <i>lii</i>	李氏木薑子
Lauraceae	<i>Litsea lii</i> Chang var. <i>nunkao-tahangensis</i> (Liao) Liao	能漢木薑子
Lauraceae	<i>Litsea morrisonensis</i> Hayata	玉山木薑子
Lauraceae	<i>Litsea rotundifolia</i> Hemsl. var. <i>oblongifolia</i> (Nees) Allen	橢圓葉木薑子
Lauraceae	<i>Neolitsea aciculata</i> (Blume) Koidz. var. <i>aciculata</i>	銳葉新木薑子
Lauraceae	<i>Neolitsea aciculata</i> (Blume) Koidz. var. <i>variabilima</i> (Hayata) J. C. Liao	變葉新木薑子
Lauraceae	<i>Neolitsea acuminatissima</i> (Hayata) Kanehira & Sasaki	高山新木薑子
Lauraceae	<i>Neolitsea buisanensis</i> Yamamoto & Kamikoti f. <i>buisanensis</i>	武威山新木薑子
Lauraceae	<i>Neolitsea buisanensis</i> Yamamoto & Kamikoti f. <i>sutsuensis</i> J. C. Liao	石厝新木薑子
Lauraceae	<i>Neolitsea daibuensis</i> Kamikoti	大武新木薑子
Lauraceae	<i>Neolitsea hiiranensis</i> Liu & Liao	南仁山新木薑子
Lauraceae	<i>Neolitsea konishii</i> (Hayata) Kanehira & Sasaki	五掌楠
Lauraceae	<i>Neolitsea parvigemma</i> (Hayata) Kanehira & Sasaki	小芽新木薑子
Lauraceae	<i>Neolitsea sericea</i> (Blume) Koidz. var. <i>aurata</i> (Hayata) Hatusima	金新木薑子

Family	Scientific name	Chinese name
Lauraceae	<i>Neolitsea sericea</i> (Blume) Koidz. var. <i>sericea</i>	白新木薑子
Lauraceae	<i>Neolitsea villosa</i> (Blume) Merr.	蘭嶼新木薑子
Loranthaceae	<i>Loranthus delavayi</i> Van Tieghem	桐樹桑寄生
Loranthaceae	<i>Viscum alniformosanae</i> Hayata	臺灣槲寄生
Menispermaceae	<i>Cocculus laurifolius</i> DC.	樟葉木防己
Menispermaceae	<i>Cocculus orbiculatus</i> (L.) DC.	木防己
Menispermaceae	<i>Cyclea gracillima</i> Diels	土防己
Menispermaceae	<i>Cyclea insularis</i> (Makino) Hatusima	蘭嶼土防己
Menispermaceae	<i>Cyclea ochiaiana</i> (Yamamoto) S. F. Huang & T. C. Huang	臺灣土防己
Menispermaceae	<i>Pericampylus formosanus</i> Diels	蓬萊藤
Menispermaceae	<i>Sinomenium acutum</i> (Thunb.) Rehd. & Wils.	漢防己
Menispermaceae	<i>Stephania cephalantha</i> Hayata	大還魂
Menispermaceae	<i>Stephania japonica</i> (Thunb. ex Murray) Miers var. <i>hispidula</i> Yamamoto	毛千金藤
Menispermaceae	<i>Stephania japonica</i> (Thunb. ex Murray) Miers var. <i>japonica</i>	千金藤
Menispermaceae	<i>Stephania merrillii</i> Diels	蘭嶼千金藤
Menispermaceae	<i>Stephania tetrandra</i> S. Moore	石蟾蜍
Menispermaceae	<i>Tinospora dentata</i> Diels	恆春青牛膽
Moraceae	<i>Broussonetia kaempferi</i> Sieb.	楮樹
Moraceae	<i>Broussonetia papyrifera</i> (L.) L'Hérit. ex Vent.	構樹
Moraceae	<i>Ficus ampelas</i> Burm. f.	菲律賓榕
Moraceae	<i>Ficus aurantiaca</i> Griff. var. <i>parvifolia</i> (Corner) Corner	大果藤榕
Moraceae	<i>Ficus cumingii</i> Miq.	對葉榕
Moraceae	<i>Ficus erecta</i> Thunb. var. <i>beecheana</i> (Hook. & Arn.) King	牛奶榕
Moraceae	<i>Ficus erecta</i> Thunb. var. <i>erecta</i>	假枇杷
Moraceae	<i>Ficus esquiroliana</i> Lévl.	黃毛榕
Moraceae	<i>Ficus fistulosa</i> Reinw. ex Bl. f. <i>benguetensis</i> (Merr.) Liu & Liao	黃果豬母乳
Moraceae	<i>Ficus fistulosa</i> Reinw. ex Bl. f. <i>fistulosa</i>	豬母乳
Moraceae	<i>Ficus formosana</i> Maxim. f. <i>formosana</i>	天仙果
Moraceae	<i>Ficus formosana</i> Maxim. f. <i>shimadai</i> Hayata	細葉天仙果
Moraceae	<i>Ficus heteropleura</i> Bl.	尖尾長葉榕
Moraceae	<i>Ficus irisana</i> Elm.	澀葉榕
Moraceae	<i>Ficus pedunculosa</i> Miq. var. <i>mearnsii</i> (Merr.) Corner	鵝鑾鼻蔓榕
Moraceae	<i>Ficus pedunculosa</i> Miq. var. <i>pedunculosa</i>	蔓榕
Moraceae	<i>Ficus pumila</i> L. var. <i>awkeotsang</i> (Makino) Corner	愛玉子
Moraceae	<i>Ficus pumila</i> L. var. <i>pumila</i>	薜荔
Moraceae	<i>Ficus ruficaulis</i> Merr. var. <i>antaensis</i> (Hayata) Hatusima & Liao	蘭嶼落葉榕
Moraceae	<i>Ficus sarmentosa</i> Buch.-Ham. ex J. E. Sm. var. <i>henryi</i> (King ex D. Oliver) Corner	阿里山珍珠蓮

Family	Scientific name	Chinese name
Moraceae	<i>Ficus sarmentosa</i> Buch.-Ham. ex J. E. Sm. var. <i>nipponica</i> (Fr. & Sav.) Corner	珍珠蓮
Moraceae	<i>Ficus septica</i> Burm. f.	大有榕
Moraceae	<i>Ficus tannoensis</i> Hayata f. <i>rhombifolia</i> Hayata	菱葉濱榕
Moraceae	<i>Ficus tannoensis</i> Hayata f. <i>tannoensis</i>	濱榕
Moraceae	<i>Ficus tinctoria</i> Forst. f.	山豬枷
Moraceae	<i>Ficus trichocarpa</i> Bl. var. <i>obtusata</i> (Hassk.) Corner	鈍葉毛果榕
Moraceae	<i>Ficus vaccinioides</i> Hemsl. ex King	越橘葉蔓榕
Moraceae	<i>Ficus variegata</i> Bl. var. <i>garciae</i> (Elm.) Corner	幹花榕
Moraceae	<i>Ficus virgata</i> Reinw. ex Blume	白肉榕
Moraceae	<i>Humulus scandens</i> (Lour.) Merr.	葎草
Moraceae	<i>Maclura cochinchinensis</i> (Lour.) Corner	柘樹
Moraceae	<i>Malaisia scandens</i> (Lour.) Planch.	盤龍木
Moraceae	<i>Morus australis</i> Poir.	小葉桑
Myricaceae	<i>Myrica rubra</i> (Lour.) Sieb. & Zucc.	楊梅
Myristicaceae	<i>Myristica ceylanica</i> A. DC. var. <i>cagayanensis</i> (Merr.) J. Sinclair	蘭嶼肉豆蔻
Myristicaceae	<i>Myristica elliptica</i> Wall. ex Hook. f. & Thomson. var. <i>simiarum</i> (A. DC.) J. Sinclair	紅頭肉豆蔻
Nyctaginaceae	<i>Pisonia aculeata</i> L.	腺果藤
Palmae	<i>Phoenix hanceana</i> Naudin var. <i>formosana</i> Beccari	臺灣海棗
Pandanaceae	<i>Freycinetia formosana</i> Hemsl.	山露兜
Pandanaceae	<i>Pandanus odoratissimus</i> L. f.	露兜樹
Piperaceae	<i>Piper arborescens</i> Roxb.	蘭嶼風藤
Piperaceae	<i>Piper betle</i> L.	荖藤
Piperaceae	<i>Piper interruptum</i> Opiz var. <i>multinervum</i> C. DC.	多脈風藤
Piperaceae	<i>Piper kadsura</i> (Choisy) Ohwi	風藤
Piperaceae	<i>Piper kawakamii</i> Hayata	恆春風藤
Piperaceae	<i>Piper philippinum</i> Miq.	菲律賓胡椒
Piperaceae	<i>Piper sintenense</i> Hatusima	薄葉風藤
Piperaceae	<i>Piper taiwanense</i> Lin & Lu	臺灣荖藤
Polygonaceae	<i>Rumex acetosa</i> L.	酸模
Polygonaceae	<i>Rumex acetosella</i> L.	小酸模
Rhamnaceae	<i>Rhamnus chingshuiensis</i> Shimizu var. <i>chingshuiensis</i>	清水鼠李
Rhamnaceae	<i>Rhamnus chingshuiensis</i> Shimizu var. <i>tashanensis</i> Liu & Wang	塔山鼠李
Rhamnaceae	<i>Rhamnus formosana</i> Matsum.	桶鈎藤
Rhamnaceae	<i>Rhamnus kanagusuki</i> Makino	變葉鼠李
Rhamnaceae	<i>Rhamnus nakaharai</i> (Hayata) Hayata	中原氏鼠李
Rhamnaceae	<i>Rhamnus parvifolia</i> Bunge	小葉鼠李
Rhamnaceae	<i>Rhamnus pilushanensis</i> Liu & Wang	畢祿山鼠李

Family	Scientific name	Chinese name
Rosaceae	<i>Filipendula kiraishiensis</i> Hayata	臺灣蚊子草
Rubiaceae	<i>Mussaenda macrophylla</i> Wall.	大葉玉葉金花
Rubiaceae	<i>Mussaenda pubescens</i> Ait. f.	毛玉葉金花
Rubiaceae	<i>Psychotria rubra</i> (Lour.) Poir.	九節木
Rubiaceae	<i>Timonius arboreus</i> Elmer	貝木
Rutaceae	<i>Melicope semecarpifolia</i> (Merr.) T. Hartley	山刈葉
Rutaceae	<i>Zanthoxylum ailanthoides</i> Sieb. & Zucc.	食茱萸
Rutaceae	<i>Zanthoxylum armatum</i> DC.	秦椒
Rutaceae	<i>Zanthoxylum integrifolium</i> (Merr.) Merr.	蘭嶼花椒
Rutaceae	<i>Zanthoxylum nitidum</i> (Roxb.) DC.	雙面刺
Rutaceae	<i>Zanthoxylum pistaciiflorum</i> Hayata	三葉花椒
Rutaceae	<i>Zanthoxylum scandens</i> Blume	藤花椒
Rutaceae	<i>Zanthoxylum schinifolium</i> Sieb. & Zucc.	翼柄花椒
Rutaceae	<i>Zanthoxylum simulans</i> Hance	刺花椒
Rutaceae	<i>Zanthoxylum wutaiense</i> Chen	屏東花椒
Salicaceae	<i>Salix fulvopubescens</i> Hayata var. <i>doi</i> (Hayata) Yang & Huang	薄葉柳
Salicaceae	<i>Salix fulvopubescens</i> Hayata var. <i>fulvopubescens</i>	褐毛柳
Salicaceae	<i>Salix fulvopubescens</i> Hayata var. <i>tagawana</i> (Koidz.) Yang & Huang	白毛柳
Salicaceae	<i>Salix kusanoi</i> (Hayata) Schneider	水社柳
Salicaceae	<i>Salix okamotoana</i> Koidz.	關山嶺柳
Salicaceae	<i>Salix taiwanalpina</i> Kimura var. <i>morrisonicola</i> (Kimura) Yang & Huang	玉山柳
Salicaceae	<i>Salix taiwanalpina</i> Kimura var. <i>taiwanalpina</i>	臺灣山柳
Salicaceae	<i>Salix taiwanalpina</i> Kimura var. <i>takasagoalpina</i> (Koidz.) Ying	高山柳
Salicaceae	<i>Salix warburgii</i> O. Seemen	水柳
Schisandraceae	<i>Schisandra arisanensis</i> Hayata	阿里山五味子
Simarubaceae	<i>Picrasma quassioides</i> Benn.	苦樹
Smilacaceae	<i>Heterosmilax indica</i> A. DC.	土伏苓
Smilacaceae	<i>Heterosmilax japonica</i> Kunth	平柄菝契
Smilacaceae	<i>Heterosmilax seisuiensis</i> (Hayata) F. T. Wang & T. Tang	臺中假土伏苓
Smilacaceae	<i>Smilax arisanensis</i> Hayata	阿里山菝契
Smilacaceae	<i>Smilax bracteata</i> Presl var. <i>bracteata</i>	假菝契
Smilacaceae	<i>Smilax bracteata</i> Presl var. <i>verruculosa</i> (Merr.) T. Koyama	糙莖菝契
Smilacaceae	<i>Smilax china</i> L.	菝契
Smilacaceae	<i>Smilax corbularia</i> Kunth	裏白菝契
Smilacaceae	<i>Smilax discotis</i> Warburg	宜蘭菝契
Smilacaceae	<i>Smilax elongato-umbellata</i> Hayata	細葉菝契
Smilacaceae	<i>Smilax glabra</i> Roxb.	光滑菝契

Family	Scientific name	Chinese name
Smilacaceae	<i>Smilax hayatae</i> T. Koyama	早田氏菝契
Smilacaceae	<i>Smilax horridiramula</i> Hayata	密刺菝契
Smilacaceae	<i>Smilax lanceifolia</i> Roxburgh	臺灣菝契
Smilacaceae	<i>Smilax luei</i> T. Koyama	呂氏菝契
Smilacaceae	<i>Smilax menispermoides</i> A. DC.	巒大菝契
Smilacaceae	<i>Smilax nantoensis</i> T. Koyama	南投菝契
Smilacaceae	<i>Smilax nipponica</i> Miquel	日本菝契
Smilacaceae	<i>Smilax ocreata</i> A. DC.	耳葉菝契
Smilacaceae	<i>Smilax riparia</i> A. DC.	烏蘇里山馬薯
Smilacaceae	<i>Smilax sieboldii</i> Miq.	臺灣山馬薯
Smilacaceae	<i>Smilax vaginata</i> Decaisne	玉山菝契
Theaceae	<i>Eurya acuminata</i> DC.	銳葉柃木
Theaceae	<i>Eurya chinensis</i> Brown	米碎柃木
Theaceae	<i>Eurya crenatifolia</i> (Yamamoto) Kobuski	假柃木
Theaceae	<i>Eurya emarginata</i> (Thunb.) Makino	凹葉柃木
Theaceae	<i>Eurya glaberrima</i> Hayata	厚葉柃木
Theaceae	<i>Eurya gnaphalocarpa</i> Hayata	毛果柃木
Theaceae	<i>Eurya leptophylla</i> Hayata	薄葉柃木
Theaceae	<i>Eurya loquiana</i> Dunn	細枝柃木
Theaceae	<i>Eurya nitida</i> Korthals var. <i>nanjenshanensis</i> Hsieh, Ling & Yang	南仁山柃木
Theaceae	<i>Eurya nitida</i> Korthals var. <i>nitida</i>	光葉柃木
Theaceae	<i>Eurya renegechiensis</i> Yamamoto	蓮花池柃木
Theaceae	<i>Eurya strigillosa</i> Hayata	粗毛柃木
Theaceae	<i>Eurya taitungensis</i> Chang	清水山柃木
Urticaceae	<i>Boehmeria clidemioides</i> Miq.	序葉苧麻
Urticaceae	<i>Boehmeria longispica</i> Steud.	長穗苧麻
Urticaceae	<i>Debregeasia orientalis</i> C. J. Chen	水麻
Urticaceae	<i>Dendrocide kotoensis</i> (Hayata ex Yamamota) Shih & Yang	紅頭咬人狗
Urticaceae	<i>Dendrocide meyeniana</i> (Walp.) Chew	咬人狗
Urticaceae	<i>Elatostema herbaceifolium</i> Hayata	臺灣樓梯草
Urticaceae	<i>Elatostema multicanaliculatum</i> Shih & Yang	多溝樓梯草
Urticaceae	<i>Elatostema rivulare</i> Shih & Yang	溪澗樓梯草
Urticaceae	<i>Elatostema strigillosum</i> Shih & Yang	微粗毛樓梯草
Urticaceae	<i>Elatostema trilobulatum</i> (Hayata) Yamazaki	裂葉樓梯草
Urticaceae	<i>Elatostema villosa</i> Shih & Yang	柔毛樓梯草
Urticaceae	<i>Leucosyke quadrinervia</i> Rob.	四脈麻
Urticaceae	<i>Pipturus arborescens</i> (Link) C. Robinson	落尾麻

Family	Scientific name	Chinese name
Vitaceae	<i>Tetrastigma alatum</i> Li	翼柄崖爬藤
Vitaceae	<i>Tetrastigma dentatum</i> (Hayata) Li	三脚蟹草
Vitaceae	<i>Tetrastigma formosanum</i> (Hemsl.) Gagnep.	三葉崖爬藤
Vitaceae	<i>Tetrastigma umbellatum</i> (Hemsl.) Nakai	臺灣崖爬藤
Zannichelliaceae	<i>Halodule pinifolia</i> (Miki) Hartog	線葉二藥藻
Zannichelliaceae	<i>Halodule uninervis</i> (Forsk.) Aschers.	單脈二藥藻



現行與未來氣候下的台灣森林植物分布預測研究

博士論文口試紀錄

應修正事項及回應說明



記錄：吳俊和

口試委員	應修正事項	回應說明
曾彥學教授	1. 第五章以係以被子植物 (angiosperms) 雌雄異株為分析對象，但論文中摘要第五章標題為「維管束植物 (vascular plants)」。應修正一致。	已修正。
鍾國芳副研究員	1. 論文各章節均已發表或發表中，文章內容包含共同作者的努力與付出，建議增列各作者的貢獻度說明。 2. 論文包含許多術語縮寫 (例如 OOB)，對非統計模型領域人員閱讀困難，請增加縮寫名詞對照表，提升閱讀方便性。 3. Dash 及 Hyphen 的使用混亂，請釐清不同符號的	1. 已在各章末段增加 Author contributions，述明每一位共同作者對該章研究成果的貢獻。目錄 (Contents) 亦增加標示 Author contributions 所在頁碼。 2. 已製作縮寫名詞對照表 (Comparison table of abbreviations)，列於摘要之後。 3. 已重新檢視並修正論文內容，修正原則如下：

口試委員	應修正事項	回應說明
	<p>途，檢視更正論文內容。</p> <p>4. 海拔遞減率採用了「百公尺」或「公里」等不同單位，請修正一致。</p> <p>5. 第四章的海拔遞減率引用了2018年Taiwania的文章，但原發表內未見所引用之數據，請檢視修正，或引用更原始的海拔遞減率文獻。</p>	<p>A. 單純的英文單字連結處，使用 hyphen (-)。</p> <p>B. 用以取代 to，或代表數值範圍者，使用 en dash (—)。</p> <p>C. 有關森林類型名稱部分，維持與原始文獻 (Li et al., 2013) 相同的用法，採用 en dash。例如 <i>Abies-Tsuga</i> forest type。</p> <p>D. 表示語意轉折或中斷處，採用 em dash (—)。</p> <p>4. 依據 Barry and Chorley 所著 <i>Atmosphere, Weather and Climate</i> (8th edition)，採用 °C/km 為本論文之海拔遞減率單位。</p> <p>5. 已修正。改用 Barry and Chorley (2009) 作為引用海拔遞減率的文獻。</p>
王震哲教授	1. 本論文使用了大量的植群調查與標本文獻資料，務	1. 前人資料對於本論文研究具有極重要的貢獻。已於論文

口試委員	應修正事項	回應說明
	<p>請對前人的辛苦成果表達致謝之意。</p> <p>2. 第四章內容仍有格式不一致之處，例如圖號、表號未列出章節代碼。</p> <p>3. 參考文獻對於中文人名的連接，部分帶有 hyphen、部分則無，請修正一致。</p> <p>4. 建議第五章增加附錄，將雌雄異株物種（dioecious species）逐一表列，以利未來的研究人員可參照與檢驗。</p>	<p>誌謝章節，述明各項資料來源並表達感謝。</p> <p>2. 已統一修正。例如修正為 Table 4.1; Fig. 4.1 等。</p> <p>3. 已將中文人名統一修正為帶有 hyphen 的連接形式。例如：H.-Y. Lin。</p> <p>4. 第五章增加 Appendix S1. List of dioecious angiosperms in Taiwan and its associated islets (p.5-31–p.5-39)。</p>

現行與未來氣候下的台灣森林植物分布預測研究



博士論文口試紀錄

後續研究建議

記錄：吳俊和

口試委員	後續研究建議
曾彥學教授	<ol style="list-style-type: none">1. 第五章對臺灣被子植物的雌雄異株地理分布趨勢進行了分析，未來可針對楊柳科、柿樹科、山茶科（柃木屬）、樟科（木薑子屬、新木薑子屬）等以雌雄異株為主的類群進行研究。另外，裸子植物亦是單獨探討的對象。2. 本論文提出高海拔森林、水青岡森林、熱帶雲霧林、熱帶季風林可能因氣候變遷而快速消失，可更深入探討與此現象有關的氣候因子，並提出適宜的保育策略。尤其是臺灣南部的熱帶霧林與季風林，兩者的季節性降雨特徵是不同的，值得進一步研究降雨與植群變遷的因果關係。3. 本研究將鐵冷杉林 (<i>Abies-Tsuga forest type</i>) 合併為同一林帶，與我們熟悉的冷杉林、鐵杉林的植群分類不太一致。建議未來可發展更細緻的林型分類與預測技術，將鐵杉林與冷杉林區分開來。4. 針對已知的易受氣候變遷衝擊森林類型，例如水青岡，應加強與林務單位的合作，對易危生態系推動具體的保護工作。5. 臺灣杜鵑是臺灣中海拔很特殊的一種林型，但在本論文未針對該林型有任何探討，建議可增納臺灣杜鵑林型的分析。
陳子英教授	<ol style="list-style-type: none">1. 植群預測模型在特定森林類型的錯誤率較高，例如熱帶季風

口試委員	後續研究建議
授	<p>林，由於該林型與地形及風衝等因素相關性高、或是某些森林僅特定生長在臨海的第一道稜線上，但現有氣候模型不易反映這種細微尺度的棲地特色，導致預測結果較差。宜思考如何找到更適合代表生物分布的氣候因子，並提高環境因子的空間解析度，進一步改良現有的預測模型。</p> <p>2. 本研究發現龜山島、綠島及蘭嶼的雌雄異株物種比例較高，除了與這些小島與臺灣本島的隔離程度外，是否與小島形成的時間有關？也許可進一步探討。</p> <p>3. 雌雄異株物種的比例，在陸生與水生植物間是否不同？以水鳥傳播為主的水生物種，是否有特殊的植物性別比例？濕地植物相有沒有特殊的植物性別特色？均為值得研究的議題。</p>
鍾國芳副 研究員	<p>1. <i>Clim. regression</i> 氣候模型值得推廣給有興趣的生態研究者使用。</p> <p>2. 如同曾彥學教授建議，未來可進一步將冷杉及鐵杉林帶區別開來，以符臺灣多數森林生態研究者的植群分類概念。</p> <p>3. 本論文探討了現行（1960-2009）與未來（2016-2100）氣候，若技術與資料許可，建議可再發展古氣候（paleo climate）的研究。</p>
謝長富教 授	<p>1. 目前的植群預測模型對於熱帶季風林的預測準確率較低，可能受到小尺度地形與季風交互作用的影響。建議未來的氣候模型可朝風衝現象做更細緻的模擬，並可作為後續研究與發表的主軸。</p> <p>2. 楠櫨林帶的預測準確率也偏低，可能與該植群帶由多個群叢</p>

口試委員	後續研究建議
	<p>混雜組成所致。未來可利用更細緻的植群分類單元，分別建構各群叢的棲位模型，也許可改善現有的預測準確度。</p>
<p>王震哲教授</p>	<ol style="list-style-type: none"> 1. 第四章提出高海拔森林及水青岡森林面積很可能因氣候變遷而縮減，熱帶霧林及熱帶季風林也可能受到嚴重威脅。前者是大部分研究報告已提出的結論，後者則是較值得注意的研究結果。建議針對後者，更詳細地討論可能導致此一現象的暖化情境、環境改變量及氣候條件組合。 2. 第五章提出雌雄異株物種比例與海拔的趨勢關係，授粉者可能是主要的因素，但因資料不足，未能有完整的分析比較。未來可加強這部分的研究。 3. 西部離島雖然雌雄異株物種比例較低，但這些離島的海拔落差也相對較小。建議進一步比較這些離島與臺灣低海拔地區的雌雄異株比例與物種組成的差異。
<p>胡哲明教授</p>	<p>本論文發掘許多值得進一步發展的研究議題，例如：</p> <ol style="list-style-type: none"> 1. 未來可從植物生理面建立物種的氣候適存曲線，並與分布模型曲線進行交互驗證。 2. 本研究已從較高的地理尺度及植物性別的形態面向，整理出雌雄異株物種的分布趨勢。未來可從自交與異交的功能面向、譜系關係、授粉者組成、或針對特定植物類群等，進行更多的植物性別研究議題探討。